

# **Dynamics of polymer lasers**

**Cover:**

The molecular structure on the cover represents a repeat unit of a prototype conjugated light-emitting polymer. The parenthesis indicate that the polymer chain consists of many of these units. The parenthesis may also be viewed as the mirrors of a laser cavity with the polymer as the gain medium. Altogether the cover illustrates the subject of this thesis: *dynamics* of polymer lasers and light-emitting polymers.

# **Dynamics of polymer lasers**

## **Proefschrift**

ter verkrijging van  
de graad van Doctor aan de Universiteit Leiden,  
op gezag van de Rector Magnificus Dr. D. D. Breimer,  
hoogleraar in de faculteit der Wiskunde en  
Natuurwetenschappen en die der Geneeskunde,  
volgens besluit van het College voor Promoties  
te verdedigen op donderdag 6 juni 2002  
te klokke 15.15 uur

door

**Stephanus Anthonius van den Berg**

geboren te Noordwijk op 6 november 1974

**Promotiecommissie:**

Promotor: Prof. dr. G. W. 't Hooft  
Copromotor: Dr. E. R. Eliel  
Referent: Prof. dr. K. J. Boller (Universiteit Twente)  
Leden: Prof. dr. J. P. Woerdman  
Prof. dr. G. Nienhuis  
Dr. E. J. J. Groenen  
Prof. dr. J. W. Hofstraat (Universiteit van Amsterdam)  
Dr. H. F. M. Schoo (Technische Universiteit Eindhoven)  
Prof. dr. P. H. Kes

Dit werk maakt deel uit van het onderzoekprogramma van de Stichting voor Fundamenteel Onderzoek der Materie (FOM, financieel gesteund door de Nederlandse Organisatie voor Wetenschappelijk Onderzoek (NWO)) en Philips Research.

# Contents

---

<b>1</b>	<b>Introduction</b>	<b>7</b>
1.1	Conjugated polymers . . . . .	7
1.2	Photophysics of light-emitting polymers . . . . .	10
1.3	Gain in light-emitting polymer films . . . . .	12
1.4	Optically pumped polymer lasers . . . . .	14
1.5	This thesis . . . . .	14
<b>2</b>	<b>From amplified spontaneous emission to laser oscillation; Dynamics in a short-cavity polymer laser</b>	<b>17</b>
<b>3</b>	<b>Pulse-train formation in a gain-switched polymer laser resulting from spatial gain inhomogeneity</b>	<b>25</b>
3.1	Introduction . . . . .	25
3.2	Experimental setup . . . . .	26
3.3	Experimental results . . . . .	28
3.4	Rate equations . . . . .	31
3.5	Heuristic description . . . . .	36
3.6	Conclusion . . . . .	39
<b>4</b>	<b>Orientational relaxation in polymer and dye solutions and its consequence for the laser threshold</b>	<b>41</b>
4.1	Introduction . . . . .	41
4.2	Orientational relaxation in optically pumped polymer and dye solutions . . . . .	42
4.3	Polymer and dye lasers . . . . .	45
4.4	Conclusion . . . . .	49
<b>5</b>	<b>Study of polarization cross coupling in a polymer microlaser using double-pulse excitation</b>	<b>51</b>
5.1	Introduction . . . . .	51
5.2	Experimental setup . . . . .	53
5.3	Experimental results . . . . .	55
5.4	Model description . . . . .	58

## Contents

---

5.5	Discussion . . . . .	64
5.6	Time-integrated output . . . . .	66
5.7	Conclusion . . . . .	68
<b>6</b>	<b>Measuring the gain dynamics in a conjugated polymer film</b>	<b>71</b>
	Appendix A: The optical gain in pump-probe experiments . . . . .	79
	Appendix B: The polymer HB1221 . . . . .	81
<b>7</b>	<b>Time-domain study of emissive states in a PPV</b>	<b>83</b>
7.1	Introduction . . . . .	83
7.2	Experiment . . . . .	84
7.3	Photoluminescence decay . . . . .	85
7.4	Photoluminescence anisotropy . . . . .	89
7.5	Discussion . . . . .	91
7.6	Conclusion . . . . .	93
	<b>References</b>	<b>95</b>
	<b>Samenvatting</b>	<b>103</b>
	<b>List of publications</b>	<b>109</b>
	<b>Curriculum Vitae</b>	<b>111</b>
	<b>Nawoord</b>	<b>113</b>

# Chapter 1

---

## Introduction

### 1.1 Conjugated polymers

Conjugated polymers offer a unique combination of conducting, mechanical and light-emitting properties that makes them very attractive for a range of applications. The basis for this new generation of conducting species was laid in 1977 when Shirakawa, MacDiarmid and Heeger developed a technique to manufacture conducting polyacetylene films. For this discovery they were awarded the Nobel prize in chemistry in 2000 [1–3]. Their work initiated the development of a whole new field of research at the interface of chemistry, physics and materials science. It has also spurred a major technological effort in the research laboratories of several large-scale companies. The fact that thin films of conducting polymers are easily formed on a wide variety of substrates by applying simple techniques like spin coating and inkjet printing, brought about the commercial interest in these materials. Conducting polymers are nowadays being developed for antistatic coatings, electromagnetic shielding, corrosion inhibitors, capacitors etc. The demonstration of a plastic field-effect transistor has opened the way for the development of cheap plastic electronics for low-performance applications [4–8].

Apart from the purely electronic applications conjugated polymers show a large potential for applications in polymer photovoltaic cells [9], and in particular in polymer light-emitting diodes (LEDs) [10–14]. The development of the latter has been pushed forward by the enormous commercial interests in the display market. Polymer LEDs are not only very interesting because they can easily be produced in bulk at low cost, but also because of their excellent luminescent properties (high brightness, high contrast), low power consumption and light weight as compared to the conventional (inorganic) LEDs. This makes polymer LEDs very suitable for application in mobile phones, laptops etc. Moreover, polymer LEDs may be coated on flexible (plastic) substrates, generating the possibility of producing displays that can be folded or bent. The essentially simple production process offers the possibility of producing large area displays, which is difficult with conventional semiconductor LEDs. The ultimate goal lies in the combination

of plastic electronics with polymer LEDs, in an all plastic, flexible light-emitting device.

An ideal conjugated polymer can be viewed as an extended regular chain of carbon atoms that have alternating single and double bonds. The  $\pi$ -electrons associated with the double bonds are delocalized along the carbon chain, because they are relatively weakly bound to the carbon atoms. Such a polymer, like polyacetylene, is an intrinsic semiconductor, which can be made to conduct by oxidation (doping). This sets the framework for applying a semiconductor model to the description of the properties of conjugated polymers [15]. In that model the conjugated polymer is viewed as an infinite one dimensional chain described by a one-electron Hamiltonian with strong electron-lattice coupling [16] under disregard of Coulomb interactions and electron-electron correlations [17].

Real conjugated polymers do not adhere to this idealized model at all. Rather, geometrical and chemical defects play an all-important role, severely reducing the extent of  $\pi$ -electron overlap. Consequently, the polymer chain can be seen as a sequence of relatively short conjugated segments of varying length. In this “molecular” picture, excitations and/or charge are localized on such segments. Because of the variation in conjugation lengths, the energy levels are distributed. Charge transport in such systems, being the result of interchain hopping, has been studied in great detail during the last decade (see e.g., Ref. [18–20] and references therein).

Electroluminescence from conjugated polymers was first reported in 1990 using the material poly(*p*-phenylene vinylene) (PPV) [10], the structure of which is shown in Fig. 1.1. Light emission follows upon the recombination of electrons and holes injected from electrodes in a diode structure. Since the demonstration of electroluminescence from PPV, many PPV-derivatives have been developed with the aim to improve the solubility in common solvents, the photostability, the conductivity etc., using the enormous toolbox provided by organic chemistry [21]. Moreover, the color of the light emission can be tuned by attaching various side-groups to the PPV-backbone, providing coverage of the visible spectrum ranging from green to red [22]. An interesting property of polymers is that they can be aligned by, e.g., stretching or rubbing techniques. Aligned polymers give rise to the emission of highly polarized light, which is useful for applications in liquid-crystal displays [23, 24].

On the road to a commercially viable polymer LED many hurdles had to be overcome. The most severe problem concerns the degradation in the presence of water and/or oxygen, especially in combination with radiation in the ultraviolet or blue spectral region. By encapsulating the polymer device, its performance has been improved considerably, although degradation remains a matter of concern.

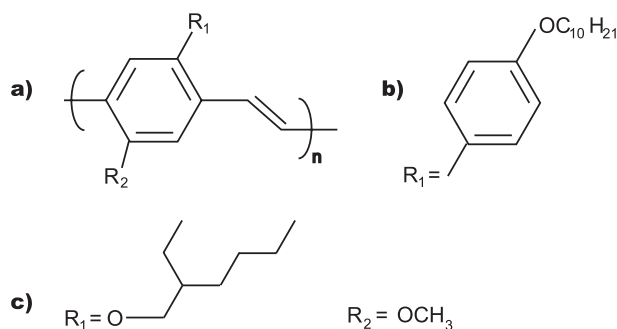


**Figure 1.1:** (a) Repeat unit of poly-(*p*-phenylene vinylene) (PPV), which emits in the yellow-green spectral region. A large variety of derivatives has been developed by adding sidegroups, e.g., at positions  $R_1$  and  $R_2$ . (b) Polymers having sidegroups like  $R_1$  have been used in part of the studies presented in this thesis (green emission). (c) Sidegroups of another derivative that has been studied in detail by many researchers: poly[2-(2'-ethylhexyloxy)-5-methoxy-1,4-phenylene vinylene] (MEH-PPV), showing orange-red emission.

Attention has also been paid to other difficulties, related to charge injection and transport, purity of the materials etc. A major challenge posed by polymer LEDs is the fact that charge transport and light emission have to be simultaneously optimized. One approach that has been popular for a number of years involves the use of material blends, with one component optimized for charge transport and the other for light emission [25, 26]. At this moment polymer LEDs are about to be produced on a commercial basis. Some prototypes of possible applications of conjugated polymers in electronics and displays are shown in Fig. 1.2.

The combination of luminescence and charge transport of conjugated polymers raises the question whether one can make a polymer injection laser in the spirit of a traditional semiconductor laser. This is not only interesting from a fundamental point of view, it is also of considerable industrial importance. Polymer lasers may be applied in, e.g., displays because of the spectral purity of laser emission. Below I will sketch the difficulties encountered when trying to make a laser based on a solid conjugated polymer film. So far an electrically pumped device has not yet been realized. The much more simple task of making an optically pumped laser based on conjugated polymers is addressed in part of the present thesis.



**Figure 1.2:** On the left: Flexible 6-inch polyimide foil with a variety of components and electronic test circuits. The circuits still operate when the foil is sharply bent. On the right: Example of a display based on polymer LEDs. Photos: Philips Research.

## 1.2 Photophysics of light-emitting polymers

The observation of electroluminescence from a light-emitting diode based on a conjugated polymer by the Cambridge group has led to a major worldwide research effort into the underlying mechanisms [10]. A large part of this effort concerns the charge injection into and transport through the light-emitting material and many device structures have been investigated. Another important issue concerns the origin of the light-emission process. Just as in a traditional LED the recombination of electrons and holes gives rise to luminescence. The photophysics however, is strongly affected by the presence of an electric field, giving rise to a reduced photoluminescence efficiency [27,28]. For all these reasons fundamental studies on the photophysics are nowadays almost exclusively performed using optical excitation.

An important characteristic of the most extensively studied light-emitting polymers is their solubility in common organic solvents (chlorobenzene, xylene, tetrahydrofuran, toluene, etc.). One can thus also study their photophysics in solution. In that state light-emitting polymers are considered to be very similar to traditional laser dyes. Indeed, when sufficiently diluted the photoluminescence (PL) quantum efficiency can be very high and the radiative lifetime is of order 1 ns, just as for a laser dye. This similarity has led to the widespread acceptance of a level scheme for a light-emitting polymer (in solution) that bears great similarity with that of common laser dyes (see Fig. 1.3). The electronic ground state  $S_0$  is con-

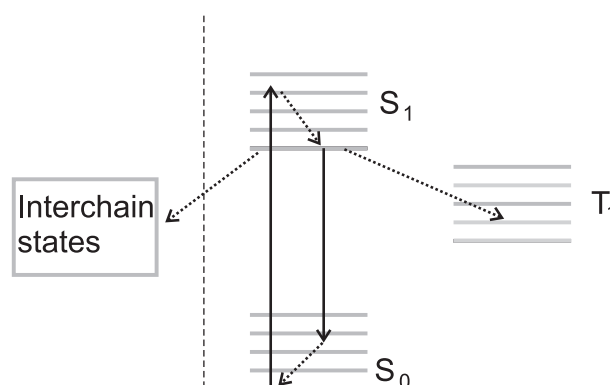


**Figure 1.3:** Level scheme of a conjugated polymer. For diluted systems interchain interactions are absent resulting in an energy scheme that is similar to a laser dye, as shown to the right of the dashed line. For a pure solid polymer film, interchain interactions must be taken into account. The exact nature of these interchain state is still heavily discussed.

nected to the first excited singlet state  $S_1$  by a dipole-allowed transition. In case of optical excitation the vibronic states of the  $S_1$  manifold are populated by the absorption of pump photons. Through fast relaxation the lowest vibronic level of the  $S_1$  state becomes populated. The latter may decay radiatively to a vibronic state within the  $S_0$  manifold, which very rapidly relaxes to the bottom of the electronic ground state. A competing process is intersystem crossing to the triplet state  $T_1$ .

In view of the above it is thus not surprising that it is quite simple to build a laser with a dissolved conjugated polymer as a gain medium, as first shown by Moses in 1992. Because of the intersystem crossing all studies of polymer-solution lasers have used a pulsed pump.

A very important difference between solutions of a laser dye and of a conjugated polymer appears when the solute concentration is increased. While the quantum efficiency of a laser dye collapses completely at concentrations of more than a few g/l, the conjugated polymers continue to readily photoluminesce up to the situation where all solvent has been removed. Thus *conjugated polymers also photoluminesce in the solid state*.

Usually, however, the PL quantum efficiency of the film is considerably lower than that of the solution. This is not surprising in view of the many additional (nonradiative) relaxation channels offered by the condensed system. Moreover, the PL *spectrum* of the film is, for most polymers, much less structured than that of the solution, and, sometimes considerably, red shifted.

Important insight into the photophysics of the film is obtained by studying the

decay of its PL as a function of emission wavelength (see also Chapter 7). In part of the spectrum, particularly in its red wing, the PL decay is slowed down relative to that of the dilute solution, in some cases by a considerable factor. It is logical to attribute the surprising features of the *film* PL to emission by interchain species, the latter being absent in a dilute solution. Nowadays, the commonly accepted view is that the slowly decaying red-shifted emission is caused by *excimers* [29, 30], that have become populated through an energy-transfer process. These excimers, being interchain states, are commonly believed to have reduced oscillator strength. This is consistent with the observation that the quantum efficiency of the film is usually reduced as compared to the dilute solution.

The picture of the PL from the film that arises involves the following features:

1. Absorption of a pump photon followed by rapid relaxation to a Coulomb-bound electron hole pair (singlet exciton) localized on a conjugated segment.
2. Rapid intrachain excitation transfer to conjugated segments of lower energy, mediated by dipole-dipole interactions.
3. Excitation transfer to weakly emissive excimers or aggregates.
4. Radiative and nonradiative decay of the weakly emitting species.

Obviously, at any moment the exciton can simply photoluminesce or be nonradiatively quenched.

The real picture is more complicated since some of the primary exciton states may not be depleted by dipole-dipole induced excitation transfer. Experimental data indicating that this may well be the case are presented in Chapter 7. All the aspects discussed here obviously have an important effect on the optical gain that can be reached in conjugated polymer films.

### 1.3 Gain in light-emitting polymer films

Net gain is required in order to make a laser, at least for the time that is needed for the generation of the stimulated output. Pump-probe spectroscopy is a powerful tool for measuring the optically induced gain (and loss) in a system. Here the polymer medium is excited with a femtosecond optical pump pulse, allowing high excitation densities to be reached. The resulting change in optical transmission ( $\Delta T/T$ ) is then measured, by probing the excited region with a very weak, ultra-short and spectrally broad probe pulse. One then measures, spectrally resolved, the gain ( $\Delta T/T > 0$ ) and photoinduced absorption ( $\Delta T/T < 0$ ) as a function of

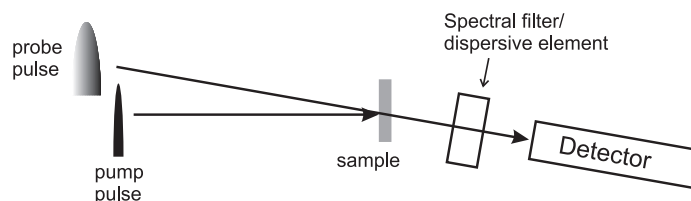


**Figure 1.4:** Pump-probe setup for measuring the optically induced change in transmission ( $\Delta T/T$ ). The sample is excited with an ultrashort pump pulse (usually of the order of 100 fs) and is subsequently probed with another ultrashort white-light pulse (the probe pulse). By scanning the delay between the pulses  $\Delta T/T$  is measured as a function of time. Using narrowband filters or dispersive elements the spectral dependence of  $\Delta T/T$  is explored.

the pump-probe delay. A schematic picture of a pump-probe setup is shown in Fig. 1.4.

The very first pump-probe studies of solid polymer films indicated that there was no gain at all [31]. In other studies net gain was demonstrated, the gain decaying on a time scale varying from a few to  $\approx 100$  ps, depending on the polymer [32, 33]. However, even for the same polymer material very different gain lifetimes have been reported [31, 34]. An important contribution to the explanation to this controversial results was made by the Cambridge group that showed that the optical gain lives shorter when a film has been subject to photo-oxidation [35]. The decay times in the films should be compared to those for conjugated polymers in solution. The latter are comparable to the photoluminescence lifetime, i.e., of order 1 ns [31, 36]. It is logical to attribute the reduction in gain lifetime associated with the transition from solution to solid film to the interchain effects mentioned in the previous section. For instance, if the excitons provide optical gain and the interchain species do not, one can associate the fast decay of the gain to the energy transfer from the excitons to the interchain species. This picture is supported by wavelength-dependent measurements of the transient gain. Transient gain is observed at short wavelength (where the excitons emit) while at longer wavelength (where the excimers emit) one observes photo-induced absorption.

As extensively discussed in a recent paper by Nguyen *et al*, the lifetime of the gain strongly depends on the morphology and quality of the films [37]. This is due to the fact that the amount of interchain interactions heavily depends on the way a particular polymer film is prepared [37]. For instance, the extent of aggregate formation has been observed to depend strongly on the solvent from which the film is cast, on the concentration of the original polymer solution, on the rotation speed during spin-coating etc. Even the excitation intensity at which

photochemical damage occurs appears to depend on the film morphology [37]. Such damage reduces the PL quantum efficiency of the film and leads to additional absorption features [36]. The importance of film morphology for the photophysics lies at the origin of much of the disagreement between experimental results of different groups since different film preparation techniques have been used.

## 1.4 Optically pumped polymer lasers

Notwithstanding the considerable progress recently made, the photophysics in pure solid films of conjugated polymers is still not fully understood. In contrast, as discussed earlier, the photophysics in solution is very similar to that of a dye, although there are some important differences. Some of these differences are studied in the present thesis, in particular how they affect the properties of a liquid polymer laser (Chapter 4). A first demonstration of lasing from a conjugated polymer was given by Moses [38]. As gain medium he used a solution of poly(2-methoxy-5-(2'-ethylhexyloxy)-1,4-PPV (MEH-PPV see Fig. 1.1) in xylene, in a configuration very similar to that of a dye laser. Other reports on lasing and amplified spontaneous emission from polymer solutions followed soon thereafter [39–42].

Laser emission from a conjugated polymer film has been demonstrated for a small set of materials in various geometries. In all cases the system was optically pumped by a pulsed laser. In 1996 the observation of laser emission by a microcavity filled with a thin film of PPV, was reported [43]. Subsequently, lasing from various PPV derivatives has been studied, using several optical feedback structures. These include planar [44, 45] and cylindrical microcavities [46, 47], microdisks, and distributed feedback (DFB) structures [48–50] (see Fig. 1.5). In some devices blends of polymers have been used, consisting of a host material to absorb the pump light, and a small amount of guest material, that becomes excited via energy transfer from host to guest (Förster transfer) [51]. Due to reduced interactions between the guest polymer chains, longer gain lifetimes and less absorption are expected, leading to lower laser thresholds [52, 53]. The subject of optically pumped polymer lasers has recently been reviewed in a number of papers [54–58].

## 1.5 This thesis

In this thesis a study of the dynamics of polymer lasers and light-emitting polymers is presented. Throughout the thesis the polymers are excited optically using

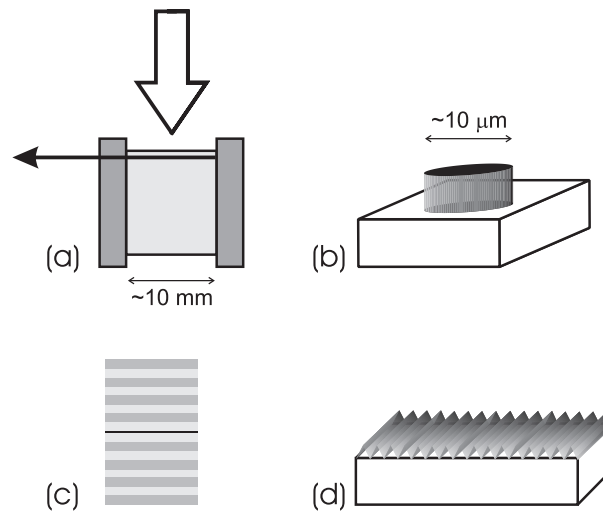


**Figure 1.5:** Several configurations of lasers based on conjugated polymers. (a) A transversally pumped cuvette, containing a polymer solution, positioned between two mirrors. (b) A microdisk laser. Feedback is provided by total internal reflection (giving rise to whispering gallery modes). (c) A planar microcavity with highly reflecting mirrors, the cavity length being of the order of a wavelength. The polymer is situated in the middle (black region). (d) A distributed feedback laser. The light is waveguided in the polymer film and optical feedback is provided by the spatial variation of the effective refractive index, having a periode of the order of a wavelength.

femtosecond pump pulses, which allows measurements on the dynamics of the polymer lasers and the light-emitting polymers with high temporal resolution.

The study of polymer lasers is performed on a polymer solution that exhibits high gain. It focusses on the laser dynamics resulting from the ultrafast excitation of the gain medium. Due to the ultrashort pump pulse the gain in the laser is turned on ‘instantaneously’ (often referred to as gain-switching), giving rise to interesting and transparent laser dynamics. Various laser configurations have been studied, all having relatively short cavity lengths, ranging from  $\approx 20 \mu\text{m}$  to 25 mm.

In Chapters 2 and 3 it is shown that a polymer laser with an inhomogeneous distribution of the gain along the axis of the cavity, emits an extended train of pulses upon excitation with a single, ultrashort pump pulse. Chapter 2 focusses on the input-output curves and the output dynamics for various cavity configurations, showing that a liquid polymer laser greatly resembles a dye laser. Chapter 3 focusses on the origin of the pulse train emitted by the polymer laser, although it is excited with a single pump pulse. It is shown that the large single-pass gain

and the rather unusual combination of time scales involved lie at the basis of the formation of the pulse train.

Although a solution of a conventional laser dye and of a light-emitting polymer are very similar, there are noticeable differences. An example is given in Chapter 4, in which the effect of the pump polarization on the laser threshold is studied in a transverse pumping geometry. It is shown that the threshold of the polymer laser strongly depends on the polarization of the pump light, which is not the case for the dye laser. The physical background of this effect lies in the very different memory times of the emitters for the polarization of the pump light. The polymer solution shows a very long memory for the polarization of the pump, which is associated with the very slow reorientation of the rigid polymer chains.

The long memory for the pump polarization in case of a dissolved polymer is exploited in Chapter 5. In that chapter a longitudinally pumped polymer micro-laser is studied by exciting it with two mutually delayed, ultrashort pulses, that are orthogonally polarized. The laser output in both polarization modes strongly depends on the interpulse delay, providing insight into the dynamics of the micro-laser and the coupling between the two polarization modes.

In Chapters 6 and 7 stimulated and spontaneous emission from a thin solid film of a conjugated polymer is studied. Chapter 6 provides a novel method for measuring the gain lifetime, which is much simpler than the conventional pump-probe technique. The method is based on double-pulse excitation of a polymer waveguide. As already discussed, the lifetime of the gain is an important parameter in the search for suitable light-emitting polymers for laser applications.

Some more insight into the photophysics in the polymer film is provided in Chapter 7, presenting a study on the dynamics and the polarization anisotropy of the photoluminescence. A polymer solution and a thin solid film are compared, showing very different behavior. Strong interchain interactions are considered to be responsible for the different photophysics.

The polymers under study are phenyl-substituted PPVs, which have been developed for applications in polymer LEDs. These materials have a high photoluminescence efficiency, both in solution and in the solid state, and are suitable for electrical pumping as well. The polymer of Chapter 7 has for a while been applied in the preproduction of commercial polymer LEDs.

Since all chapters have been written to be published as separate papers it is possible to read each chapter individually. As an unavoidable consequence there is some overlap between the various chapters.

## Chapter 2

---

# From amplified spontaneous emission to laser oscillation; Dynamics in a short-cavity polymer laser <sup>1</sup>

We present an experimental study of the input-output characteristics of an ultra-short pumped  $\pi$ -conjugated polymer in solution. By comparing the results for configurations with zero, one and two mirrors around the polymer we show that the physics is driven by amplified spontaneous emission and not by cooperative emission. This is substantiated by ps-timescale measurements of the evolution of the emission of the polymer. For the two-mirror configuration a sharply defined threshold for laser oscillation is found; the output of the laser exhibits strong pulsations.

Conjugated polymers have recently attracted widespread attention as a promising gain medium for laser applications. The most extensively studied materials are (derivatives of) poly(*p*-phenylene-vinylene) (PPV). When optically pumped these materials can be quite easily made to lase both in a dilute solution [38, 39, 41] and in a neat thin film [43, 59].

In almost all studies of lasing in conjugated polymers the device is characterized by measuring the input-output curve. An upward kink in this curve is then associated with the threshold for laser action. Alternatively, the *spectrum* of the emitted light is measured at various values of the pump intensity. The laser is said to pass through threshold when this spectrum becomes considerably narrowed. This approach is not without ambiguity since amplified spontaneous emission (ASE) also gives rise to spectral narrowing; equally an ASE device can exhibit input-output characteristics that are similar to that of a proper laser [60].

Although time-domain studies of the transient gain in an optically pumped polymer abound [61, 62], little attention has so far been paid to the temporal characteristics of the output from an optically pumped polymer device. This is surprising since it is most unlikely that the output of a polymer laser is transform-limited.

---

<sup>1</sup>S. A. van den Berg, R. H. van Schoonderwoerd den Bezemer, H. F. M. Schoo, G. W. 't Hooft, and E. R. Eliel. *Opt. Lett.* **24** 1847 (1999).

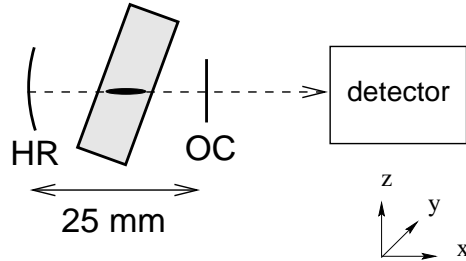


**Figure 2.1:** Schematic of the experimental setup. The shaded area represents the dye cell with the excitation region indicated by the thick line. The laser cavity is formed by the concave high reflector (HR,  $R=50$  mm) and flat output coupler (OC). To avoid optical feedback from the walls of the dye cell the latter is slightly tilted

In addition, time-domain studies are particularly suited to show whether cooperative phenomena like superfluorescence are important in polymer systems as has been suggested in a number of papers [42,63,64]. In this chapter we report on detailed measurements of input-output curves and time-domain studies of optically pumped polymer devices, thereby establishing the role of ASE, and exploring the boundary between ASE and laser oscillation.

As a gain medium we use a copolymer of PPV-derivatives which absorbs in the near UV, emits in the green (photoluminescence maximum at  $\lambda = 530$  nm) and exhibits high photoluminescent efficiency ( $> 60\%$ ) [65]. The polymer is dissolved in chlorobenzene (0.2% by weight) and continuously flows through a dye cell. It is transversally pumped in a pencil-shaped volume ( $7 \times 0.05 \times 0.05$  mm) with Fresnel number  $\approx 1$ , by an  $\approx 130$  fs long pump pulse at  $\lambda = 400$  nm. Our interest lies in the light emitted along the axis of the pencil ( $x$ -direction in Fig. 2.1). In the absence of optical feedback this light travels through the cell in a single pass, both in the positive and negative  $x$ -direction. By inserting a single mirror (99% reflectivity, concave) the light travelling in the negative  $x$ -direction is redirected through the region of excitation yielding a double-pass device. With an output coupler (10% transmission) on the opposite side of the polymer medium a laser resonator is formed. Our study of ASE and laser oscillation is based on a comparison of these three configurations.

In the experiment we measure the input and output energies of the mirrorless, single-mirror and full-resonator configurations using photodiodes (response time approximately 100 ns). Care is taken that the characteristics of the pump, such as pulse duration and polarization (parallel to  $z$ -axis) remain constant during the series of measurements, and that the output radiation is always collected within the

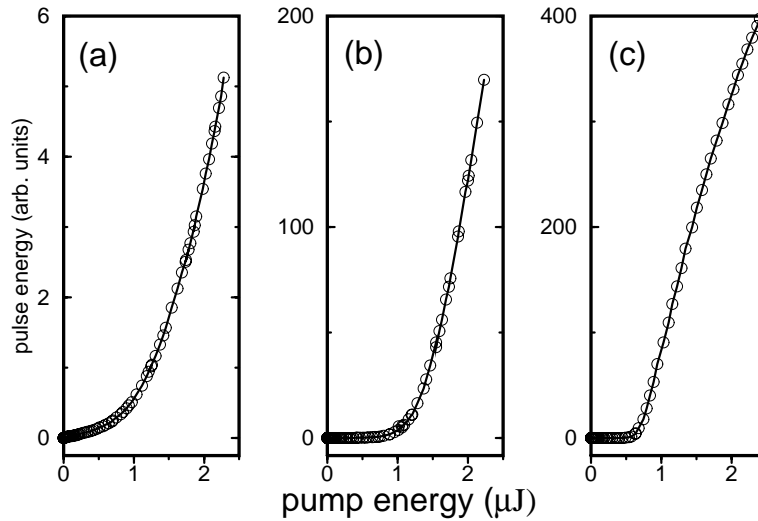


**Figure 2.2:** Light output versus pump energy for the mirrorless (a), single-mirror (b), and full-cavity (c), setup. Note the quantitative differences of the signal for the three configurations.

same solid angle ( $4 \times 10^{-3} \pi$  sr). The latter corresponds to the emission angle of the full resonator at high pump energy. The results are presented in Fig. 2.2. The curve for the full resonator (right frame) exhibits the characteristics of a laser: a well-defined polarization ( $> 99 : 1$ , parallel to pump polarization) and a well-defined threshold at  $0.6 \mu\text{J}$  pump energy with a vastly different efficiency below and above threshold. The curvature of the input-output curve at high pump energy indicates the onset of saturation of the inversion. The single-mirror results (middle frame) have some of the same flavor but a sharp threshold is not found. This applies even more to the mirrorless case (frame at left) where nothing like a threshold appears. Yet in all cases the dependence between output and pump energy is highly nonlinear.

The results of Fig. 2.2 can easily be understood in terms of a system that starts up from spontaneous emission and exhibits optical gain (at sufficiently high pump energy). The keywords that apply to Figs. 2.2a and 2.2b are therefore amplified spontaneous emission and mirrorless lasing [60]. Strong support for this point of view comes from the time-domain studies that are presented below.

In our experiment the polymer is pumped by a pulse that is substantially shorter than either its spontaneous lifetime or the relevant transit time through the excited volume. Consequently the inversion is generated instantaneously at time  $t = 0$  and the inversion and photon densities evolve completely freely. The evolution of the

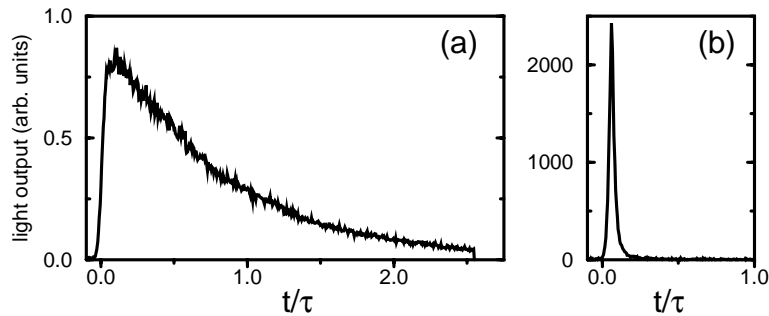


**Figure 2.3:** Temporal evolution of the light output for the single-pass setup upon pumping with an ultra-short excitation pulse. The time axis is normalized to the spontaneous-emission lifetime (0.86 ns). (a) Very low pump energy. (b) At high pump energy ( $2\mu\text{J}$ ) a pulse of  $\approx 20$  ps duration is emitted; the height of this pulse is  $\approx 2500$  times stronger than that of frame (a).

latter is studied by recording the light output of the polymer using a streak camera with a time resolution of approximately 10 ps. The results for the mirrorless (single-pass) configuration are shown in Fig. 2.3 for very low (left frame) and high (right frame) excitation densities. At low pump energy the emission decays exponentially, the decay time representing the fluorescence lifetime (0.86 ns). In contrast, at high pump energy ( $2\mu\text{J}$ ), one observes highly nonexponential decay; actually a pulse is emitted with a width of approximately 20 ps. This pulse appears at a well-defined and reproducible time after excitation. Therefore, this pulse can not originate from superfluorescence since, in that case, the pulse delay should exhibit appreciable jitter reflecting the quantum fluctuations in the system [66].

The formation of such a short pulse can be explained as follows: As a result of spontaneous emission the excited polymer starts to emit light at  $t = 0$ . The light is amplified by stimulated emission as it travels through the inverted volume. The largest gain is experienced by the on-axis radiation originating at the far side of this volume and emitted at  $t = 0$ ; the emission is at its peak when this light leaves the gain volume. Subsequently, the light output decreases because the inversion and thus the amplification decay. In the limit that the inversion decays by spontaneous emission only the output is proportional to  $[\exp(g_0 \exp(-t/\tau)) - 1]$  with  $\tau$  the spontaneous-emission lifetime. The initial amplification  $g_0$  is simply given by  $g_0 = \sigma l N(0)$ , where  $\sigma$ ,  $l$  and  $N(0)$  represent the stimulated-emission cross section, the length of the gain medium and the inversion at  $t = 0$ , respectively. Here we have neglected the transit time through the pumped volume ( $\approx 40$  ps) since it is much shorter than the decay time  $\tau$  of the inversion ( $\approx 860$  ps). For large values of  $g_0$  the output changes very rapidly even for  $t \ll \tau$ . In this high-gain limit the

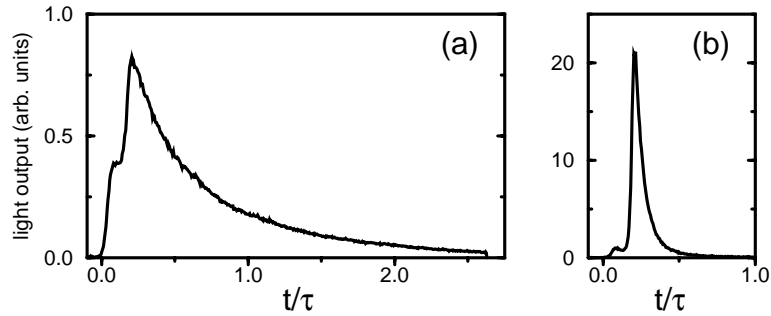


**Figure 2.4:** Dynamics for the double-pass configuration. (a) Low pump energy ( $0.4 \mu\text{J}$ ). (b) Higher pump energy ( $0.8 \mu\text{J}$ ). In both cases the first and second peak represent light that makes a single pass and a double pass through the gain medium, respectively.

half-life of the emission can be estimated as  $t_{1/2}/\tau = \ln 2/g_0$ . Assuming the decay time to be equal to half the pulse width, we estimate  $g_0$  to be roughly 50 for an output pulse of width 20 ps. If gain depletion by stimulated emission becomes important the collapse of the output will be even faster and the gain-transit time comes into play. This simple picture of pulse formation is supported by solving the laser rate equations for this system (in analogy to e.g. Ref. [67]).

The single-pass amplification can be characterized by putting a mirror right behind the dye cell, thereby redirecting the backward travelling light through the excited medium. Relative to the light that makes a single pass the light that double passes the gain medium then arrives at the camera with a slight delay, in our case of about 85 ps (see Fig. 2.4). Comparing the amplitudes of the two signals yields the single-pass amplification. For low excitation densities there is very little amplification since the retro-reflected signal is equal to the original signal: the signals simply add up (Fig. 2.4, left frame). However if the gain medium is strongly pumped the double-pass signal becomes very large compared to that of the direct output thus elegantly demonstrating the existence of gain in the system (right frame of Fig. 2.4). Here the pump energy is chosen in such a way that both signals can easily be seen. At even higher pump energies, of order  $1.5 \mu\text{J}$ , the second pulse is approximately 70 times larger than the first one. For this value of the pump energy stimulated emission dominates, both in the first and second pass. It is the stimulated emission in the second pass that provides this device with the large output as seen in the input-output characteristic of Fig. 2.2 and lies at the origin of the differences between Figs. 2.2a and 2.2b. Note that the value of 70 for the amplification represents a lower bound since there are appreciable Fresnel and diffraction losses associated with coupling the light in and out of

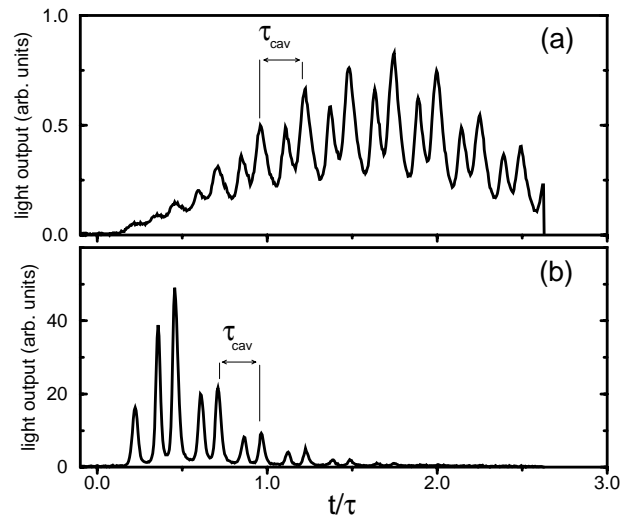


**Figure 2.5:** Dynamics of the laser just below (a) and far above threshold (b). The output of the laser consists of two interleaved pulse trains representing light circulating in opposite directions through the cavity. The cavity round-trip time  $\tau_{\text{cav}} \approx 200$  ps is indicated.

the dye cell. The fact that in the second pass the gain coefficient is still large shows that the inversion is at most marginally depleted during the first pass. This provides additional evidence that cooperative emission does not lie at the origin of the phenomenon observed here.

For the full-resonator configuration the light that propagates along the cavity axis will initially evolve exactly in the same way as described above. Now both the high reflector and the output coupler redirect a large fraction of the emitted radiation back into the gain medium. Figure 2.5 shows the experimental results just below threshold (top frame) and far above threshold (bottom frame). Close to threshold the power builds up slowly, initially mainly due to spontaneous emission. Stimulated emission becomes important and pulsations appear when the intracavity photon density has grown sufficiently. In the present case this happens after  $\approx 3$  round trips. After several additional round trips the gain becomes smaller than the losses since the inversion is being reduced continuously; after roughly 1.5 ns the intracavity flux simply dies away. Far above threshold the stimulated emission is already important from the start (see Fig.2.5b) and a very pronounced pulse structure develops almost immediately. Maximum output is reached in only a few round trips, much fewer than in the case of a weak pump. This shows that the inversion is now depleted by stimulated emission. The results of Fig. 2.5a ele-

gantly illustrate the advantages of having optical feedback: In the absence of such feedback there is insufficient time (or gain length) for the stimulated emission to start up at low pump energies.

The time-domain results shown above provide strong confirmation of our interpretation of the input-output characteristics of the polymer material in the three configurations studied. For the mirrorless and single-mirror configurations amplified spontaneous emission - and not superfluorescence - is the driving mechanism resulting in short pulses at high pump energy. For the full-cavity configuration lasing is observed above a sharp, well-defined threshold. Pulsations appear in the output of the laser as result of the gain being large and inhomogeneously distributed over the cavity. In the next chapter the origin of the pulse-train formation is thoroughly investigated.



## Chapter 3

---

### **Pulse-train formation in a gain-switched polymer laser resulting from spatial gain inhomogeneity<sup>1</sup>**

We present an experimental study of the dynamics of a polymer laser upon excitation with an ultrashort pump pulse. The laser is unusual in the sense that the cavity length is such that the cavity round-trip time is intermediate between the duration of the pump pulse and the spontaneous-emission time of the gain medium. The cavity is only partly filled with gain medium. The unusual timescales in combination with the spatial gain distribution result in the emission of a neat and regular train of short pulses. Its generation can be viewed as a special case of gain switching. A one-dimensional rate-equation model that takes the nonuniformity of the gain explicitly into account is presented. The model describes both the evolution of the inversion, which is also measured experimentally, and the dynamics of the output in great detail and yields excellent agreement with the experimental results. A heuristic description of the arisal of the pulse train in terms of amplified spontaneous emission and gain depletion is given.

#### **3.1 Introduction**

Gain switching is a well-known technique for short-pulse generation, and has been applied to a wide variety of laser systems like semiconductor lasers [68, 69], Ti:Sapphire lasers [70–72] and gas lasers [73]. It is accomplished by modulating the pump on a time scale short compared to the spontaneous-emission lifetime of the upper laser level. The ensuing time-varying gain then gives rise to the production of a laser pulse that is much shorter than the spontaneous-emission lifetime, and, in some cases, even substantially shorter than the pump pulse. Synchronous pumping can be viewed as an extension of gain switching. Here the gain medium is excited repetitively, with the excitation rate synchronized to the cavity length.

---

<sup>1</sup>S. A. van den Berg, G. W. 't Hooft, and E. R. Eliel. Phys. Rev. A **63** 063809 (2001).

Due to this repetitive gain switching mode-locking is achieved and a stable train of short pulses, considerably shorter than the pump pulses, is emitted [74, 75].

Here we study the dynamics of the light emitted by a short-cavity polymer laser that is pumped by a single ultrashort pulse. The cavity dimensions of this laser are such that the cavity round-trip time is intermediate between the duration of the pump pulse and the spontaneous-emission time of the gain medium. Additionally, the gain medium only partly fills the cavity. Such a laser shows interesting dynamics [76]. Because of the short duration of the pump pulse the dynamics can be transparently analyzed. The pump pulse is so short that the laser evolves completely freely and gain switching provides a proper framework for a description of its dynamics.

In contrast to most gain-switched systems our short-cavity polymer laser does not emit a single short pulse. Rather it emits a neat and regular train of short pulses; we attribute this to a combination of the unusually ordered timescales and the inhomogeneous distribution of the gain along the cavity axis. Since gain switching still provides a useful framework for the understanding of the phenomena we interpret the pulse train as a result of multiple gain switching.

In this chapter we show the results of an experimental study of the pulse evolution and the dynamics of the population of the upper laser level from the very start, both below and above the laser threshold. Due to the convenient choice of cavity round-trip time we are able to record various aspects of this pulse train, such as the rise and decay time of the individual pulses and the evolution of the train in great detail. We notice that the pulse repetition rate is given by twice the longitudinal mode spacing and that the pulse train shows odd-even staggering. All results are explained with help of a ‘local’ rate-equation model, i.e., a model where the spatial distribution of gain and loss is explicitly taken into account. The rate equations are solved numerically.

## 3.2 Experimental setup

In the experiment we employ a 25 mm long cavity consisting of a concave high reflector (50 mm radius of curvature) and a flat output coupler ( $T_{OC} = 10\%$ ). Approximately at its center sits a dye cell through which the polymer solution flows continuously (see Fig. 3.1). The cell is slightly tilted ( $\approx 10^\circ$ ) relative to the cavity axis in order to avoid optical feedback from its walls. As gain medium we use a 0.2% by weight solution of a copolymer of poly(*p*-phenylene vinylene)-derivatives in chlorobenzene. PPV is a popular and well-known light-emitting polymer and laser action in PPV and its derivatives has been observed both in solution and in solid state [38, 43, 55, 56]. Details on the materials used in our

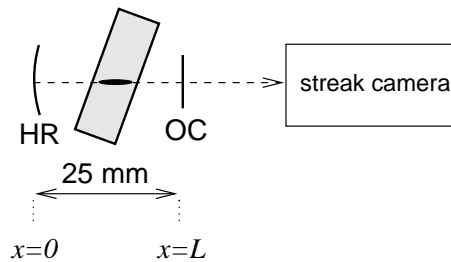


**Figure 3.1:** Schematic of the experimental setup: The shaded area represents the dye cell, with the excitation region indicated by the oval. To avoid optical feedback from the walls of the dye cell the latter is slightly tilted.

studies have been published in Ref. [65]. The radiative lifetime of this material in solution is 0.86 ns; its absorption and emission spectra are shown in Fig. 3.2, where also the polymer repeat units are shown.

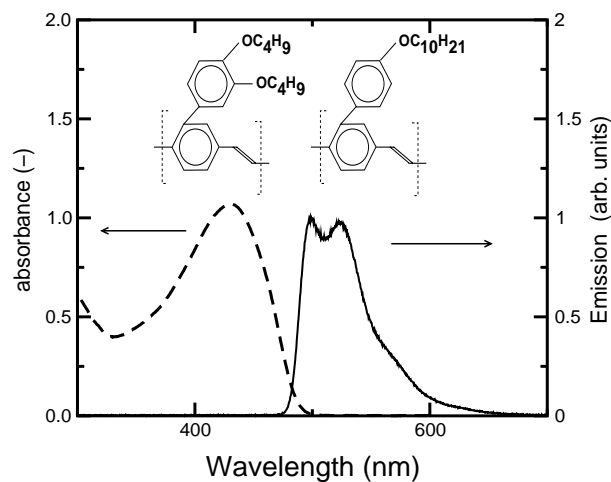


**Figure 3.2:** Absorption and emission spectra of the dissolved copolymer. The two repeat units are shown with the spectra.

The polymer laser is side-pumped with 130 fs pulses at  $\lambda = 400$  nm with a repetition rate of 1 kHz. The pump pulses are generated with a Ti:Sapphire regenerative amplifier system (Spectra Physics, Spitfire), seeded by a Ti:Sapphire oscillator (KM-labs). The 800 nm output of the Ti:Sapphire laser system is frequency doubled in  $\beta$ -barium borate (BBO). The blue pump light is focussed into a pencil-shaped volume ( $\approx 7$  mm  $\times$  0.05 mm  $\times$  0.05 mm) inside the polymer solu-

tion, the transverse dimension of the volume being of the same order as that of the fundamental mode of the laser resonator. The polarization of the pump is perpendicular to the cavity axis. Above threshold the laser emits light in a narrow band ( $\Delta\lambda \approx 12$  nm) centered at  $\lambda = 530$  nm. We simultaneously measure the dynamics of the light emitted into lasing, and into nonlasing modes, i.e. in a sideways direction. The latter provides us with a measure of the evolution of the population of the upper laser level [77–79]. In all experiments on the laser dynamics we employ a streak camera (Hamamatsu, C1587) providing us with a temporal resolution of approximately 10 ps.

### 3.3 Experimental results

For a range of pump-pulse energies, from slightly below to far above threshold, we have measured the temporal evolution of the light emitted by the polymer laser upon excitation by a *single* ultrashort pulse. These pump energies are indicated on the input-output curve that is presented in Fig. 3.3.

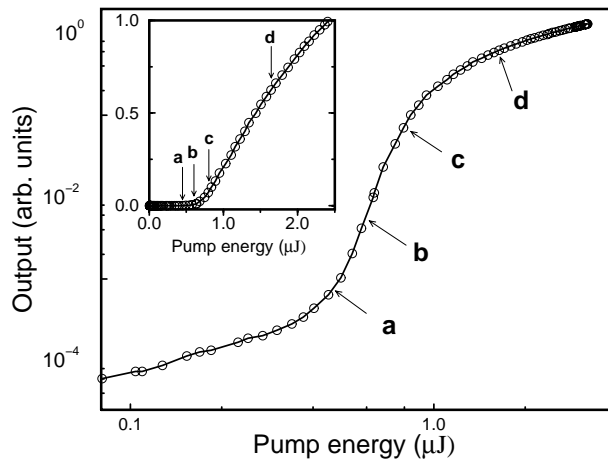


**Figure 3.3:** Input-output curve of the polymer laser. The time-integrated light output as measured within a small solid angle, is plotted versus pump energy on a double-logarithmic scale. In the inset the same curve is plotted on a linear scale. The pump energies at which our measurements have been performed are indicated.

As shown by Fig. 3.4 a stable pulse train develops for all values of the pump <sup>2</sup>. On the scale shown here, the pump pulse (at  $t = 0$ ) is infinitely short. Figure 3.4a

<sup>2</sup>To obtain a good signal-to-noise ratio we average the signal over several seconds. As a check we compare these results with single-shot measurements and find no significant differences.

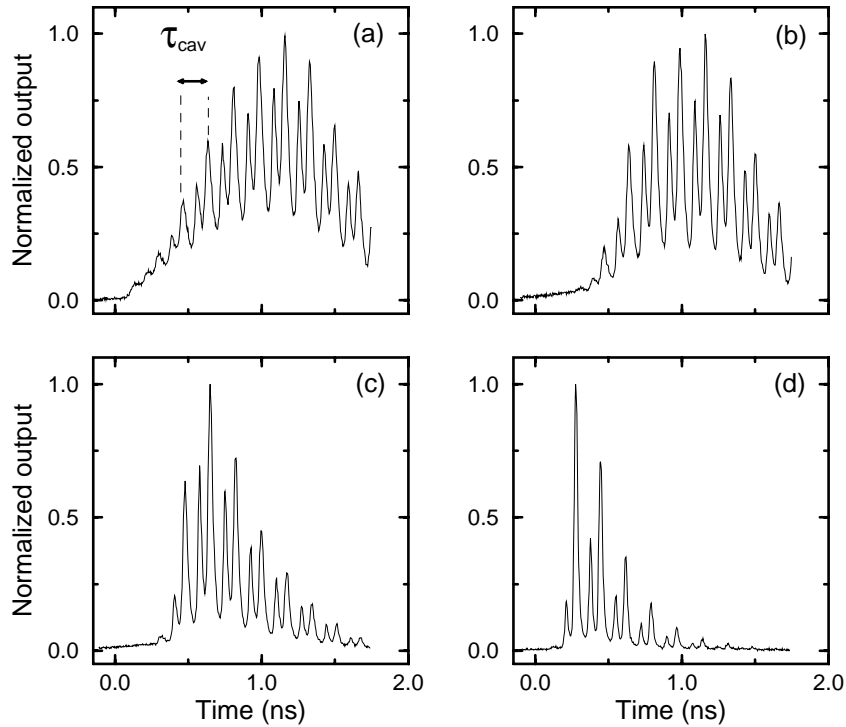


**Figure 3.4:** Temporal dynamics of the polymer laser output for pump energies ranging from below threshold to far above threshold, as indicated in Fig. 3.3. Pump parameters:  $r = 0.77$ ,  $r = 1$ ,  $r = 1.3$ ,  $r = 2.8$ , for graphs (a)-(d), respectively. The pump parameter is defined as the pump energy normalized to the experimentally determined threshold value of the pump energy.

shows the output just below threshold: initially the output grows rather smoothly but pulsations start to appear after a few cavity round trips. The output keeps growing while the modulation depth increases and the pulses become narrower. The pulse-train envelope shows a maximum after  $\approx 1.1$  ns. As indicated in the figure two pulses are emitted within one cavity round-trip time, i.e. the laser emits two interleaved pulse trains. It is observed that the envelopes of both pulse trains are quite different, in other words: the laser output exhibits odd-even staggering. These points will be discussed in more detail later in this chapter.

The other frames of Fig. 3.4, containing the results for higher and higher pump energies, show a basically similar behavior, although the initial growth of the signal is less easily observed. The pulse structure, however, is much more fully developed, i.e., the modulation depth is substantially larger. Overall one notices

that further above threshold the highest peak occurs earlier and earlier. Below we will show that this is caused by gain depletion.

Figure 3.5 shows the evolution of the sideways emitted photoluminescence for the same values of the pump strengths as in Fig. 3.4. Curve (a) shows the

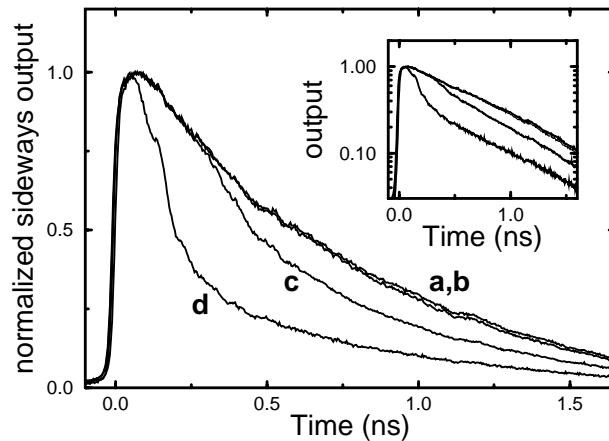


**Figure 3.5:** Population decay, measured by means of sideways emitted light. The indices a-d correspond to the pump energies indicated in Figs. 3.3 and 3.4. The inset shows the results on a logarithmic scale.

results for the case where the laser is operated below threshold. As can be seen from the straight line in the inset, where the curves are plotted on a logarithmic scale, the population decays exponentially in this case. The slope of this line yields the photoluminescence lifetime of the material. Curves (b) through (d) show the dynamics of the upper-laser level population for pump strengths ranging from slightly above to approximately 3 times threshold, i.e. through the range where gain depletion becomes important. This is best illustrated in curve (c): initially, the population of the upper laser level decays by spontaneous emission only. However, the intracavity intensity grows and after approximately 0.3 ns stimulated emission leads to substantial depletion of the inversion. In curve (d) the gain depletion sets in almost immediately; here the population of the upper laser level is seen to decrease in a stepwise fashion. These steps are correlated with the transit of the optical pulses through the gain medium.

### 3.4 Rate equations

As a laser material a dissolved light-emitting polymer shows very similar behavior to that of a laser dye in solution [38, 55, 56]. We therefore assume the gain to be homogeneously broadened, the intraband relaxation to be very rapid and the lower laser level to be empty [67]. Hence the inversion is given by the population of the upper laser level. We thus model our laser as a homogeneously broadened ideal four-level laser [56]. Furthermore we use a one-dimensional description where we separate the intracavity photon density in two fluxes that travel in opposite directions through the cavity. This approach has been fruitfully applied to other systems where the gain and/or loss are inhomogeneously distributed [80, 81]. Examples are systems based on travelling-wave amplified spontaneous emission [67, 82–84] and semiconductor lasers where the spontaneous-emission noise is described in such terms [85].

For the evolution of the inversion density  $N(x, t)$  and for the left- and right-travelling photon densities ( $n^-(x, t)$  and  $n^+(x, t)$ , respectively) we write the following rate equations (in analogy with Ref. [67]):

$$\begin{aligned} \frac{\partial N(x, t)}{\partial t} &= -\gamma N(x, t) - c \sigma \eta N(x, t)(n^+(x, t) + n^-(x, t)), \\ \frac{\partial n^+(x, t)}{\partial x} + \frac{\eta}{c} \cdot \frac{\partial n^+(x, t)}{\partial t} &= \sigma N(x, t) n^+(x, t) + \frac{\gamma \beta \eta}{c} N(x, t), \\ -\frac{\partial n^-(x, t)}{\partial x} + \frac{\eta}{c} \cdot \frac{\partial n^-(x, t)}{\partial t} &= \sigma N(x, t) n^-(x, t) + \frac{\gamma \beta \eta}{c} N(x, t). \end{aligned} \quad (3.1)$$

These rate equations are defined on the interval  $x = 0$  through  $L$ , where  $L$  is the length of the cavity. In Eq. (3.1),  $\gamma$  is the spontaneous-emission rate,  $\sigma$  denotes the stimulated-emission cross section,  $\eta$  the refractive index of the polymer solution,  $c$  the speed of light in vacuum, and  $\beta$  the fraction of spontaneous photons emitted in the lasing mode. Note that Eq. (3.1) does not contain the usual pump term. The pump pulse is so short in comparison to all other relevant time scales that its effect is well represented by setting the value of the inversion density distribution  $N(x, 0)$  at  $t = 0$ . Also, again in contrast to common practice, our rate equations do not include a term describing the cavity losses. In our laser the dominant losses are not homogeneously distributed over the cavity, as is usually assumed, rather they are localized at the output coupler and at the windows of the flow cell. The localized losses are taken into account via the conditions by which the left- and right-travelling photon densities are coupled at the cavity mirrors:

$$n^+(0,t) = T_{\text{cell}}^2 \cdot n^-(0,t), \quad (3.2)$$

$$n^-(L,t) = R_{\text{OC}} \cdot T_{\text{cell}}^2 \cdot n^+(L,t). \quad (3.3)$$

Here  $L = 25$  mm represents the distance between the mirrors,  $R_{\text{OC}} = 0.9$  the power reflection coefficient of the output coupler (for the high reflector we assume  $R_{\text{HR}} = 1$ ), while  $T_{\text{cell}} \approx 0.85$  is the power transmission coefficient of a single window of the flow cell. This number is rather low because of diffraction losses at the edges of the flow cell.

We numerically solve the set of coupled rate equations presented in Eq. (3.1), combined with the coupling relations of Eqs. (3.2) and (3.3). As initial conditions we take  $n^\pm(x,0) = 0$  and  $N(x,0) = N_0 \exp(-(x-x_0)^2/w^2)$ . As indicated, the initial inversion is assumed to have a Gaussian distribution (since the gain medium is transversely pumped) with a full width at half maximum equal to about  $\frac{1}{3}$  of the cavity length ( $w = L/6\sqrt{\ln 2}$ ). We position the gain medium close to the center of the cavity ( $x_0 \approx L/2$ ). For our simulation we use the following values for the numerical coefficients:  $\gamma = 1.5 \times 10^9 \text{ s}^{-1}$ ,  $\eta = 1.5$ ,  $c = 3 \cdot 10^8 \text{ m/s}$ ,  $\sigma = 10^{-16} \text{ cm}^2$  (order of magnitude of conventional laser dye) and  $\beta = 10^{-6}$ . To solve the rate equations we use an Euler-type method, dividing the cavity in small steps, and approximating the differentials by finite steps ( $\Delta x = L/100$  and  $\Delta t = \eta \Delta x / c$ ).

The results for the photon flux  $cn^+(L,t)$  at the output coupler are shown in Fig. 3.6 for several values of the peak inversion density  $N_0$ , normalized to its value at the laser threshold. The latter is found from an input-output curve that is calculated from the same rate equations. In full agreement with the experimental results of Fig. 3.4 the calculated photon flux exhibits a pulsed structure that develops after a few round trips. The calculated flux shows the same periodicity as in the experiment and exhibits the odd-even staggering of the pulse heights. The excellent agreement of the results of the model with the experimental data indicates that our model is sufficiently detailed. Hence one may conclude that our model accurately describes the coupling between the left and right travelling solutions and that additional couplings (e.g. grating formation) are rightfully neglected. The accuracy of the numerical method has been verified by showing that the same results are obtained when the step size is reduced.

Additional insight into the laser dynamics is obtained from the simulation of the evolution of the inversion density in the center of the gain medium:  $N(L/2,t)$ . The results for this quantity are shown in Fig. 3.7 for the same four values of the pump energy as in Fig. 3.6. In curves (a) and (b), corresponding to the pulse trains of Figs. 3.6a and 3.6b, the inversion density decays in a purely exponential fashion, i.e., the gain is not depleted by the stimulated-emission process. Initially,

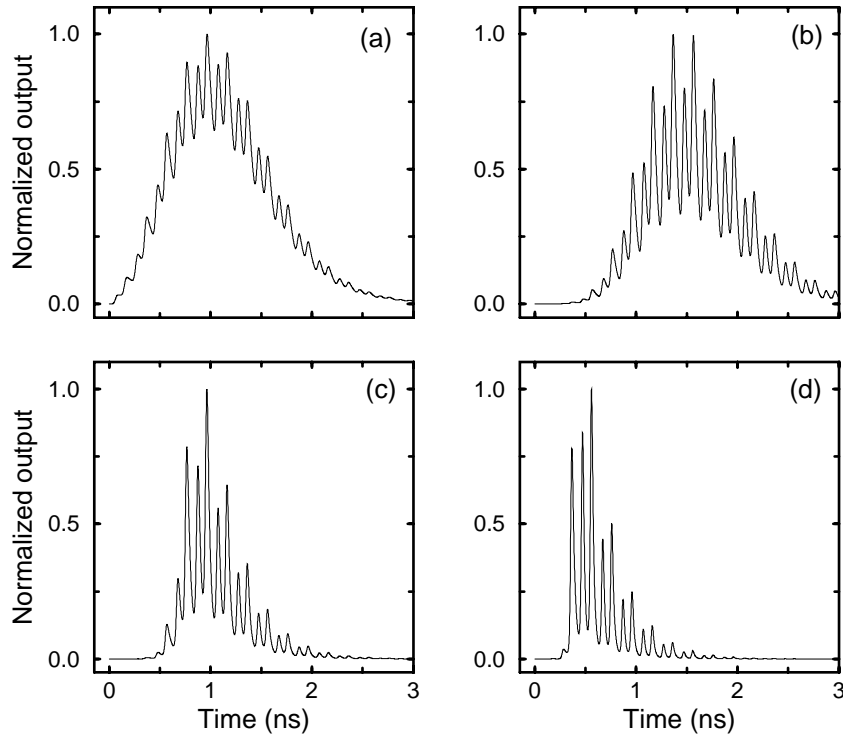


**Figure 3.6:** Simulation of the dynamics at various pump energies from just below threshold to five times above threshold.

curve (c) also follows exponential decay. However, after  $\approx 0.6$  ns the reduction of the inversion accelerates very rapidly. This point corresponds to the onset of gain depletion. In curve (d) the inversion decays very rapidly almost from the start. Here the initial gain is so high that gain depletion sets in immediately. In curves (c) and (d) one notices that the reduction of the inversion has step-like features. These steps can be associated with the passage of the short optical pulse through the gain medium.

The horizontal line in Fig. 3.7 indicates the equivalent cavity loss. It is now easy to understand the overall features of the pulse trains in Fig. 3.6. The pulse height will grow as long as the inversion is larger than the value indicated by this line. And, obviously, the pulse height will decrease (rapidly) when the inversion has dropped below this line. The intersection of the various curves in Fig. 3.7 with the 'loss line' sets the position of the maximum in each pulse train. As we will demonstrate below optical gain is an essential ingredient for generation of the strongly modulated output. Since the inversion density in Fig. 3.7 always

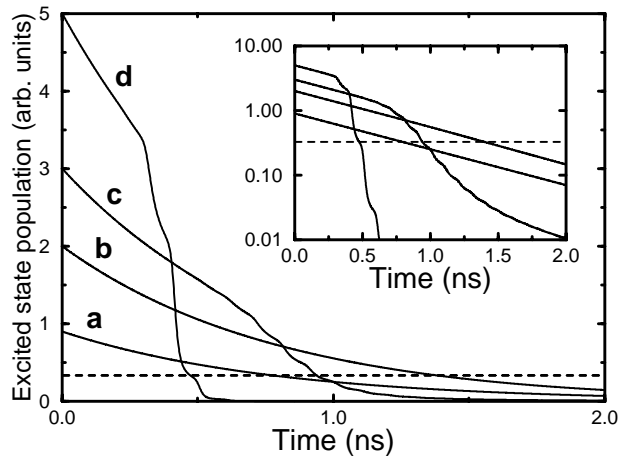


**Figure 3.7:** Calculation of the population decay corresponding to the dynamics shown in Fig. 3.6. Note the onset of gain saturation and the steplike decay of the inversion in curves (c) and (d). The dashed line indicates the population of the excited state at which the gain is equal to the losses. The cross-points of the ‘loss-line’ and the decay curves indicate the time at which maximum output is reached (compare to Fig. 3.6).

starts above the loss line, net gain is present in all cases and consequently pulse sharpening is observed for all curves in Fig. 3.6

Here one clearly sees that the common threshold condition formulated as ‘the gain is equal to the loss’ is ill-defined for this system. Because of its time dependence, the gain equals the loss only at a specific time  $t_e$ . For  $t < t_e$  the gain exceeds the loss, resulting in amplification of the intracavity photon flux, while for  $t > t_e$  the system is predominantly lossy. As argued above, under these conditions, pulses will arise due to stimulated emission. However, when the initial inversion is not too large, the stimulated-emission process may come to an end before a powerful coherent beam is formed. Consequently, the time-integrated laser output may indicate that the laser is below threshold, even though, initially, the gain exceeded the loss, tempting one to conclude that the laser is above threshold. The lack of clarity in the threshold definition for this type of systems is succinctly discussed in Ref. [71].

Based on its appearance, one may be tempted to interpret the pulse train emitted by our laser as an example of a relaxation oscillation (spiking). However, relaxation oscillations in lasers develop because of depletion and subsequent recovery of the population of the upper laser level [60]. In our system the pump is switched off immediately; hence this population can not recover. It is thus in-

appropriate to view the pulse train as a relaxation oscillation. As we will show below an appropriate interpretation for the generation and sharpening of the output pulses can be given in terms of gain switching.

Usually, gain switching is achieved by modulating the gain (or loss) in a time short compared to the spontaneous lifetime of the laser medium. After such a switch the intracavity intensity builds up by amplified spontaneous emission. The subsequent depletion of the gain brings the pulse to an end, resulting in a short output pulse. The dynamics of the gain thus lie at the heart of the emission of such a short pulse. In our laser the light experiences not only a variation of the gain in the temporal domain, but also in the spatial domain, because the laser medium is localized at the center of the cavity. This spatial variation causes the light to experience an additional modulation of the gain. On the time scale of the spontaneous lifetime the light thus *repetitively* experiences gain switching, although the medium is excited only once.

In order to stress the importance of the spatial distribution of the inversion in the cavity, we compare the calculated dynamics of Fig. 3.6b to a calculation of the pulse evolution under excitation with a four times larger pump spot inside the same laser cavity (with the same number of excited species inside). Figure 3.8 shows the laser output for both excitation spots. The upper frame shows the results

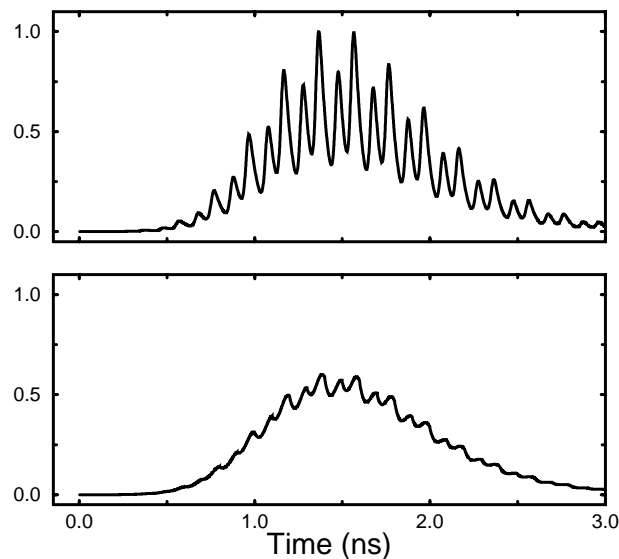


**Figure 3.8:** Comparison between the evolution as shown in Fig.3.6b (upper frame) and a laser that is pumped with an excitation stripe that is 4 times larger (lower frame). The number of excited molecules is the same in both cases.

of Fig. 3.6b, while the output for the four times larger pump spot is presented in the lower frame. For the larger pump spot the output clearly exhibits a much weaker modulation than for the smaller pump spot, yet the overall shape is the same. This shows that the spatial distribution of the gain has a major impact on the detailed temporal output of our laser. The regime of normal gain switching can be found by filling the cavity uniformly with gain. In that case the modulation disappears almost completely<sup>3</sup>, but the overall shape is conserved. This shows that the pulse-train *envelope* of our laser represents an example of normal gain switching.

### 3.5 Heuristic description

An heuristic description of the pulse train is obtained by analyzing the light intensity at the output coupler during the first round trip after the pump pulse, as shown in Fig. 3.9, an enlargement of Fig. 3.6b. In the left frame one sees the first pulse that is coupled out of the cavity, containing the light that, immediately after excitation, propagates in the direction of the output coupler. During the rising

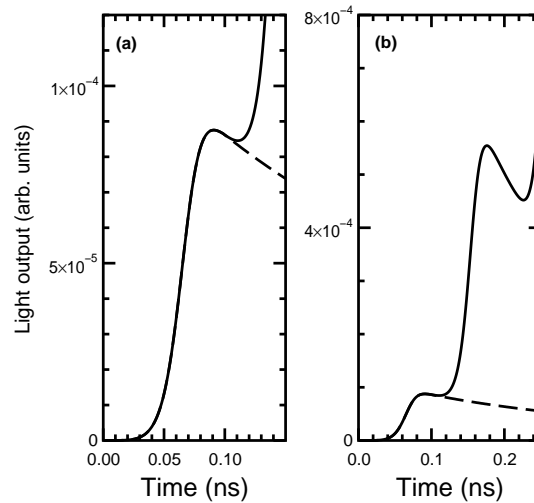


**Figure 3.9:** Detail of the initiation of the pulse train. Frame (a) shows only the first pulse while frame (b) shows both the first and second pulse. The dashed line shows the decay of the output if no mirrors would have been present.

<sup>3</sup>Note that the output of the laser is also slightly modulated when the gain is homogeneously distributed over the cavity. In that limit the modulation is the result of the high losses which are localized at the mirrors, inducing an inhomogeneous photon distribution in the cavity [73, 85].

slope of the pulse the signal grows because an ever larger part of the gain medium contributes to the light intensity at the output coupler. This continues until the full length of the gain medium contributes. Beyond that point the signal starts to decrease because the inversion is decaying over the full length of the gain medium. The dashed line shows how the light output would continue to decay if no mirrors would be present. Due to the mirrors, however, additional light arrives at the output coupler after some time, light that originally was emitted towards the high reflector. Because of the delay between the arrival of the retroreflected light and the roll-over of the light that arrived first at the output coupler, the output signal will exhibit a small dip. This dip occurs because the cavity is not completely filled with gain, the photoluminescence lifetime is finite, and because the pump pulse is so short<sup>4</sup>.

The small dip is responsible for the development of the strongly modulated output that appears after some round trips through the cavity. This is illustrated by the results shown in the right frame of Fig. 3.9, where the first and second pulse are shown together (note the different scale as compared to frame (a)). From the height difference between the first and second peak one sees that the light has experienced gain during its second pass through the gain medium. One also sees that the dip following the second pulse is considerably deeper than the first dip. This can be understood when we see the second pulse as a nonlinearly amplified version of the first pulse: With a decaying inversion the front of the light travelling through the gain medium experiences more amplification than the tail. As a result a sharpened peak is emitted [60].

The emission of the subsequent peaks is now easily described since we have entered the regime where stimulated emission dominates. The evolution of the pulse train is now very similar to that in a regenerative amplifier [87] with the first (and second) peak acting as a seed. Repetitive nonlinear amplification results in the strongly modulated output. Note that the spontaneous-emission lifetime (0.86 ns) exceeds the cavity round-trip time (0.17 ns), a necessary requirement for having gain during several round trips.

As discussed earlier there are two essentially separate but interleaved pulse trains that emerge from the cavity resulting in a pulse repetition rate twice the longitudinal mode spacing<sup>5</sup>. Obviously, the pulse trains experience coupling since they feed from the same gain. Except from this fact, these pulse trains are largely

---

<sup>4</sup>It is easily seen that the two light signals will not be distinguishable when the cavity is completely filled. In that case no 'pulse front' can be assigned and the photon density in the cavity is essentially homogeneous. The same argument applies when the pump pulse has a duration larger or equal to half the cavity round-trip time [86].

<sup>5</sup>Double or multiple pulsing is also known to occur in mode-locked lasers [88, 89], the origin of the multiple pulsing being different in that case.

independent. This becomes clear when, in the calculation, one moves the gain medium along the cavity axis, to a position somewhat closer to the high reflector than to the output coupler (distance ratio 9:11). In that situation the calculated pulse train shows the odd-even staggering as observed in the experiment. In terms of the two interleaved pulse trains the odd-even staggering is very simply explained: The odd-numbered pulses have their origin in light that, directly after excitation, travels towards the output coupler, returning to the gain medium at a time  $1.1 L/c$ . The even-numbered pulses, however, grow out of the light that, initially, moves towards the high reflector, making a second pass through the gain medium at a time  $0.9L/c$ . The time of second passage is thus different for the two light pulses. Since the gain continuously diminishes, the pulse that arrives earliest will, at each round trip, experience a larger gain as compared to the other. The small asymmetry has already been included in the model presented above (Fig. 3.6), reproducing the considerable amplitude odd-even staggering of the pulses in Fig. 3.4. Figure 3.10 serves to illustrate the asymmetry by marking the time of passage of the pulses through the gain medium during subsequent round trips through the cavity. Also indicated in Fig. 3.10 is the evolution of the gain for the case that gain depletion does not come into play [cf. Figs. 3.6a

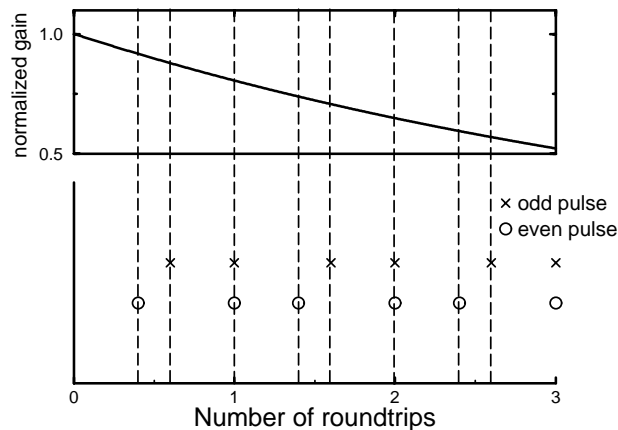


**Figure 3.10:** Visualization of the moments of passage through the gain medium for the odd (cross) and even (circle) pulses. Because of the asymmetric position of the gain medium inside the cavity the odd and even pulses do not always pass through the gain medium at exactly the same moment. Each  $(m + \frac{1}{2})$  round trip ( $m=0,1,2,..$ ) the even pulse passes the gain medium a bit earlier than the odd pulse. Since the gain is continuously decaying (as shown by the curve in the upper half of the Figure), the even pulse experiences more gain than the odd pulse during this passage. This effect gives rise to the odd-even staggering of the pulse heights.

and 3.6b]. The gain asymmetry will give rise to a substantial asymmetry in the pulse heights of the two trains since the amplification depends exponentially on the gain.

### **3.6 Conclusion**

We have performed a detailed experimental time-domain study of the output of a short-cavity polymer laser upon excitation by a single femtosecond pump pulse. In the experiment the gain medium only partially fills the cavity and the duration of the pump pulse is very much shorter than the cavity round-trip time, which, in turn, is shorter than the spontaneous emission lifetime of the gain medium. Although the gain medium is excited only once, a whole train of pulses is emitted. This behavior occurs because the spatial distribution of the gain medium makes the light to experience repetitive gain switching. We show that our results can be well reproduced by a one-dimensional rate-equation model that takes the nonuniformity of the cavity explicitly into account. This model exhibits the build up and decay of the pulse train, the odd-even staggering of the pulses when the gain medium is positioned somewhat asymmetrically in the laser cavity, and allows us to calculate the decay of the inversion. We find excellent agreement with the experiment.



## Chapter 4

---

# **Orientalional relaxation in polymer and dye solutions and its consequence for the laser threshold<sup>1</sup>**

We compare orientational relaxation phenomena of a light-emitting polymer and a, spectroscopically similar, conventional laser dye in solvents of comparable viscosity. The orientational relaxation time of the laser dye is found to be much smaller than that of the polymer. This result is attributed to the large difference in shape between the two light-emitting materials. We demonstrate that these very different reorientation times have a major influence on the operation of a gain-switched laser based on these gain media, in particular on its threshold.

### **4.1 Introduction**

It is a broadly held view that light-emitting polymers and traditional dyes have very similar properties as laser gain media, at least when they are dissolved in an appropriate solvent [38, 40, 41]. Both types of material exhibit broad absorption and emission bands with small or negligible overlap, and have excited-state lifetimes of approximately a nanosecond. However, a dye molecule has a very different shape as compared to a polymer chain. A dye molecule is a rather compact unit with a relatively small molecular weight ( $M \approx 500$  atomic units). Light-emitting polymers, in contrast, form an extended structure with a well-defined backbone; they have molecular weights of order  $10^5 - 10^6$  atomic units.

In the absence of external influences, the orientational distribution of the transition dipole moments of either dye or light-emitting polymer, is isotropic. However, it is well known that the absorption of linearly polarized light results in an excited-state population with an *anisotropic* orientational distribution of dipole moments. Due to this anisotropy the luminescence of the material is polarized, the preferential polarization direction being parallel to that of the exciting light.

---

<sup>1</sup>S. A. van den Berg, G. W. 't Hooft, and E. R. Eliel, Chem. Phys. Lett. **347** 167 (2001).

In time, the excited-state anisotropy diminishes as a result of, e.g., orientational diffusion. Under the assumption that this diffusion is isotropic, it can be specified in terms of a single diffusion coefficient  $D$  or a relaxation rate  $\alpha = 6D$  [90]. Such relaxation phenomena have been studied extensively for a large variety of dyes in all possible solvents [91–95]. It has been shown that the dipolar reorientation time is roughly proportional to the viscosity of the solvent and the molecular volume of the solute [96]. Because of their vastly different shape one expects the polymer to reorient much more slowly than the dye molecule, at least if the viscosity of the solvents are roughly equal.

Both materials are used as active materials in optically pumped lasers. Since the pump-induced dipolar anisotropy and its persistence play a major role in the operation of such lasers, as has been shown for numerous types of dye lasers in various pumping configurations [97–102], it is to be expected that polymer and dye lasers may exhibit some differences in this respect. The aim of this chapter is to bring to light how the morphological differences between a laser dye and a light-emitting polymer affect both the polarized photoluminescence and the laser action of these materials in solution. The first effect is studied by determining the decay rate of an optically induced dipolar non-equilibrium in these materials. The second effect is explored by measuring the input-output characteristics of short-cavity lasers, based on either material, for different choices of the pump polarization.

## 4.2 Orientational relaxation in optically pumped polymer and dye solutions

Our two light-emitting materials are a copolymer of two poly-(*p*-phenylene-vinylene) (PPV)-derivatives (alkoxy-substituted 2-phenyl PPVs) [65], dissolved in chlorobenzene (2 g/l), on the one hand, and the laser dye Coumarin 153, dissolved in methanol (2.4 g/l), on the other hand. Both materials absorb in the near UV and emit in the green spectral region with a peak at  $\lambda \approx 530$  nm. We create a dipolar nonequilibrium (anisotropy) by exciting the materials very weakly with the linearly polarized output of a frequency doubled ( $\lambda = 400$  nm) Ti:sapphire laser that generates  $\approx 130$  fs pulses with a 82 MHz repetition rate. We use time-correlated single-photon counting to record the decay of the fluorescence, polarized either parallel or perpendicular to the pump polarization. The measurements are performed at room temperature.

In Fig. 4.1 we show the temporal evolution of the polarized photoluminescence of the polymer. Curve (a) shows the polarization component of the luminescence

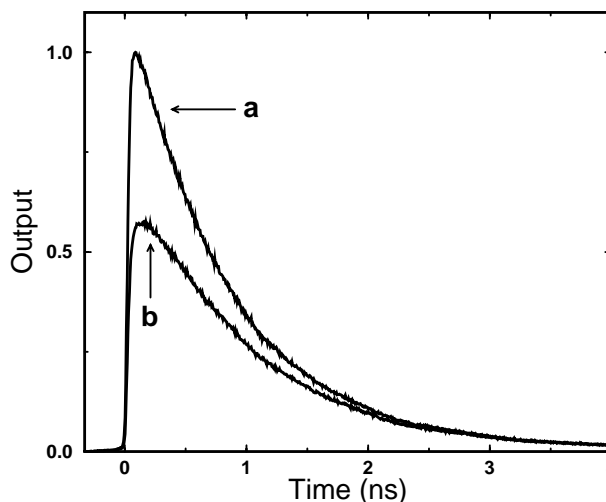


**Figure 4.1:** Decay of the two polarization components parallel (a) and perpendicular (b) to the pump polarization for the light-emitting polymer in chlorobenzene.

parallel to that of the pump ( $I_{\parallel}(t)$ ), whereas curve (b) shows the perpendicular polarization component ( $I_{\perp}(t)$ ). We observe that the anisotropy is quite substantial initially ( $I_{\parallel}/I_{\perp} \approx 2$  at  $t = 0$ ), and that it decays on a time scale exceeding the spontaneous-emission lifetime of the fluorophore ( $\tau_{\text{sp,polymer}} = 0.86$  ns). Note that the duration of the pump pulse (130 fs) is negligibly short on the time scale shown.

Figure 4.2 shows similar data for the laser dye. Also here curve (a) shows the polarization component of the luminescence parallel to that of the pump ( $I_{\parallel}(t)$ ), and curve (b) shows the perpendicular polarization component ( $I_{\perp}(t)$ ). In this case the decay occurs within 50 ps, a limit imposed by the time resolution of the measurement system. Measurements with a streak camera (not shown here), provide us with a orientational relaxation time of about 30 ps. This value agrees quite nicely with data found in a recent detailed study of rotational dynamics of this dye in many different solvents [94]. Note that this relaxation time is very much shorter than the spontaneous-emission lifetime of this material ( $\tau_{\text{sp,dye}} = 3.7$  ns).

Summarizing, in the polymer the polarization anisotropy is long-lived, while in the dye it is almost immediately washed out. Because the solvents that we use (chlorobenzene and methanol, respectively) have almost equal viscosity at room temperature we can, in first order, neglect their influence. Consequently, we associate the large difference in the decay rate of the induced anisotropy to the morphological effects that have briefly been mentioned in the introduction: Because of its compactness, the dye molecule can tumble in the solvent and therefore rather

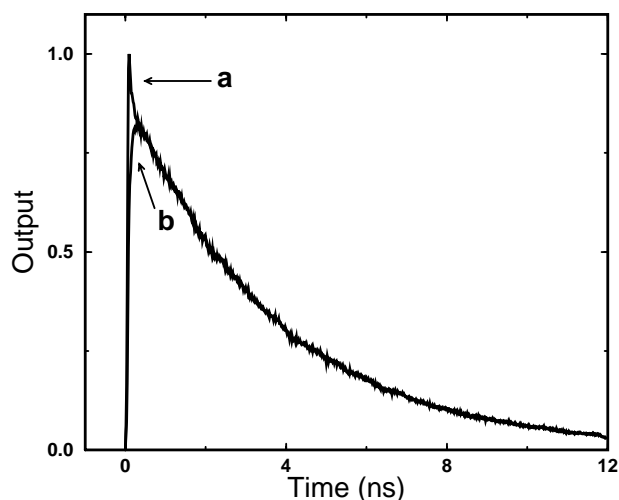


**Figure 4.2:** Decay of the two polarizations components parallel (a) and perpendicular (b) to the pump polarization for Coumarin 153 in methanol.

easily reorient its dipole. In the light-emitting polymer, the dipoles are fixed to the large, kinematically sluggish polymer backbone and can therefore not so rapidly change their orientation.

To substantiate our picture of physical reorientation, we have measured the orientational relaxation time of the dissolved polymer for a range of temperatures. From such measurements we find that the reorientation time of the polymer in chlorobenzene increases by a factor of 4 when the temperature is reduced from  $+20\text{ }^{\circ}\text{C}$  to  $-40\text{ }^{\circ}\text{C}$  (close to the freezing point of chlorobenzene). This factor agrees quite well with the increase in viscosity of the solvent.

A simple classical dipole model [103] allows us to analyze the results of Figs. 4.1 and 4.2 somewhat more quantitatively. For this we consider an ensemble of dipoles whose random orientations are fixed in space. When such an ensemble is excited with linearly polarized light, the luminescence will be polarized preferentially parallel to the polarization of the exciting light ( $I_{\parallel}/I_{\perp} = 3$ ). In a real system this ratio may not attain this value, for instance in systems where the directions of the absorption and emission dipoles do not completely coincide, e.g., due to intraband relaxation [103].

In solution, however, the molecules have motional freedom and orientational relaxation must be taken into account. In order to model this diffusive process we decompose the dipole distribution into an ensemble  $N_{\parallel}(t)$ , parallel to the pump polarization, and two ensembles  $N_{\perp}(t)$  along the two mutually orthogonal axes

perpendicular to the pump polarization. The total number of dipoles is thus given by  $N(t) = N_{\parallel}(t) + 2N_{\perp}(t)$ . Defining  $\Delta(t) = N_{\parallel}(t) - N_{\perp}(t)$  as the orientational excess, we write:

$$\frac{dN(t)}{dt} = -\gamma N(t), \quad (4.1)$$

$$\frac{d\Delta(t)}{dt} = -(\gamma + \alpha)\Delta(t), \quad (4.2)$$

where  $\gamma$  represents the spontaneous-emission rate of the emitter and  $\alpha$  its reorientation rate in the solvent, assuming isotropic diffusion [90]. The solution of these equations is given by:

$$N_{\parallel}(t) = \frac{1}{3}N_0(1 + 2R_0 \exp(-\alpha t)) \exp(-\gamma t) \quad (4.3)$$

$$N_{\perp}(t) = \frac{1}{3}N_0(1 - R_0 \exp(-\alpha t)) \exp(-\gamma t), \quad (4.4)$$

with  $N_0$  the total amount of excited molecules at  $t = 0$  and  $R_0 = R(0)$  the fluorescence polarization anisotropy at  $t = 0$ . The quantity  $R(t) = (I_{\parallel}(t) - I_{\perp}(t)) / (I_{\parallel}(t) + 2I_{\perp}(t))$  is a convenient measure for the polarization anisotropy of the luminescence. Since  $I_{\parallel(\perp)}(t) \propto N_{\parallel(\perp)}(t)$  we may write:  $R(t) = \Delta(t)/N(t) \propto \exp(-\alpha t)$ . From the polarization-resolved fluorescence decay curves of the polymer (Fig. 4.1) we find the characteristic orientational relaxation time of this material in chlorobenzene at room temperature to be  $\alpha^{-1} = 1.3$  ns. This value is comparable to earlier reported values for the reorientation time of dissolved polymers at room temperature [41].

### 4.3 Polymer and dye lasers

In the study of the lasing properties of our two materials, we employ a 25 mm long symmetrical laser cavity consisting of a high reflector and an output coupler (see Fig. 4.3). Both mirrors have a radius of curvature of 40 mm; the transmissivity of the output coupler is 10%. The cavity is made to have a negligible polarization anisotropy. In the center of this cavity sits a dye cell through which the dye or polymer solution flows continuously. This gain medium is side-pumped with 130 fs pulses at  $\lambda = 400$  nm at a repetition rate of 1 kHz, the pump light being focussed into a pencil-shaped volume (4 mm  $\times$  0.05 mm  $\times$  0.05 mm) inside the solution and polarized either parallel or perpendicular to the axis of the cavity. Because of the ultrashort nature of the pump pulse the laser operates in the gain-switched regime [104].

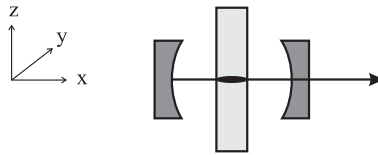


**Figure 4.3:** Schematic of the experimental setup: A laser cavity consisting of two concave mirrors and a dye cell, with the transversally excited region indicated by the oval.

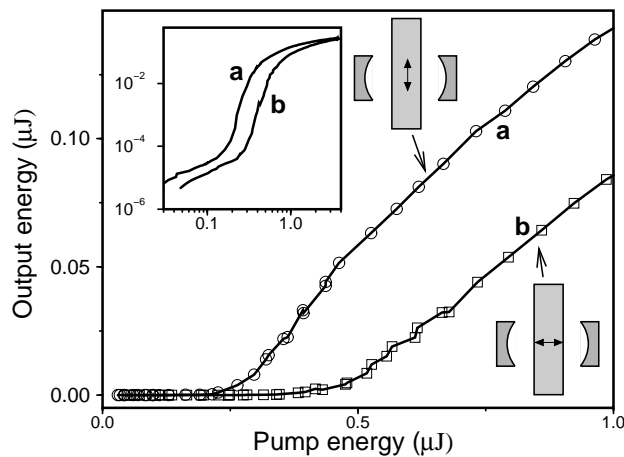


**Figure 4.4:** Input-output curve of the polymer laser for two polarizations of the pump light. The time-integrated light output, as measured within a small solid angle, is plotted versus pump energy on a linear scale. In the inset the same curve is plotted on a double-logarithmic scale.

Figure 4.4 shows the input-output characteristics of the polymer laser for polarizations of the pump light parallel and perpendicular to the axis of the cavity. Curve (a) shows the results for the normal case where the pump is polarized perpendicular to the cavity axis, while curve (b) corresponds to the unusual case where the pump is polarized parallel to the cavity axis. We observe that the threshold of the polymer laser is very different for these two modes of pumping, the threshold for pumping parallel to the cavity axis exceeding the threshold for pumping perpendicular to the cavity axis by almost a factor of two. In contrast, in the dye laser the effect of the pump polarization on the laser threshold is hardly observable (see Fig. 4.5).

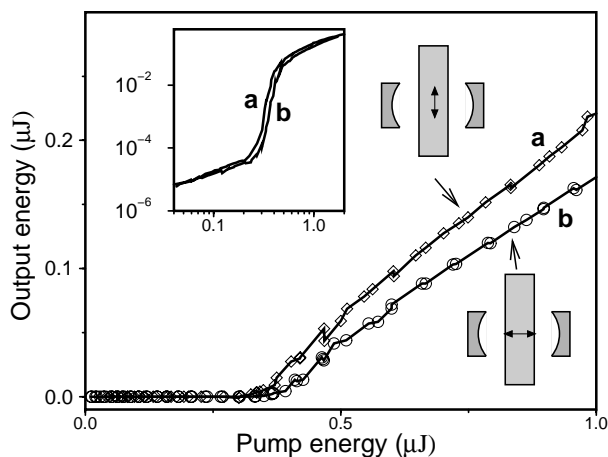


**Figure 4.5:** Input-output curves of the laser with Coumarin 153 as gain medium for two polarizations of the pump light.

Below threshold, the laser output is dominated by spontaneous emission. The inset of Fig. 4.4 shows that, for the polymer solution, the output is about two times larger for the pump polarization perpendicular to the axis of the cavity, as compared to the case with the pump polarization parallel to the cavity axis. In contrast, for the laser dye, the output level does not depend on the polarization of the pump (see the inset of Fig. 4.5). These results are in excellent agreement with the measurements of the polarized luminescence discussed earlier.

Let us first analyze the case that the pump polarization points in a direction ( $z$ ) *perpendicular* to the cavity axis ( $x$ ). Radiation in the cavity mode then experiences gain anisotropy (dichroism) as a result of the pump-induced excess dipolar alignment in the  $z$ -direction. Consequently, both media will emit radiation that is polarized along the  $z$ -axis, thereby profiting from the excess gain. Secondly, in the case that the pump polarization points *along* the cavity ( $x$ )-axis, radiation in the cavity mode does not experience gain anisotropy, since its polarization (which lies in the  $y-z$ -plane) is oriented perpendicular to the excess alignment. Comparing the two pump polarizations we notice that the induced excess gain is accessible for the lasing mode in the cavity in case of the  $z$ -polarized pump, while not being accessible in case of the  $x$ -polarized pump. In the latter case the laser thus experiences less gain.

This picture of a laser with anisotropic gain applies particularly well to the

polymer because its gain anisotropy persists over at least a spontaneous-emission lifetime. From the data of Fig. 4.1 one can deduce that the gain of the polymer is reduced by almost a factor of 2 when the pump and emission polarizations are orthogonal to each other instead of parallel. This factor reappears in the ratio of the laser thresholds for the two polarizations of the pump (see Fig. 4.4).

The rapid orientational relaxation of the dye suggests that a different scenario applies here. Whatever pump polarization is chosen, the gain medium has effectively become isotropic on the time scale of a single cavity round trip ( $\approx 170$  ps). Possible differences in output of the dye laser thus originate in the early start-up phase of the laser, at a time when stimulated emission does not yet dominate the output. The dye laser may then be described as a polarization isotropic amplifier injected by a weakly polarized seed for the  $z$ -polarized pump, and, alternatively, injected by an unpolarized seed for the  $x$ -polarized pump. Since the output energy of the amplifier depends exponentially on the pump energy but only linearly on the injected seed energy, the effect of the seed energy on the input-output curve is very small. Thus indistinguishable threshold levels result.

We have also measured the degree of polarization ( $P = (I_{\parallel} - I_{\perp}) / (I_{\parallel} + I_{\perp})$ ) of the output of the two lasers for the case that the pump is polarized perpendicular to the cavity axis. For the case that the laser is driven two times above threshold we find  $P = 0.92$  for the polymer, while for the dye we find  $P = 0.71$ . In view of the different relaxation times of the dichroism it is not surprising that the polarization of the polymer laser is so much better defined. For both materials the laser output is completely unpolarized ( $P = 0$ ) when the pump is polarized parallel to the axis of the cavity. One is tempted to find this result trivial in view of the symmetry of the setup: it has neither gain nor loss anisotropy. However, it is well known that many lasers, in spite of such full symmetry, usually emit highly polarized light. An example of such a laser is a vertical-cavity surface-emitting laser (VCSEL), where inevitable small anisotropies (e.g. due to strain), in combination with mode competition drive the laser towards a single mode with a well-defined polarization [105]. The difference between such a VCSEL and the lasers discussed in the present chapter lies in the fact that the VCSEL is operated in, or close to, steady state while our lasers are operated very far from steady state. Our system is gain-switched, that is, the excitation pulse is negligibly short as compared to all other timescales in the system, and its output is highly dynamic [76, 104]. At any time the system is far from steady state, which implies that there is no time for selecting a well-defined polarization state through mode competition [106], although small anisotropies are certainly present in our system as well.

## **4.4 Conclusion**

Time-resolved measurements have been performed to show that orientational relaxation phenomena in a solution of light-emitting polymers occur on a much longer time scale as compared to a conventional laser dye in solution. This result is attributed to shape and size differences between the constituent materials. In a polymer laser the polarized pump light induces dichroism that persists over a time comparable to the spontaneous-emission lifetime of the emitter. As a result the threshold of a polymer laser strongly depends on the polarization of the pump light. In contrast, due to the fast randomization of orientation of the dye molecules, the input-output curves of the dye laser hardly depend on the polarization of the pump.

We gratefully acknowledge Dr. H.F.M. Schoo for providing us with the polymer materials.



## Chapter 5

---

# Study of polarization cross coupling in a polymer microlaser using double-pulse excitation<sup>1</sup>

We have studied the coupling of the two polarization modes of a polymer microlaser by pumping its gain medium with two mutually delayed orthogonally polarized femtosecond pump pulses, which have a variable interpulse delay. Because the dominant anisotropy in the laser is induced by the pump and the various time scales associated with this setup are well-separated, insight into the dynamics of the system is obtained by this method. Both time-resolved and time-integrated measurements of the output of the microlaser demonstrate strong cross-coupling and memory effects between the polarization modes. These can be assigned to the interplay between the optical fields in the cavity and the inversion. The most remarkable result is that the dominant output polarization switches direction when the interpulse delay is varied. Using a simple model, both for the polarization properties of the polymer and for the polymer laser, we discuss the underlying physics of the polarization cross coupling. An attractive aspect of our gain material, i.e., a light-emitting polymer in solution, is its long memory for the polarization anisotropy induced by the pump; such a material provides a transparent model system.

### 5.1 Introduction

The polarization state of the output of a laser is a subject of recurrent interest; it has been studied for almost all types of lasers, from HeNe lasers in the early days [107–109] to vertical-cavity surface-emitting lasers (VCSELs) [110, 111], (multimode) fiber lasers [112, 113], etc. in the present day. A large part of this work has been concerned with the polarization behavior of CW-operating

---

<sup>1</sup>S. A. van den Berg, V. A. Sautenkov, G. W. 't Hooft, and E. R. Eliel, Phys. Rev. A, to appear in June 2002.

lasers. Recently, however, with the advent of e.g. passively Q-switched single-mode microchip lasers, the pulsed regime has attracted considerable attention as well [114].

It is well known that dispersive (birefringent) and gain/loss (dichroic) anisotropies play an important role in determining the polarization state of the light emitted by the laser; these anisotropies can have both linear and nonlinear character. The richness of this field, and thus the recurrent interest, stems from the fact that the effective anisotropy of the laser as a whole is determined by such factors as the laser material itself, the cavity surrounding it, the pumping process and the time scales associated with these factors. Consequently, for each new laser material or laser configuration this question has to be addressed.

Complexities arise as the various anisotropies may have different principal axes, or have different ellipticity (linear versus circular dichroism and/or birefringence). Nevertheless, most lasers can be made to oscillate in a state of stable polarization by making one anisotropy much larger than all others. For example, in a cavity with Brewster-angled interfaces the loss is so strongly anisotropic that the laser will emit linearly polarized light, even in the presence of additional anisotropies [99].

An interesting case is that where the dominant anisotropy is introduced via the pumping process; this is the case in dye lasers with isotropic cavities that are pumped by the linearly polarized output of another laser [115]. Here the anisotropy arises because the field of the pump laser selectively interacts with those dye molecules whose transition dipole is more or less aligned with the polarization vector of the pump-laser field. The effective anisotropy can be large or small, depending on the fact whether the anisotropy decays rapidly (in solvents of low viscosity) slowly (in viscous solvents) or not at all (in solid matrices) [94]. In optically pumped VCSELs a similar situation arises; a gain anisotropy can be introduced in that system by pumping with *circularly* polarized light. The decay of this gain anisotropy is, however, so fast [116] that it usually does not play an important role when the laser is operated in the CW regime. Only when the laser is driven by fs pump pulses this anisotropy can be made to express itself [117, 118].

In recent years lasers with light-emitting polymers as gain medium have attracted considerable attention [54–57]. This new type of gain medium can be applied both as a thin solid film [43, 59] and in solution [38, 39, 41]. Light-emitting polymers in solution show many similarities with standard laser dyes [38, 39, 55, 56]. For instance, when the polymer solution is pumped with linearly polarized light an anisotropy in the optical gain is induced, just as in a laser dye. Actually, this gain anisotropy persists for a very long time, much longer than for a laser dye that is dissolved in a solution with comparable viscosity [119]. The long memory

for the pump polarization is directly related to the long reorientation time ( $> 1$  ns) of the extended polymer chains. Just like for a dye laser the emitted polarization of the polymer laser will therefore be parallel to that of the pump light, if no polarizing elements are present in the cavity. Since the reorientation time exceeds the spontaneous lifetime of the polymer [119], the polymer chains can be considered fixed in space on the time scale of many experiments. A solution of light-emitting polymers therefore forms a perfect model system for polarization experiments.

In this chapter we study a microcavity polymer laser by exciting the gain medium with *two* mutually delayed, orthogonally polarized femtosecond pulses. The double-pulse excitation leads to surprising polarization cross-coupling effects in the microlaser. These effects come to light because of the ordering of the important time scales associated with using a femtosecond pump, a microcavity laser and a gain medium for which the relaxation of the pump-induced anisotropy is negligibly slow. By varying the delay between the two pump pulses, insight into the interplay between the two signal fields and the inversion in the microlaser is obtained.

This chapter is organized as follows: In Sec. 5.2 the experimental setup is discussed, followed by the results of real-time measurements on the output of the polymer laser upon double-pulse excitation (Sec. 5.3). A measurement of the time-integrated output in each polarization state as a function of the interpulse delay is briefly discussed. Subsequently, a model for the polymer laser is developed in which the induced anisotropies in the angular distribution of the gain are explicitly taken into account (Sec. 5.4). The real-time output and the effective optical gain that is associated with the individual polarization components, are calculated numerically for various values of the interpulse delay. These results provide insight into the coupling between the polarization modes in the microcavity laser. The underlying physics of the polarization cross coupling is discussed in Sec. 5.5. In Sec. 5.6 the time-integrated output of both polarization components as a function of the interpulse delay is discussed more thoroughly. We show that the time-integrated data provide information on the duration of the pulse that is emitted by the microlaser. Both simulations and experimental results are presented for various pump energies, showing a strong dependence of the cross coupling on the pump strength.

## 5.2 Experimental setup

To explore the polarization properties and the dynamics in the polymer microlaser, we pump its gain medium with two temporally separated, orthogonally polarized ultrashort pulses. The microcavity consists of two flat dielectric mirrors, separated

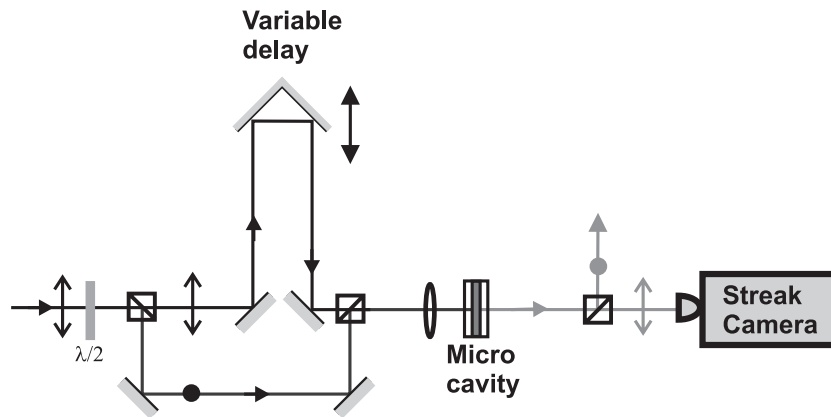


**Figure 5.1:** Schematic of the experimental setup. A pump pulse is split into two pulses with mutually orthogonal polarizations (indicated by  $\uparrow$  and  $\bullet$ ). The delay between the two pulses is controlled by the variable delay line. The polarization components of the light that is emitted by the microcavity laser are separated on a polarizing beam splitter and, after spectral filtering (not shown), sent to individual detectors.

by a  $17 \mu\text{m}$  thin spacer. The mirrors are highly reflective for  $\lambda = 510 - 550 \text{ nm}$  ( $R > 99\%$ ) and nonreflective around the pump wavelength of  $400 \text{ nm}$  ( $T > 85\%$ ). The volume between the mirrors is filled with a chlorobenzene solution (refractive index  $\eta = 1.523$ ) of a copolymer of two alkoxy-substituted 2-phenyl poly-(*p*-phenylene-vinylene)s [65], at a concentration of  $2\text{g/l}$ . The polymer absorbs in the blue, while it emits in the green spectral region. The emission and absorption spectra and the repeat units are shown in Fig. 3.2.

The polymer laser is pumped longitudinally with  $130 \text{ fs}$  pulses at  $\lambda = 400 \text{ nm}$  at a repetition rate of  $10 \text{ Hz}$ . The pump pulses are generated by a Ti:sapphire regenerative amplifier system (Spectra Physics, Spitfire), seeded by a Ti:sapphire oscillator (Kapteyn-Murnane laboratories). The  $800 \text{ nm}$  output of the Ti:sapphire laser system is frequency doubled in a  $0.5 \text{ mm}$  thick  $\beta$ -barium borate crystal. The resulting near UV beam is split into two orthogonally polarized beams by the use of a half-wave plate and a polarizing beamsplitter (see Fig. 5.1). The horizontally polarized pump pulse passes through a variable delay line, after which the paths of both pulses are recombined on a second polarizer. This pump beam is then brought to a focus in the laser cavity, resulting in an excitation spot with a diameter of about  $10 \mu\text{m}$ . The two polarization components of the microlaser's output are separated by a polarizer. In part of the experiments the horizontal polarization output is recorded by a streak camera (Hamamatsu, C1587), allowing us to

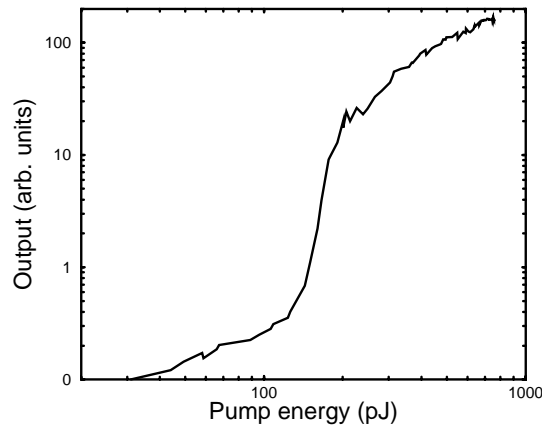


**Figure 5.2:** Input-output curve of the polymer microlasers measured under single pulse excitation.

perform measurements in the time domain with a temporal resolution of  $\approx 10$  ps. In other experiments both polarization components of the output are recorded by slow photodiodes and integrated in separate gated integrators.

## 5.3 Experimental results

### 5.3.1 Characteristics of the polymer microlaser

First we present some characteristics of the microlaser as it is pumped by just a single femtosecond pulse. In Fig. 5.2 its input-output curve is presented, displaying a clear threshold at a pump energy of about 0.2 nJ. The output of the polymer laser is linearly polarized, parallel to the polarization of the pump. As expected from the cylindrical symmetry of the laser, a very similar input-output curve is obtained when the laser is pumped with the excitation beam having the orthogonal polarization.

In Fig. 5.3 the spectrum of the light emitted by the polymer laser is shown when the laser operates far below (a) and far above (b) threshold, respectively. The below-threshold spectrum nicely shows the longitudinal modes spacing, as imposed by the cavity length and the refractive index of the polymer solution. Above threshold only a few modes contribute to the laser emission of the cavity. In both spectra the width of the peaks is determined by the resolution of our spectrometer.

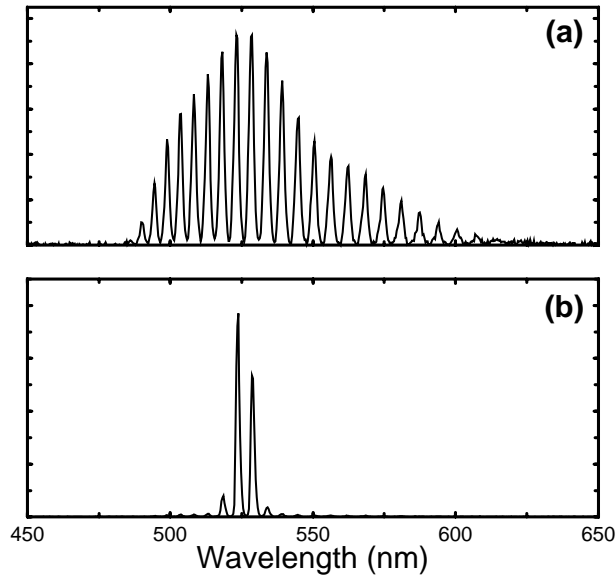


**Figure 5.3:** Emission spectra of the polymer microlaser for excitation below (a) and far above (b) threshold, respectively.

### 5.3.2 Experiments in the time domain

The results of our time-domain experiments on the output of the laser are presented in Fig. 5.4, for various values of the interpulse delay. The laser is pumped at about 1.6 times the threshold energy (i.e. the normalized pump parameter  $r = 1.6$ ). Only the horizontally polarized output component has been detected and is displayed. The experimental curves are presented in such a way that the vertically polarized pump pulse arrives at  $t = 0$ . In curve (a) the horizontally polarized pump pulse arrives much earlier ( $\approx 180$  ps) than its vertically polarized companion. The curve shows how a single pulse appears (duration  $\approx 30$  ps, buildup time  $\approx 40$  ps) shortly after the horizontally polarized pump pulse, while no noticeable (horizontally polarized) output is generated after the vertically polarized pump pulse. That pump pulse generates a vertically polarized output pulse which is not detected in our setup. In short, we observe a single pulse in the horizontally polarized output channel upon excitation by two time-separated, orthogonally polarized pump pulses. It demonstrates that, for each pulse, the output polarization is completely determined by the polarization of the associated pump pulse.

The result shown in curve (a) of Fig. 5.4 represents the response to the first pump pulse with the second pump pulse appearing at a time that the output of the

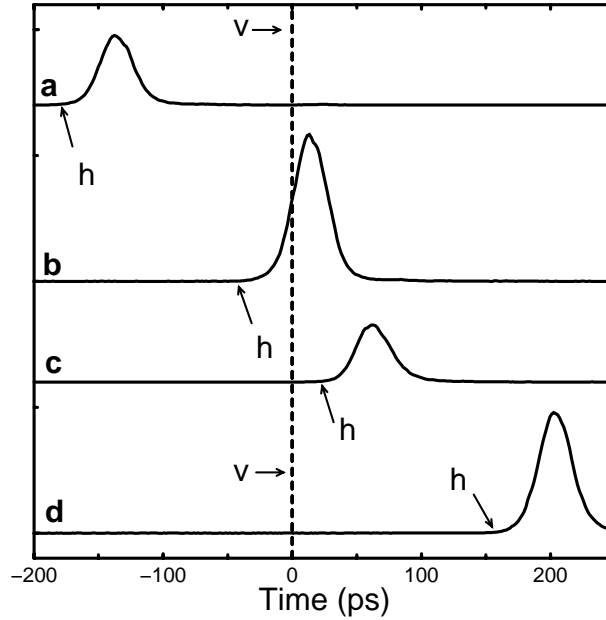


**Figure 5.4:** Results of time-domain measurements of the horizontally polarized output of the polymer microlaser for values of the several delay between the horizontally and vertically polarized pump. The vertically polarized pump pulse always arrives at  $t = 0$ . The arrows indicate the time at which the horizontally polarized pump pulse arrives. The pump energy is approximately 1.6 times the threshold value. All curves are drawn on the same scale but have been given an offset for clarity of presentation.

first output pulse is completely over. It thus shows the system response to a single isolated pump pulse and therefore serves as a reference for further measurements.

The situation is different when the interpulse delay is short, or if the order of the pump pulses is interchanged. For instance, curve (b) shows the output pulse for the case that the horizontal pump pulse is still first, but the interpulse delay is short (43 ps). When comparing this output pulse with that of curve (a) one sees that the horizontally polarized output of the laser is strongly enhanced: evidently, it profits from the second (vertically-polarized) pump pulse. Curve (c) shows the situation in which the horizontally polarized pump pulse arrives somewhat *after* ( $\approx 24$  ps) the vertically polarized pump. This case appears to be *unfavorable* for the horizontal output: it is slightly reduced compared to the reference pulse of curve (a). When the horizontally polarized pump pulse comes considerably later than the vertically polarized pump, as in curve (d), the horizontally polarized

output is again enhanced.

The results shown here indicate that the two polarization modes of the laser are coupled and that their coupling depends strongly on the order and delay of the two pump pulses. When comparing the various curves of Fig. 5.4, one notices an appreciable lack of symmetry relative to zero delay. For instance, for long interpulse delay (curve (a) and (d)), the horizontally polarized output is enhanced if the *last* pump pulse is horizontally polarized. In contrast, for short interpulse delay as in curves (b) and (c), the horizontally polarized output is enhanced when the *first* pump pulse is horizontally polarized. This nontrivial correlation between the order of the pump pulses and the laser output suggests that memory effects are important.

### 5.3.3 Time-integrated data

In all cases discussed above we have measured the horizontally polarized output. For reasons of symmetry, the vertically polarized output shows very similar behavior. This implies that, *independent of which input polarization comes first*, for *short* interpulse delay the output polarization corresponding to the first pump pulse exceeds the output component parallel to the second pump pulse. On the contrary, for *long* interpulse delay the output component corresponding to the second pump pulse exceeds the output component corresponding to the first pump pulse. Consequently, at some interpulse delay, henceforth called the switch point, the output in the two polarization channels must be equal. We have explored this switch by measuring the *time-integrated* output for both polarizations as a function of the interpulse delay. The results are displayed in Fig. 5.5, showing the values of the time-integrated vertically (dashed line) and horizontally (solid line) polarized outputs of the microlaser for  $r = 1.6$ . For negative values of the interpulse delay the vertically polarized pump pulse excites the gain medium first, while for a positive interpulse delay the horizontal polarization comes first. Because of the symmetry around zero delay the curves are each others mirror images with respect to  $\Delta\tau = 0$ .

The time-integrated curves show the same overall behavior as the time-domain measurements. Indeed, one sees that the dominant output polarization of the laser switches when the interpulse delay is scanned. For this pump value the switch points lie at an interpulse delay of  $\Delta\tau \approx \pm 60$  ps.

## 5.4 Model description

In this section we will develop a simple and effective model to describe the polarization and dynamics of the individual output pulses of our polymer laser. It

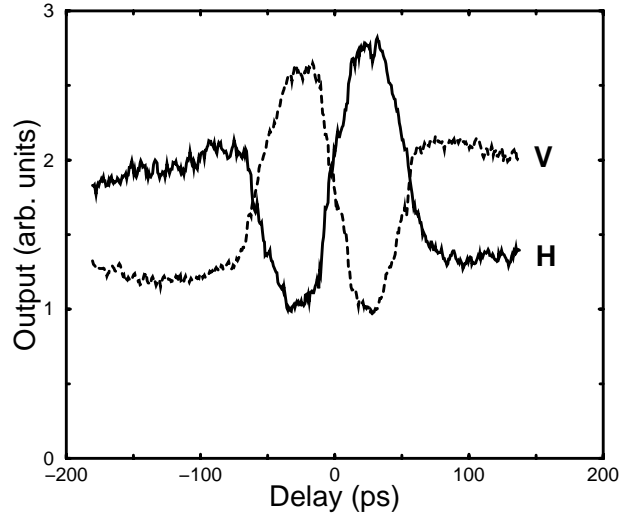


**Figure 5.5:** Time-integrated values for the horizontally (solid line) and vertically (dashed line) polarized outputs of the polymer microlaser, measured as a function of interpulse delay. The laser is pumped approximately 1.6 times above threshold.

is based on a combination of a specific model for the light-emitting polymer and a rate-equation description. The latter describes the evolution of the number of photons with horizontal and vertical polarization, and that of the anisotropic inversion of the gain medium. The large difference between the duration of the pump pulse, the cavity decay time, the spontaneous-emission lifetime and the dipolar-orientation relaxation time makes it possible to apply such a simple model.

#### 5.4.1 Polymer

To describe the polarization properties of the polymer laser we view the polymer as an ensemble of dipoles that are fixed to the backbone of the polymer. Because of the random orientation of these backbones, we model our polymer solution as an ensemble of randomly oriented dipole absorbers/emitters. For simplicity we will assume that the absorption and emission dipoles are parallel.

Absorption of linearly polarized pump light creates an anisotropic distribution of dipoles in the excited state since the probability of absorption is given by  $P_{\text{abs}} = |\vec{\mu} \cdot \vec{E}_{\text{pump}}|^2$ . Here  $\vec{\mu}$  is the electric dipole moment associated with a relevant unit of the polymer, and  $\vec{E}_{\text{pump}}$  represents the pump field. Our pump is sufficiently weak that we may assume that the absorption does not get saturated and that the ground state remains isotropic. One can easily show that for e.g., a horizontally

polarized pump pulse, the initial distribution of dipoles in the excited state, projected onto the polarization plane of the pump light (which is the transverse plane of the cavity in our case), is described by  $N(\theta, 0) = 2N_0 \cos^2 \theta$ , where  $N_0$  represents the effective number of excited dipoles. The angle  $\theta$  is defined with respect to the horizontal axis.

The orientational relaxation time of our dissolved polymer has been measured to be of the order of a few ns [119], much larger than the time scale of the present experiment. We can therefore safely assume that the initially created anisotropy in the excited state does not relax during the experiment. In this respect the polymer in solution behaves very similar to laser dye molecules in polymer matrices [120] or rare-earth ions in amorphous hosts like glass [121]. The probability of emission of a linearly polarized photon into a mode of the laser cavity is given by  $P_{\text{em}} = |\vec{\mu} \cdot \vec{E}_{\text{signal}}|^2 = \mu^2 E_{\text{signal}}^2 \cos^2 \theta$ , with  $\vec{E}_{\text{signal}}$ , the generated field. By integrating over all dipoles one can show that the intensity of the fluorescence polarized parallel to the pump polarization exceeds that of the fluorescence with orthogonal polarization by a factor of three [103].

#### 5.4.2 Rate equations

In accord with many other authors [55–57], we model our polymer laser as a homogeneously broadened, ideal four-level system [104]. Since the gain medium fills the cavity completely, we assume that the gain and losses are homogeneously distributed along the length of the cavity. In order to model the polarization properties of the microcavity, we take into account the angular distribution of excited dipoles, projected on the polarization plane of the pump radiation. We separately consider the horizontally and vertically polarized components of the signal field. The evolution of the inversion  $N(\theta, t)$  and the horizontally and vertically polarized photon numbers ( $n_h(t)$  and  $n_v(t)$ , respectively) are described by the following rate equations:

$$\begin{aligned} \frac{\partial N(\theta, t)}{\partial t} &= -\gamma N(\theta, t) - \gamma \beta N(\theta, t) [n_h(t) \cos^2 \theta + n_v(t) \sin^2 \theta], \\ \frac{dn_h(t)}{dt} &= \int_0^{2\pi} [\gamma \beta N(\theta, t) (n_h(t) + 1) \cos^2 \theta] d\theta - \gamma_c n_h(t), \\ \frac{dn_v(t)}{dt} &= \int_0^{2\pi} [\gamma \beta N(\theta, t) (n_v(t) + 1) \sin^2 \theta] d\theta - \gamma_c n_v(t). \end{aligned} \quad (5.1)$$

Here  $\gamma$  is the spontaneous-emission rate,  $\gamma_c$  the cavity decay rate, and  $\beta$  denotes the fraction of spontaneous photons emitted into the lasing mode. The equations are very similar to those presented in Ref. [122] and Ref [123]. Note that

Eq.(5.1) does not contain the usual pump term. In our experiment the pump pulse is so short ( $\approx 130$  fs) compared to the other time scales that the polymer laser operates in the gain-switched regime [104]. The effect of the pump pulse is well represented by setting the value of the orientational distribution of the inversion  $N(\theta, 0)$  at  $t = 0$ . The effect of the second orthogonally polarized pump pulse is taken into account by suddenly increasing the inversion  $N(\theta, \Delta\tau)$  remaining at time  $\Delta\tau$  to the value  $N'(\theta, \Delta\tau) = N(\theta, \Delta\tau) + N(\theta + \pi/2, 0)$ .

For the discussion below it is insightful to introduce effective gain functions for the two polarization directions.

$$K(t) = \int_0^{2\pi} N(\theta, t) \cos^2 \theta d\theta, \quad (5.2)$$

$$M(t) = \int_0^{2\pi} N(\theta, t) \sin^2 \theta d\theta. \quad (5.3)$$

Obviously, these effective gain functions are not independent since any change of  $N(\theta, t)$ , will affect both  $K(t)$  and  $M(t)$ . The rate equations then take the form:

$$\begin{aligned} \frac{\partial N(\theta, t)}{\partial t} &= -\gamma N(\theta, t) - \gamma\beta N(\theta, t)[n_h(t) \cos^2 \theta + n_v(t) \sin^2 \theta], \\ \frac{dn_h(t)}{dt} &= \gamma\beta(n_h(t) + 1)K(t) - \gamma_c n_h(t), \\ \frac{dn_v(t)}{dt} &= \gamma\beta(n_v(t) + 1)M(t) - \gamma_c n_v(t). \end{aligned} \quad (5.4)$$

The equations are solved numerically, using an Euler-type method in which the differentials  $dt$  and  $d\theta$  are approximated by finite steps.

### 5.4.3 Numerical results

We will present numerical results for the case that the first pump pulse is horizontally polarized and arrives at  $t = 0$ . The resulting angular distribution of the inversion at  $t = 0$  is given by  $N(\theta, 0) = 2N_0 \cos^2 \theta$ . Subsequently, this dipole distribution gets modified by spontaneous and stimulated-emission processes giving rise to an output pulse with a polarization parallel to that of the pump. At time  $\Delta\tau$ , the equally strong vertically polarized pump pulse arrives, adding a contribution of  $2N_0 \sin^2 \theta$  to the inversion  $N(\theta, \Delta\tau)$  which is left at that time.

In all our calculations we use the following values for the numerical coefficients:  $\gamma^{-1} = 0.86$  ns,  $\gamma_c^{-1} = 2.8$  ps,  $\beta = 4 \cdot 10^{-5}$ . The spontaneous emission rate  $\gamma$  has been measured directly, the cavity decay rate  $\gamma_c$  is estimated from the round-trip time of the cavity and the finesse; the latter is measured to be  $\mathcal{F} \approx 100$ . The

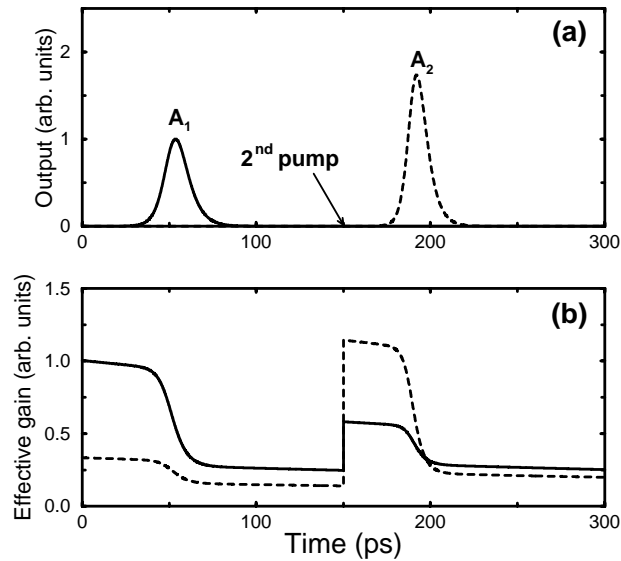


**Figure 5.6:** Numerical simulation of the real-time horizontally (solid line) and vertically (dashed line) polarized outputs of the laser for an interpulse delay of 150 ps (frame (a)). The horizontally polarized pump pulse arrives at  $t = 0$ . The moment of excitation by the second, vertically polarized pulse is indicated. Frame (b) shows the gain functions  $K(t)$  (solid) and  $M(t)$  (dashed), corresponding to the effective gain along the horizontal and vertical axes, respectively. The laser is pumped 1.6 times above threshold.

value for the coefficient  $\beta$  is based on the cavity volume and the spectral width of the photoluminescence spectrum [60].

Figure 5.6a shows the output in both polarization modes when the interpulse delay is long (150 ps). Here the laser, as pumped by a single pump pulse, operates 1.6 times above threshold. The pump pulse that arrives at  $t = 0$ , generates an output pulse with a build-up time of  $\approx 50$  ps (peak  $A_1$ ) and a polarization direction parallel to that of the pump. Just as curve (a) of Fig. 5.4 this output pulse is the result of excitation by a single pump pulse; it therefore serves as a reference. The second, much delayed, orthogonally polarized pump pulse leads to a second output pulse (peak  $A_2$ ), which is more powerful than the first pulse and is polarized parallel to its own pump pulse. Figure 5.6b shows, for this case of long interpulse delay, the evolution of the effective gain functions  $K(t)$  (solid line) and  $M(t)$  (dashed line), for the horizontally and vertically polarized signal fields, respectively. Note that  $K(0) : M(0) = 3 : 1$ , as follows from the dipole model. Due to the second pump pulse the gain functions are boosted (with the ratio 1 : 3) at

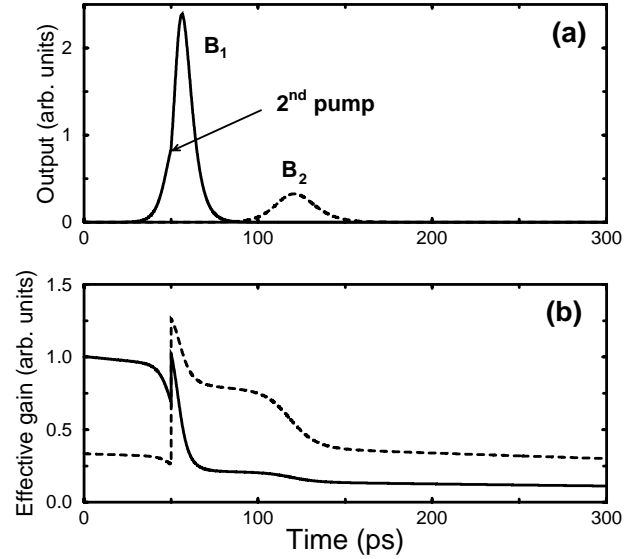


**Figure 5.7:** Results of the numerical simulation of the horizontally (solid line) and vertically (dashed line) polarized outputs of the laser for an interpulse delay of 50 ps (frame (a)). The horizontally polarized pump pulse arrives at  $t = 0$ . The moment of excitation by the second, vertically polarized pulse is indicated. Frame (b) shows the gain functions  $K(t)$  (solid) and  $M(t)$  (dashed), corresponding to the effective gain for the horizontal and vertical polarizations, respectively. The laser is pumped 1.6 times above threshold.

$t = 150$  ps. Since some inversion is still present at that time, the gain functions reach higher values than those at  $t = 0$ .

Fig. 5.7a shows the output in both polarization modes for short interpulse delay (50 ps). In this case the optical field in the cavity, being the result of the first pump pulse, is close to its peak value when the second pump pulse arrives. Now the first output pulse is enhanced (peak  $B_1$ ), as compared to the reference value, while the orthogonally polarized second pulse (peak  $B_2$ ) experiencing an increased build-up time, is suppressed. Fig. 5.7b shows that in this case the gain functions are boosted just at the time that stimulated emission starts to deplete them.

In conclusion, the numerical results show, just like the experiment, the existence of two regimes of interpulse delay. Long delays give rise to an enhanced second pulse, relative to the first pulse, while short delays generate a reduced second pulse.

## 5.5 Discussion

The numerical results of Figs. 5.6 and Fig. 5.7 are in excellent agreement with the measurements shown in Fig. 5.4. Figure 5.6, representing the results for long interpulse delay, shows the output with polarization parallel to the first pump pulse (peak  $A_1$ ) and that with polarization parallel to the second pump pulse (peak  $A_2$ ). Peaks  $A_1$  and  $A_2$  thus correspond to curves (a) and (d) of Fig. 5.4, respectively. In the short delay regime (Fig. 5.7), peaks  $B_1$  and  $B_2$  represent the output being polarized parallel to the first and second pump pulse, respectively. Peak  $B_1$  can be associated with curve (b) of Fig. 5.4, and curve  $B_2$  with curve (c) of the same figure.

Having established the existence of two regimes of interpulse delay in both the experiment and the numerical calculations we will now focus on the underlying physics. When the interpulse delay is long as in Fig. 5.6, the first output pulse has completed its full evolution by the time the second pump pulse arrives. The power associated with the tail of the first output pulse is thus comparable with the spontaneous emission flux that is emitted by the still partially excited gain medium. The output pulse following the second pump pulse thus has to build up from the noise just as the first pulse. The increased output level of the second pulse is caused by the fact that the first pulse has not fully depleted the excitation generated by the first pump pulse (see Fig. 5.6b). Consequently, the second output pulse can profit from this remnant. Obviously, for this picture to apply the interpulse delay should be small as compared to the spontaneous-emission lifetime. In the present experiment the time scales are such that this condition is fulfilled.

An interesting aspect of Fig. 5.6b is that it shows the coupling of the effective gain functions  $K(t)$  (solid line) and  $M(t)$  (dashed line) for the horizontally and vertically polarized outputs, respectively. The large initial value of  $K(t)$  gives rise to a relatively fast build up of the horizontally polarized signal field. This field depletes the inversion, affecting both gain functions  $K(t)$  and  $M(t)$ . This coupling of the gain functions originates from the fact that any dipole in the distribution  $N(\theta, t)$  contributes, with different weight factors, to both gain functions. When any dipole disappears out of the angular distribution of the inversion  $N(\theta, t)$ , both  $K(t)$  and  $M(t)$  decrease.

For short interpulse delay the evolution of the first signal pulse is not yet complete (as in Fig. 5.7). Now the first signal pulse can profit from the extra inversion supplied by the second pump pulse. This is well visible in Fig. 5.7b where the second pump pulse arrives at a time that the first signal pulse is effectively depleting its gain  $K(t)$ , represented by the solid line. Instantaneously, this gain function gets a (relatively small) boost, but now gain and signal field are large simultaneously,

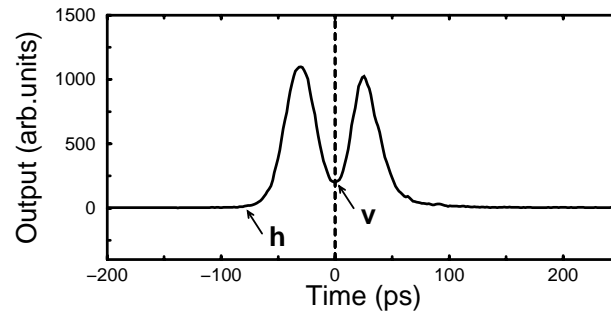


**Figure 5.8:** Measurement of the pulse shape of the horizontally polarized output for an intermediate value of the delay ( $\approx 80$  ps) between the horizontally and vertically polarized pump. The vertically polarized pump pulse arrives at  $t = 0$ .

resulting in a big boost of the output and very efficient depletion of the gain  $K(t)$ . Interestingly, the gain  $M(t)$  for the initially non-lasing polarization has become quite large as a result of the two pump pulses, but it is ‘sympathetically’ depleted by the first output pulse. The remaining value of  $M(t)$  is just sufficient to generate a comparatively weak vertically-polarized output pulse. This second pulse is smaller than the reference value of Fig. 5.6 because the gain it experiences during buildup has partially been removed by the first pulse.

In the results presented so far the polymer laser emits two signal pulses, one for each polarization channel. This holds for almost all values of the interpulse delay. However, for values of this delay slightly larger than that of Fig. 5.7 the decaying first signal pulse is revived by the second pump pulse. A double pulse appears in the channel corresponding to the polarization of the first pump pulse followed by a single signal pulse in the other output channel. A time-domain measurement on the double pulsed output is shown in Fig. 5.8. The physics, here, is the same as that discussed in the framework of Fig. 5.7.

Just like the output boost of the signal in Fig. 5.7, the revival of the signal pulse in Fig. 5.8 is driven by a pump pulse of the ‘wrong’ polarization. After the second pump pulse, the gain anisotropy strongly favors the nonlasing polarization mode. However, the latter contains very few photons in contrast to the lasing polarization mode; the result is highly efficient stimulated emission in the lasing polarization mode and normal (slow) buildup of the polarization mode that had been nonlasing so far. A memory effect similar to the one observed here has been observed in polarization-switching CW-driven VCSELs [124]. In that case the memory effect expresses itself as hysteresis of the lasing polarization across the polarization switch point.

An important property of our polymer gain material is that the pump-induced

gain anisotropy relaxes so slowly that this relaxation can be neglected, considerably simplifying the analysis. If, instead, we would have studied a standard laser dye in a low-viscosity solvent we would not have been allowed to make such a simplifying assumption. For instance, for Coumarin 153 (a dye that photoluminesces in the same spectral region as our polymer), dissolved in methanol, the dipolar reorientation time at room temperature is  $\approx 35$  ps [94, 119]. This reorientation time is of the same order as the buildup time of the signal pulse in our laser under the prevailing pumping conditions. In that case there is appreciable relaxation of the gain anisotropy during the buildup time, but the relaxation is too slow to follow the (anisotropic) depletion of the gain when the signal pulse is really strong. The result is that the first signal pulse experiences reduced gain because of the reduced anisotropy, and that the excitation is less effectively depleted. This leads to the conclusion that the enhancement/suppression in the limit of short interpulse delay will be reduced. For long interpulse delay the second signal pulse can considerably profit from the remaining excitation which has become completely isotropic during the interpulse delay. Consequently, the enhancement of the second output pulse will be larger in this limit. This reasoning shows that for intermediate relaxation times of the gain anisotropy the physical picture of the polarization cross coupling gets more complicated. In the limit that the reorientation time is sufficiently fast that it can follow the gain depletion, the gain has become effectively isotropic at all times; in that limit the polarization properties of the laser will be mainly determined by unintended cavity anisotropies.

## 5.6 Time-integrated output

The discussion of the previous sections provides an excellent framework to understand our experimental results on the time-integrated signals in the horizontal and vertical output channels as shown in Fig. 5.5. For the remaining discussion we will restrict ourselves to positive values of the delay, where the horizontal pump pulse precedes its vertical partner. In that case the reference value is given by the level of the horizontal output at long delay, as in Figs. 5.4a and 5.6a. Figure 5.5 shows the enhancement of the vertical output at long delay and that of the horizontal output at short delay. It also shows that at short delay, the vertically polarized output is suppressed. For the pump strength of Fig. 5.5 (normalized pump parameter  $r = 1.6$ ), the switch point lies at a delay of about 60 ps.

Clearly, the overall features of these time-integrated data, i.e., suppression or enhancement, and the existence of a switch point where the time-integrated output in both channels are equal, will persist when the laser is driven closer to or further above threshold. This is indeed the case, as shown in Fig. 5.9, where the

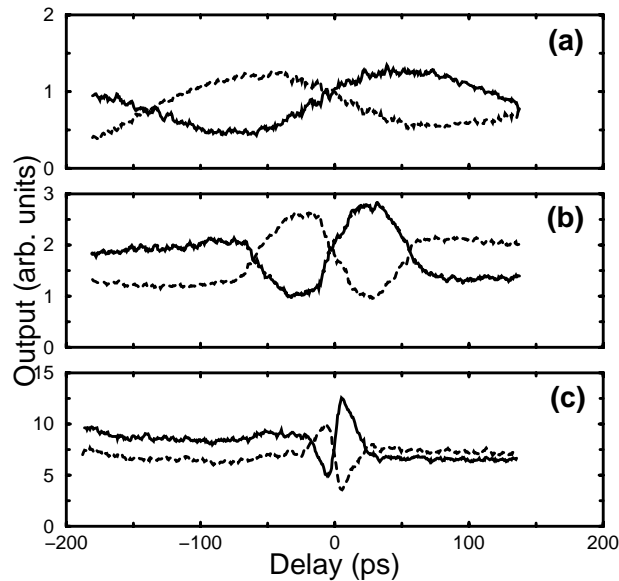


**Figure 5.9:** Measurement of the time-integrated outputs of the horizontally (solid line) and vertically (dashed line) polarized components as a function of the inter-pulse delay for values of the normalized pump parameter equal to  $r = 1.2$  (a),  $r = 1.6$  (b) and  $r = 6$  (c).

time-integrated output in both channels as a function of pump delay is plotted for values of the pump parameter equal to  $r = 1.2$ ,  $1.6$  and  $6$ . For increasing pump strength one sees that the switch occurs at shorter and shorter delay, and that the difference in output level at long delays gets smaller. These experimental results are fully corroborated by the time-integrated results of our rate-equation model as presented in Fig. 5.10. The underlying physics is that when the pump parameter is increased the pulses get more powerful while their build-up time decreases. Consequently, the gain will deplete more fully and do so at an earlier time. The boundary between the regimes of short and long inter-pulse delay, roughly given by the end of the first emitted pulse, thus also shifts to earlier times. For large values of the pump parameter and large inter-pulse delay the first emitted pulse will so effectively deplete the gain, that the remainder is exceedingly small. This applies to both the gain functions  $K(t)$  and  $M(t)$ . The second pump pulse will now generate a gain that is essentially the same as that available to the first pulse (see Fig. 5.10c). The labels  $A_{1,2}$  and  $B_{1,2}$  as indicated in Fig. 5.10b correspond to the peaks having the same labels in Fig. 5.6 and Fig. 5.7, respectively

The switch occurs when the time-integrated outputs in both polarization chan-

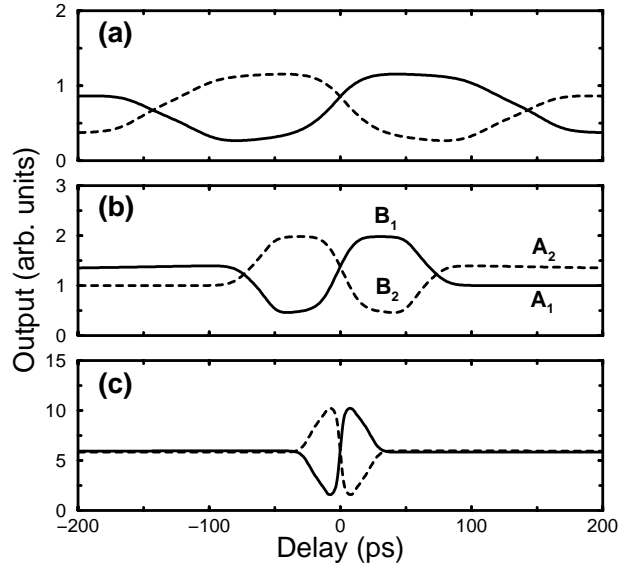


**Figure 5.10:** Results of a numerical simulation of the horizontally (solid line) and vertically (dashed line) polarized time-integrated outputs for values of the normalized pump parameter equal to  $r = 1.2$  (a),  $r = 1.6$  (b) and  $r = 6$  (c) as a function of the delay time between the pump pulses. Positive delay corresponds to the horizontally polarized pump pulse arriving first.

nels are equal. At that value of the interpulse delay the second pump pulse excites the gain medium just when the first output pulse has extinguished. This value of the delay thus provides a convenient measure for the buildup and decay of a single pulse from such a microlaser. Therefore, the time-integrated signals allow us to get a value of a characteristic time much shorter than the response time of the measurement instruments that are used. The switch also tells us the maximum pulse repetition rate with which this laser can be driven so that it delivers well-separated output pulses, free of a CW background.

## 5.7 Conclusion

A polymer microlaser driven by two mutually delayed, orthogonally polarized, femtosecond pulses has a pulsed output in the two polarization modes defined by the polarization of the pump pulses. These two output pulses show strong cross coupling with a remarkable dependence on the interpulse delay. The basis for this interesting behavior lies in the pump-induced gain anisotropy (the dominant

anisotropy in the microlaser) and the very different time scales of our polymer microlaser. These are the duration of the pump pulse ( $\approx 0.1$  ps), the buildup and decay of the intracavity field (10 – 100 ps, depending on the pump energy), the spontaneous-emission lifetime of our fluorophore ( $\approx 1$  ns) and the dipolar orientational relaxation time ( $> 1$  ns). An important property of the polymer is that the latter time is unusually long, considerably simplifying the physical picture.

We distinguish two regimes: for short delay the second pump pulse arrives at the moment that the signal field in the cavity, resulting from the first pump pulse, is still large. For long delay the second pulse arrives at the moment that the field resulting from the first pump pulse has become negligibly small, but some excitation may still be present in the gain medium. The existence of these regimes fully explains the observation that the dominant output polarization of the microlaser switches direction when the interpulse delay is scanned.

For small interpulse delay the field that is already present in the cavity benefits immediately from the fresh inversion that is provided by the second (orthogonally polarized) pulse. In contrast, the other polarization mode, still needs to build up from the spontaneous-emission level. As a result, the latter experiences less gain and is therefore suppressed in this regime. For long delay, however, no field resulting from the first pump pulse is left when the inversion is boosted by the second pump pulse. In that case, the second output pulse profits from the excitation left by the first pump pulse and is, consequently, enhanced. The existence of these two regimes, a direct result of the specific order of the various time scales in the microlaser, forms the physical basis for the cross-coupling effects that we discuss here.

An attractive aspect of our configuration with orthogonal pump pulses lies in the fact that the effect of the individual pump pulses on the laser output can be easily separated by measuring both polarization components separately. In this way much more information on the dynamics can be retrieved as compared to the case where two pump pulses with parallel polarization were used.



## Chapter 6

---

### Measuring the gain dynamics in a conjugated polymer film<sup>1</sup>

We present a simple method for measuring the gain lifetime in a conjugated polymer film by optically exciting the film with two mutually delayed ultrashort pump pulses. When the pump is set at such a power level that amplified spontaneous emission marginally develops along the polymer waveguide, the total output emitted from its edge decays exponentially as a function of the interpulse delay. The corresponding decay time represents the lifetime of the gain of the polymer material.

Conjugated polymers are believed to carry great promise for application as gain material in organic solid-state lasers. They cover the whole visible spectral range and offer the prospect of being electrically driven. Recently, a first electrically driven organic laser has been realized using a crystalline material [125], but lasing from conjugated polymers has so far only been achieved in an optically pumped device. In the first optically pumped thin-film polymer laser a planar microcavity was employed [43]. Since then various other optically driven polymer lasers have been reported, also with cylindrical microcavities [47, 126] and distributed-feedback structures [48–50]. In most cases the polymer film is applied by spin coating a polymer solution on top of a substrate, resulting in a layer that is a few hundred nm thick.

In the planar microcavity, the polymer layer is sandwiched between two highly reflecting mirrors. The laser light then propagates perpendicular to the active layer, just as in a vertical-cavity surface-emitting semiconductor laser. In this configuration the gain length is limited by the thickness of the layer or the absorption length of the pump light (which usually doesn't exceed 100 nm). Contrary, this limit doesn't occur for configurations in which the generated field propagates along the polymer film, acting as a waveguide. In this case the gain length is determined by the dimensions of the excitation beam, which offers the possibility to

---

<sup>1</sup>S. A. van den Berg, V. A. Sautenkoy, G. W. 't Hooft, and E. R. Eliel, submitted for publication.

generate strong amplified spontaneous emission (ASE) along the waveguide, even in the absence of any feedback [127–129].

To characterize the suitability of a specific conjugated polymer film for laser applications, the gain and loss and their corresponding dynamics need to be measured. The pump-probe technique has proven to be especially powerful here, providing a tool to measure stimulated emission and photoinduced absorption on a sub-picosecond time scale [32, 33, 36, 130–133]. In this technique, the polymer film is excited with a femtosecond pump pulse and the resulting change in optical transmission ( $\Delta T/T$ ) is measured as a function of time by probing the excited region with a very weak, delayed, ultrashort probe pulse. Usually the probe pulse has a very broad spectrum, allowing spectrally resolved measurements of stimulated emission ( $\Delta T/T > 0$ ) and photoinduced absorption ( $\Delta T/T < 0$ ). The setup for pump-probe measurements is sketched in Chapter 1, Fig. 1.4. In addition to yielding the actual value of  $\Delta T/T$  at zero delay for all probe wavelengths, this technique also provides data on the variation of  $\Delta T/T$  as a function of time. Specifically, one can determine the decay time of the stimulated emission. In order to achieve lasing in a given device, this decay time should at least exceed the time that is needed for the laser field to build up in this device. In solid polymer films  $\Delta T/T$  usually diminishes on a time scale much shorter than the photoluminescence lifetime of the polymer. Various mechanisms which have been heavily discussed in literature lie at the root of this fast decay [42, 131, 134–136]. These include photo-oxidation [35], film morphology [37] and pump intensity [132].

In this chapter we put forward a new and simple method for measuring the decay time of the gain in thin solid films of a conjugated polymer. We employ the waveguide configuration and excite the film in a pencil-shaped region using *two* pump pulses, with a variable interpulse delay. We measure the time-integrated output of the optically excited stripe as a function of interpulse delay. We directly extract the gain lifetime from these measurements.

Our sample is made by spin coating a heated and stirred solution of a PPV-copolymer in toluene (5 mg/ml) on top of a glass substrate. The copolymer, referred to as HB1221, consists of four different phenyl-PPVs (25% each, see Appendix B); the chemical structure and synthesis route have been published in Ref. [137]. The substrate-film-air stack (with refractive indices  $\eta_{\text{glass}} = 1.46$ ,  $\eta_{\text{poly}} \approx 1.7$  and  $\eta_{\text{air}} = 1$ , respectively) forms an asymmetrical waveguide with a thickness of  $\approx 100$  nm, supporting the propagation of the fundamental TE-mode [128, 138]. After spin coating the substrate is broken in order to access the more homogeneous part of the film in the middle of the substrate and to create a sample with relatively sharp edges. We excite the film with two ultrashort pump pulses ( $\approx 130$  fs,  $\lambda = 400$  nm, 1 kHz repetition rate), one being delayed relative

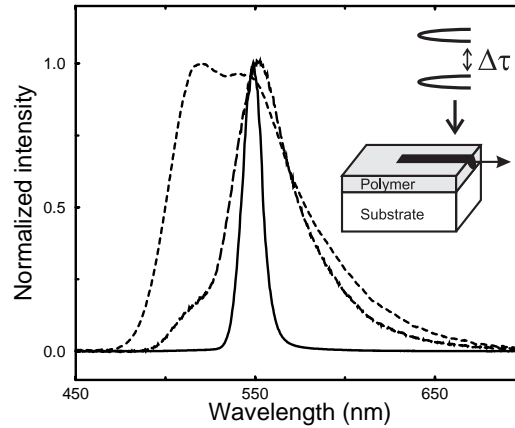


**Figure 6.1:** Emission spectra measured for various pump energies. The dashed curve shows the spontaneous-emission spectrum that is emitted from the surface of the waveguide for very low pump intensity. The solid and long-dashed curves show the output emitted from the edge of the waveguide at high pump energy ( $> 10$  nJ) and some intermediate pump energy, respectively.

to the other. We shape the excitation beam using lenses and a slit to make the intensity distribution homogeneous. Subsequently it is focussed into a stripe of  $1 \times 0.02$  mm on the sample. We measure the light emitted along the stripe. The setup is shown in the inset of Fig. 6.1.

First we provide some characteristics of the polymer waveguide under single-pulse excitation. The spectrum of the emitted light, as obtained with a fiber spectrometer having a resolution of 1 nm, is shown in Fig. 6.1 for a range of pump energies. At low pulse energy ( $< 1$  nJ) the broad photoluminescence spectrum of the polymer film is observed (dashed curve). When the pulse energy is increased a narrow peak develops at  $\lambda = 548$  nm (long-dashed curve), which completely comes to dominate the output at even higher pump energies (10 nJ, solid curve). Another characteristic is the input-output curve of the stripe as shown in Fig. 6.2.

It shows the temporally and spectrally integrated output that is emitted from the edge of the polymer film. The signal is measured with a slow photodiode in combination with a gated integrator. Notwithstanding the absence of a feedback structure, the curve shows a clear threshold around 5 nJ. In the vicinity of this point the input-output curve is highly nonlinear. We will employ this nonlinearity to obtain insight into the dynamics of the gain.

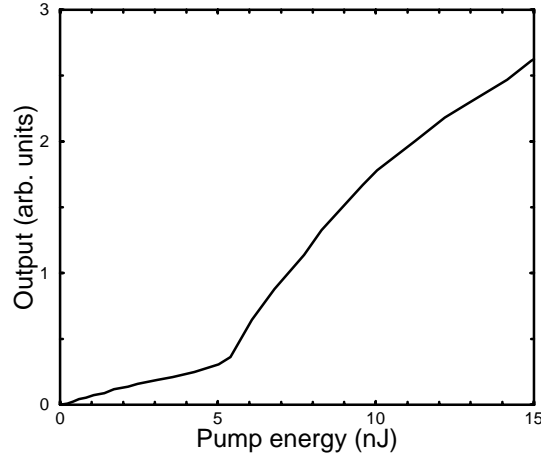


**Figure 6.2:** The temporally and spectrally integrated output as emitted from the edge of the waveguide measured as a function of the pump energy.

The output spectral power on one side of the stripe with length  $l$  is given by:

$$P(\lambda, t) = A(\lambda) \frac{g(\lambda, t)}{g(\lambda, t) - \alpha} (e^{(g(\lambda, t) - \alpha)l} - 1). \quad (6.1)$$

Here,  $g(\lambda, t)$  represents the net optical gain, as induced by the pump pulse. The linear absorption in the waveguide is denoted by  $\alpha$ ;  $A(\lambda)$  is related to the photoluminescence spectral power per unit wavelength. The optical gain is associated with the presence of primary excitons, which may be described as a four-level system. The gain lifetime is determined by radiative and nonradiative decay of the exciton population. Eq. (6.1) has been derived from the laser rate equations, assuming that the gain decays slowly as compared to the single-pass transit time along the stripe ( $\approx 5$  ps); the latter time will be neglected henceforth. Because we use ultrashort pump pulses, the gain coefficient is at its maximum value at  $t = 0$  and subsequently diminishes. We assume the gain decays via a single exponential.

In order to measure the decay time of the gain in our waveguide we excite the polymer film at such a power level that there is very little stimulated emission, the output being dominated by spontaneous emission (e.g. at 4 nJ, see Fig 6.2). After some delay we reexcite the film with a second pump pulse, identical to the first. We measure the time-integrated signal emitted by the stripe upon this dual-pulse excitation as a function of the interpulse delay. For excitation with two pump pulses of equal intensity, having an interpulse delay  $\Delta\tau$ , the emission is given by Eq.(6.1), with:

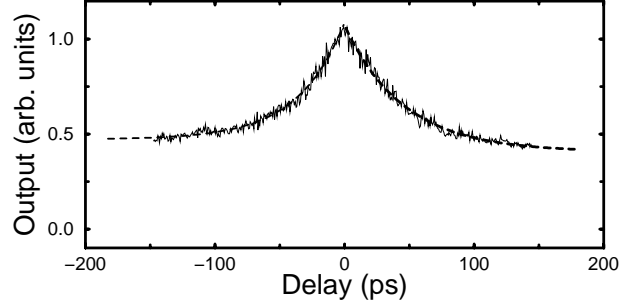


**Figure 6.3:** The total edge-emission under double-pulse excitation (4 nJ/pulse), measured as a function of the interpulse delay. The dashed lines represent single exponential fits.

$$g_d(\lambda, t) = \begin{cases} g_s(\lambda, t) & t < \Delta\tau \\ g_s(\lambda, t) + g_s(\lambda, t - \Delta\tau) & t \geq \Delta\tau. \end{cases} \quad (6.2)$$

Here  $g_d(\lambda, t)$  represents the double-pulse gain coefficient, while the gain upon single-pulse excitation is represented by  $g_s(\lambda, t)$ . We now define  $U_s$  and  $U_d(\Delta\tau)$  as the output energies at the edge of the film for single and double pulse excitation, respectively. The output energy is obtained by integrating  $P(\lambda, t)$  over both time and wavelength. When the delay is much longer than the lifetime of the gain, the time-integrated double-pulse output simply equals twice the single-pulse output ( $U_d(\Delta\tau) = 2U_s$ ). However, when the delay is short, the double pulse output  $U_d(\Delta\tau)$  is larger than  $2U_s$  because of the nonlinearity of Eq.(6.1). This is most easily seen at zero delay. The input-output curve immediately shows that the output at 8 nJ pump energy is considerably larger than twice the output at 4 nJ. It is easy to show that, for  $0 < (g_s(0) - \alpha)l < 1$ , the excess output

$$U_{\text{excess}}(\Delta\tau) = U_d(\Delta\tau) - 2U_s \quad (6.3)$$

decays exponentially as a function of the interpulse delay  $\Delta\tau$ , assuming  $g_s$  to decay exponentially. In particular, it can be shown that the decay rate of  $U_{\text{excess}}$  directly yields the decay rate of the gain coefficient  $g_s(t)$ .

In Fig. 6.3 we show the time-integrated output that is emitted from the edge of our substrate as a function of the interpulse delay at a single-pulse excitation energy of 4 nJ/pulse ( $\approx 20 \mu\text{J}/\text{cm}^2$ ). As expected, the curve is symmetrical with respect to zero delay. The fitted exponentials (dashed curves), are in excellent agreement with the experimental data, indicating that the excess output indeed decays exponentially, the decay time being  $\approx 40$  ps. The gain coefficient is thus

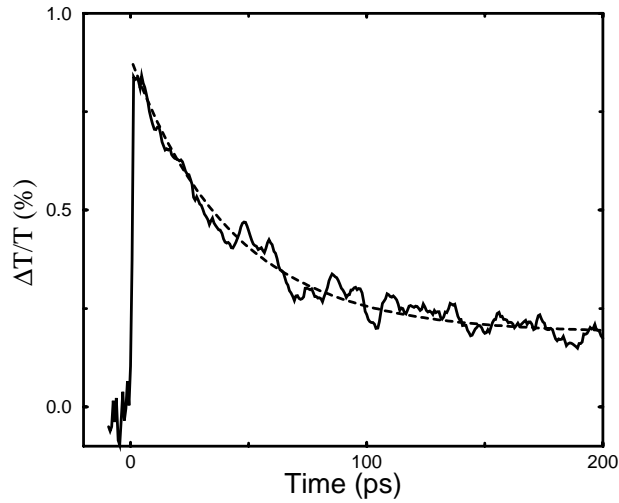


**Figure 6.4:** Measurement of the lifetime of the gain at 548 nm using the pump-probe technique for a pump intensity of  $\approx 80 \mu\text{J}/\text{cm}^2$ . The dashed line represents a single exponential curve fit.

estimated to have a decay time of  $\approx 40$  ps as well. The asymptotic values of the fits correspond to twice the single pulse output, since in the long-delay limit the two output pulses become independent.

In order to check the validity of our approach we have also applied the conventional pump-probe technique to our sample, again using a low excitation density ( $\approx 80 \mu\text{J}/\text{cm}^2$ ). The probe wavelength has been set at  $\lambda = 548$  nm (gain maximum), the same wavelength as selected by the gain medium when ASE develops in the waveguide. The results are shown in Fig. 6.4, representing a single exponential decay of 43 ps, in excellent agreement with the result obtained with the method introduced in this chapter.

Our technique thus provides a reliable tool to measure the lifetime of the gain in a thin film of light-emitting polymers. The primary advantage of the technique introduced here is its simplicity. No white-light generation is required and due to the long gain length, the signals are large. This makes the method well suited for studying systems that exhibit very small gain. Moreover the gain lifetime is automatically measured at the wavelength at which the net gain is maximum and stimulated emission will build up.

In conclusion, when pumping a polymer waveguide with two excitation pulses at such a power level that the excitation energy of a single pump pulse is just below the threshold value for ASE, the total output upon double pulse excitation

### *Measuring the gain dynamics in a conjugated polymer film*

---

strongly depends on the interpulse delay. We have shown that this behavior can be exploited to measure the lifetime of the gain in a very simple way: the total output emitted from the edge of the waveguide decays exponentially as a function of the interpulse delay with a characteristic time that represents the lifetime of the gain.



## Appendix A

---

### The optical gain in pump-probe experiments

In this chapter I have focussed on the method developed by us to measure transient gain in polymeric thin films, and on the decay of that gain. The value of the measured small-signal gain has, however, not been addressed: this forms the subject of this appendix.

In Fig. 6.4 the amplification of the probe pulse is  $\approx 0.8\%$  at  $t = 0$ . Since the thickness of the polymer layer is  $\approx 100$  nm, the optical gain at  $t = 0$  is found to be approximately  $800 \text{ cm}^{-1}$ . About 50% of the pump light is absorbed in the film. If we assume that all absorbed pump photons lead to excitons that contribute to the gain, the stimulated emission cross-section  $\sigma$  can be estimated from  $g = \sigma Nl$ . Here  $g$  represents the total gain in the film ( $g = 0.008$ ),  $N$  is the density of absorbed photons and  $l$  denotes the film thickness. In the experiment the pump energy per unit area is about  $80 \mu\text{J}/\text{cm}^2$ , corresponding to an excitation density of  $N = 8 \times 10^{18} \text{ cm}^{-3}$ . These values provide us with a cross-section  $\sigma \approx 10^{-16} \text{ cm}^2$ , in good agreement with values reported for other conjugated polymers [55,57].

In order to avoid saturation, the measurement discussed above has been performed at a relatively low pump energy. Higher peak values of the gain are obtained at increased pump energies, with values up to 4%. A result of a pump-probe measurement at an excitation energy of about  $1 \text{ mJ}/\text{cm}^2$  is shown in Fig. A.1. At such high pump energies the gain is observed to decay much faster as compared to the situation of Fig.6.4. (Note the different scale of the time-axis.) In the present case the decay cannot be fit with a single exponential. As shown in the figure, a biexponential fit, however, works out well. Here we fix the decay time of the slow component to the value (43 ps) found from the curve fit of Fig. 6.4. The fast component is then found to decay within  $\approx 5$  ps. From the rising slope at  $t = 0$  the time resolution is estimated to be better than 1 ps. Obviously, the fast decay is related to a process that depends nonlinearly on the pump energy. In the literature several mechanisms have been brought forward to explain the fast component, such as exciton-exciton annihilation and amplified spontaneous emission (ASE) [139]. In the present case depletion of the gain by ASE in the plane of the polymer film is quite possible, since the size of the pump spot ( $\approx 20 \mu\text{m}$ ) in the pump-probe experiment may well be sufficiently large.

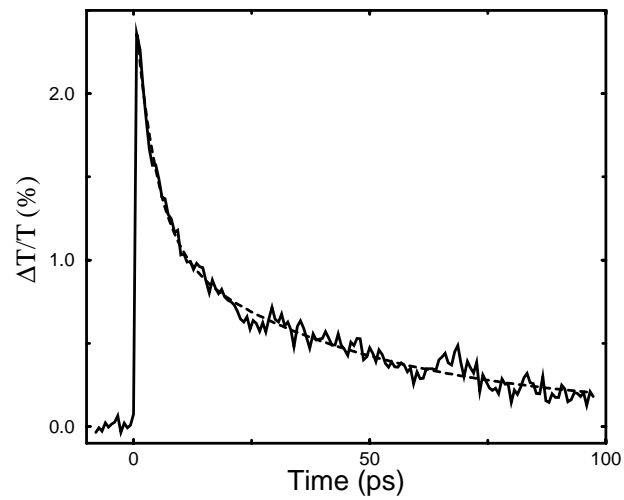


**Figure A.1:** Pump-probe results for a pump energy of about  $1 \text{ mJ/cm}^2$ . The dashed line represents a biexponential fit.

Although an optical gain of over  $1000 \text{ cm}^{-1}$  (a few % in 100 nm) looks promising for building a laser, one should realize that this gain decays very rapidly. This explains why all solid polymer lasers that have been realized so far have short cavities, since only in that case a sufficient number of cavity round trips can be made within the gain lifetime.

## Appendix B

### The polymer HB1221

The conjugated polymer HB1221 used in Chapter 5 has been developed for use in electroluminescent devices [137]. It is a copolymer consisting of four different phenyl-PPVs, mixed in equal weight. The repeat units are shown in Fig. B.1.

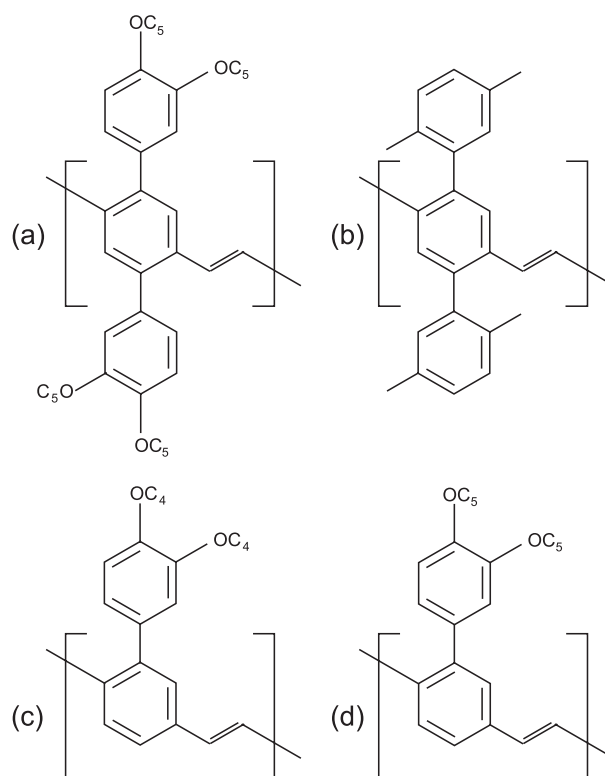


**Figure B.1:** The polymer HB1221, consisting of the units: (a) 2,5-bis(3,4-bis(3-methylbutyloxy)phenyl)-*p*-phenylene vinylene; (b) 2,5-bis(2,5-dimethylphenyl)-*p*-phenylene vinylene; (c) 2-(3',4'-bis(2-methylpropyloxy)phenyl)-*p*-phenylene vinylene; (d) 2-(3',4'-bis(2-methylbutyloxy)phenyl)-*p*-phenylene vinylene.



## Chapter 7

---

### Time-domain study of emissive states in a PPV<sup>1</sup>

We report on the photophysics of a phenyl-substituted PPV both in solution and as a film. For both systems, we have studied the decay of the photoluminescence and of the emission anisotropy for a large set of wavelengths spanning the entire photoluminescence spectrum. At long wavelengths the decay behavior is that of an interchain species. At the shortest wavelengths the decay of the photoluminescence from the film is observed to have a long-lived component, in addition to the rapidly decaying component usually associated with energy transfer. We attribute this slow component to emission by isolated intrachain excitons with reduced nonradiative relaxation.

#### 7.1 Introduction

The first operation of a light-emitting diode based on electroluminescence from poly(*p*-phenylene-vinylene), PPV [10], has been followed by a large worldwide effort to discover new and efficient organic electroluminescent materials, to understand their conducting and luminescent properties, and to develop technologies to enable applications. A prime attraction of these materials is that they are like a semiconductor in that they emit light and allow charge transport, and that they can be processed like a plastic. Exactly because of this combination conjugated polymers are believed to carry great promise for completely novel applications such as flexible, miniature displays or extremely large luminescent panels. An attractive feature of these materials is the possibility of chemical tuning, i.e., the emission wavelength can be adjusted by modifying the chemical structure of the polymer, in particular the sidegroups attached to their main chain [22].

The photophysics of these materials is, notwithstanding an intense effort, not yet completely understood. This applies in particular to the technologically relevant situation where the polymer forms a thin film. But even when the polymer is

---

<sup>1</sup>V. A. Sautenkov, S. A. van den Berg, G. W. 't Hooft, and E. R. Eliel, submitted for publication.

in solution at low concentration, the picture is more complicated than one would expect [140, 141]. The main difficulty arises because all these materials contain a variety of emitting species. This is not caused by a lack of chemical purity; rather it is intrinsic to the fact that polymer chains overlap with themselves and with each other.

The general accepted view is that, in low-concentration solutions, the photoluminescence (PL) is primarily due to the decay of the primary exciton [140], more properly called a Coulomb-bound electron-hole pair. This decay gives rise to a characteristic PL spectrum consisting of a 0-0 band and well-resolved vibronic side modes. The PL quantum yield is high ( $> 50\%$ ) and the decay time of the photoluminescence is of order 0.3-1.2 ns. The characteristics of light-emitting polymer *films*, made from the same material, are usually quite different. The PL quantum yield is considerably reduced [31, 142] and, for many polymers, the PL spectrum is much less well structured, is broadened and considerably red shifted. The decay time of the PL is, for many conjugated polymer films, larger than that of the corresponding solutions. Time-resolved measurements of the photoluminescence reveal the presence of a weak, long-lived red emission [30, 37, 143, 144]. This red emission, being characteristic for the film, is commonly associated with the emission by *interchain* species such as aggregates [145, 146], excimers, exciplexes [147], polaron pairs [148, 149], spatially indirect excitons [145], etc. Such interchain species are expected to have a lower oscillator strength than the primary exciton [30].

Information about intrachain and interchain processes in polymers has also been obtained by measuring the polarization anisotropy of the (time-dependent) photoluminescence [146, 150–152]. This anisotropy is sensitive to energy migration inside the inhomogeneously broadened density of states. In this chapter we present a study of the photophysics of a phenyl-substituted PPV, developed to have a high PL efficiency in the condensed phase. We measure the PL spectrum, the spectrally resolved PL decay, and the time and spectrally resolved PL anisotropy for both a neat film and a solution of the polymer. By comparing the results for the film with those for the solution we are able to separate intrachain from interchain effects.

## 7.2 Experiment

The conjugated polymer under study is the phenyl-substituted PPV, poly[2-phenyl-(2'-decyloxy)-1,4-phenylene-vinylene]. It exhibits good solubility in standard organic solvents and has a high electroluminescent efficiency when made into a thin film [65]. Our base material is a solution of the polymer in chlorobenzene at a

concentration of 1 g/l. We fill a small cuvette with the solution to measure the PL spectrum and PL decay of the solution. Additionally, we form thin films by spin coating the solution on a BK7 substrate in a dry nitrogen atmosphere. The samples are kept and studied permanently under such atmosphere to avoid degradation due to the presence of oxygen and/or water. The optical density of the films is measured to be approximately 2 at a wavelength of 400 nm.

We excite the polymer, either in solution or as a thin film, with the frequency-doubled output ( $\lambda = 400$  nm) of an ultrafast (60 fs pulse duration) Ti:sapphire laser (Kapteyn-Murnane Laboratories) operating at a repetition rate of 82 MHz. The excitation pulses from the laser are heavily attenuated in order to remain in the linear-response regime and to avoid degradation of the sample. The laser beam is vertically polarized and is focussed to a spot of 1 mm diameter at the sample. The photoluminescence emitted by the film is collected with a lens and imaged on the input aperture of our detection equipment. Steady-state PL spectra are recorded with a simple fiber-optic spectrometer (Ocean Optics S2000), while we use time-correlated single-photon counting to measure PL in the time domain. With a multichannel-plate based photomultiplier (Hamamatsu model R3809U-52) our setup has a temporal resolution of  $\approx 40$  ps. In the time-domain measurements we use spectral filters (bandwidth 10 nm,  $10^{-7}$  out-of-band transmission) to select specific wavelength bands in the range 472 – 600 nm. We include a polarizer in our setup to separately record the polarized and sensitized luminescence.

Figure 7.1 shows the steady-state absorption spectrum together with the time-integrated PL spectrum of the polymer, both in solution (dashed curves) and as a thin film (solid lines). For the solution the absorption spectrum peaks at  $\lambda = 430$  nm, whereas the PL spectrum has its maximum at  $\lambda = 490$  nm. The absorption spectrum of the film is similar to that of the solution, peaking at  $\lambda = 428$  nm. As compared to that of the solution, the PL spectrum of the film is red shifted, relatively broad and structureless, with a peak at  $\lambda = 538$  nm. When excited with more powerful pump pulses, generated by an amplified laser system, we observe amplified stimulated emission from our film, centered around  $\lambda = 545$  nm.

### 7.3 Photoluminescence decay

For the polymer *in solution* the temporal evolution of the PL is almost wavelength independent and is well described by a single exponential:

$$S = S_0 \exp(-\gamma t), \quad (7.1)$$

where  $\gamma$  represents the PL decay rate. The decay takes place due to a combination of radiative (spontaneous emission) and nonradiative processes, which have, for

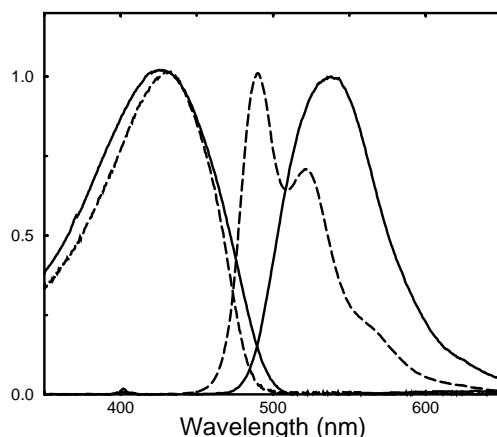


**Figure 7.1:** Absorption and photoluminescence spectra of the phenyl-substituted PPV polymer under study. The dashed lines show the spectra for the polymer dissolved in chlorobenzene while the solid lines display the absorption and emission spectrum of a spin-coated polymer film.

the polymer at hand, roughly equal rates. Curve (a) in Fig. 7.2 shows the decay of the PL of the dissolved polymer as measured in a narrow interval around  $\lambda = 472$  nm, i.e., in the blue wing of the pure singlet-exciton transition (see Fig. 7.1).

The PL decay of the *thin film* shows a strong wavelength dependence, and can no longer be described by a single exponential. Rather, the PL decay shows both a fast and a slow component, the latter becoming slower with increasing wavelength. Additionally, for the longer emission wavelength, one observes that the PL rise time is no longer instrumentally limited as is the case for shorter emission wavelengths. To illustrate the wavelength dependence of the PL decay we include in Fig. 7.2 decay curves for the thin film (solid lines), as recorded in wavelength bands around  $\lambda = 472$  (curve (b)) and  $\lambda = 600$  nm (curve (c)). To simplify the comparison of the various decay curves in Fig. 7.2, they have all been normalized to unity at their respective maxima.

In the standard description of light emission by conjugated polymers *intra-chain* energy migration and relaxation play an important role [153]. The singlet exciton, generated through the photo-excitation process, is thought to migrate from regions of short conjugation length to regions of longer conjugation length, thereby reducing its energy. This process takes place on a time scale of order 100 ps. Additionally, there can be *interchain* energy transfer due to dipole-dipole coupling, for instance through the Förster process [154]. This model is generally believed to be incomplete. Experimental evidence abounds that one has to assume

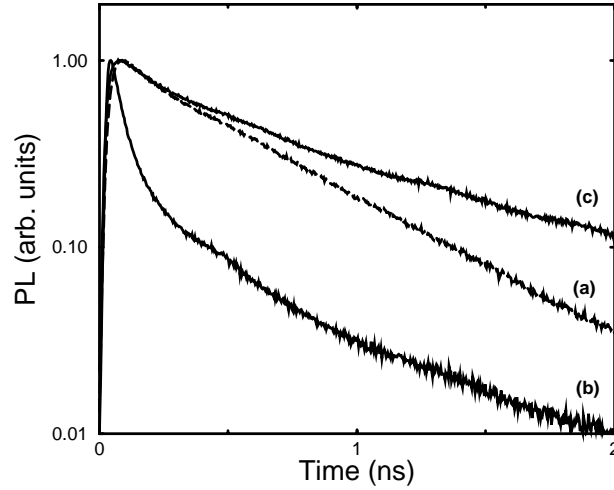


**Figure 7.2:** Decay of the photoluminescence of the polymer as excited by an ultrashort pulse at  $\lambda = 400$  nm. Curve (a) shows the emission at  $\lambda = 472$  nm by the dissolved polymer while curves (b) and (c) give the results for the polymer film at a wavelength of  $\lambda = 472$  nm and  $\lambda = 600$  nm, respectively.

the presence of at least two types of excitation: intrachain excitons and long-lived, red-emitting interchain species, such as excimers. These excitations are coupled through a one-way transfer from exciton to excimer. This transfer takes place in a time comparable to the response time of our setup ( $\approx 40$  ps). Note that not all primary excitons need to follow this path. The presence of a long-lived component in the film PL at  $\lambda = 472$  nm suggests that at least some of the primary excitons survive.

We parametrize the PL decay by a biexponential:

$$S(t, \lambda) = S_{\text{fast}}^{\lambda} \exp(-\gamma_{\text{fast}}^{\lambda} t) + S_{\text{slow}}^{\lambda} \exp(-\gamma_{\text{slow}}^{\lambda} t), \quad (7.2)$$

where  $S_{\text{fast}}^{\lambda}$  and  $S_{\text{slow}}^{\lambda}$  are proportional to the population of the fast-decaying and the slow-decaying species that emit at wavelength  $\lambda$ , respectively. These species decay at rates  $\gamma_{\text{fast}}^{\lambda}$  and  $\gamma_{\text{slow}}^{\lambda}$  respectively. Figure 7.2 shows that the slowly decaying component can indeed be described by an exponential. Our parametric description of the luminescence fits our experimental data quite well, particularly at longer wavelengths.

For  $\lambda > 515$  nm we associate the slowly decaying component of the PL with the excimer, and the component with fast decay with the exciton, each emitting at that specific wavelength. In the extreme blue wing of the PL spectrum we make a different connection; there we associate the fast decaying component of

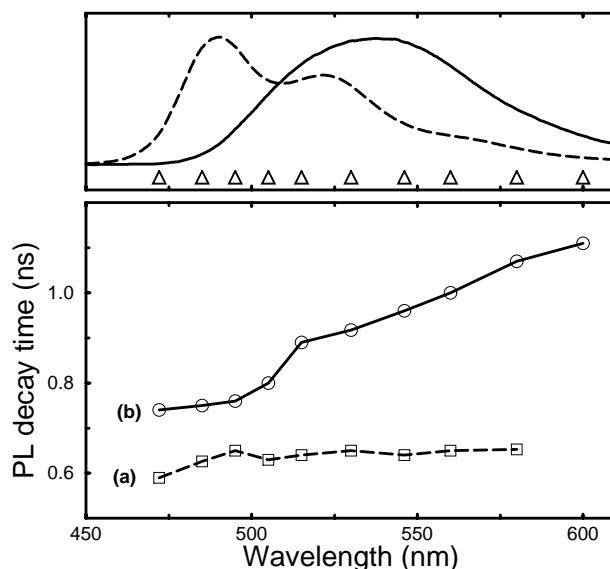


**Figure 7.3:** Upper frame: PL spectra measured for a solution (dashed line) and for a film (solid line). The triangles indicate the midband positions of the narrow-bandwidth (10 nm) filters to selectively measure the wavelength dependent PL decay. Lower frame: The dashed curve shows the wavelength dependence of the decay time of the PL from a solution; the solid curve displays the behavior of the decay constant associated with the slow component of the PL emitted by a film.

the PL with the (nonradiative) relaxation of the bulk of the exciton population, while the slow decay represents the evolution of a class of high-energy excitons that have strongly reduced nonradiative decay; henceforth we will refer to these excited states as ‘isolated excitons’. The rapid decay of the bulk of the population of high-energy excitons is due to nonradiative processes such as intrachain and interchain energy transfer and coupling to excimer states. In that light it does not come as a surprise that Eq. (7.2) does not fit our data so well at short wavelengths. One can hardly expect the complicated energy transfer process to be described by a biexponential.

From the fits one can extract values for the two decay rates  $\gamma_{\text{fast}}^{\lambda}$  ( $\leq 5 \times 10^9$   $\text{s}^{-1}$ ) and  $\gamma_{\text{slow}}^{\lambda}$ . In Fig. 7.3 we show the values of  $\tau_{\text{slow}}^{\lambda} = (\gamma_{\text{slow}}^{\lambda})^{-1}$  as a function of emission wavelength. For reference purposes we have included the decay time for the polymer in solution as obtained from a fit of the appropriate data with a curve described by Eq. (7.1). Figure 7.3 also shows that the film PL (at least its slow component) decays at a rate that is appreciably slower than that of the solution. This observation corroborates our assumption that an interchain species

is involved in the slow decay of the film PL.

## 7.4 Photoluminescence anisotropy

Additional information about interchain interactions can be obtained from a time-domain study of the photoluminescence anisotropy [146, 150], given by:

$$r(t, \lambda) = \frac{S_{\parallel}(t, \lambda) - S_{\perp}(t, \lambda)}{S_{\parallel}(t, \lambda) + 2S_{\perp}(t, \lambda)}. \quad (7.3)$$

Here  $S_{\parallel}(t, \lambda)$  and  $S_{\perp}(t, \lambda)$  represent the strength of the polarized and sensitized PL signals at wavelength  $\lambda$  as a function of time. Modelling the conjugated polymer, both in solution and in the film, as an ensemble of randomly oriented dipoles one finds (for  $t = 0$ )  $r(0) = 0.4$  ( $S_{\parallel}(0)/S_{\perp}(0) = 3$ ), if the absorbing and emitting dipoles are parallel. Beyond  $t = 0$ , the photoluminescence anisotropy (PLA) decays due to orientational relaxation. In a polymer solution this happens through orientational diffusion of the polymer chains [119]. In the film, the decay of  $r(t, \lambda)$  is due to intrachain and interchain excitation transfer, or creation of interchain states.

In our experiments we find that  $r(t, \lambda)$  never exceeds the value 0.3, even for the solution at  $t = 0$ . This implies either misalignment of the absorbing and emitting

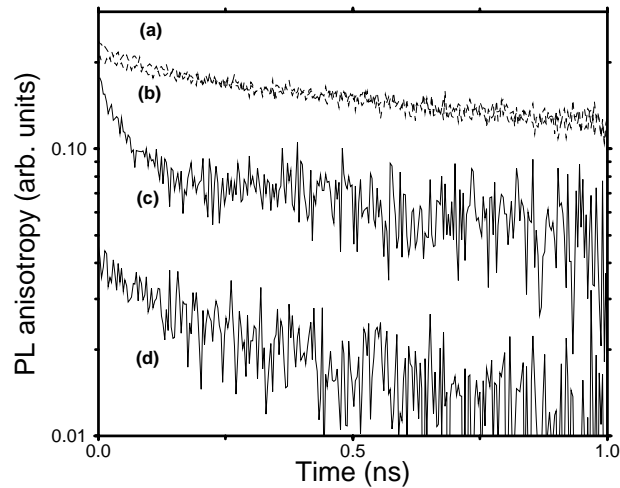


**Figure 7.4:** Time-dependent anisotropy of the emission from a solution (curve (a) for  $\lambda = 472$  nm and curve (b) for  $\lambda = 580$  nm), and from a film (curve (c) for  $\lambda = 472$  nm and curve (d) for  $\lambda = 600$  nm).

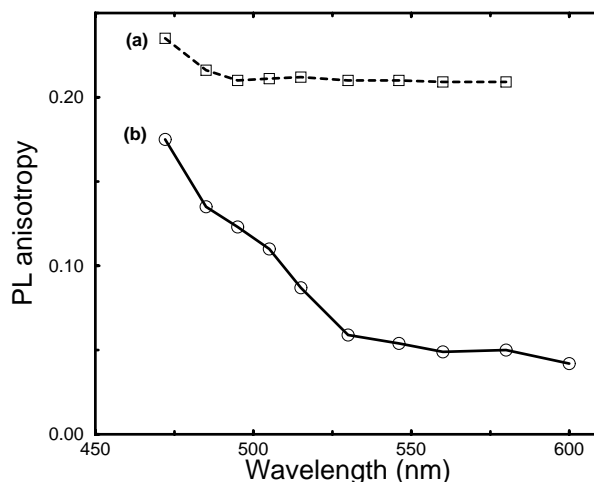


**Figure 7.5:** Wavelength dependence of the PL anisotropy at  $t = 0$  for the polymer solution (dashed curve), and for a polymer film (solid curve).

dipoles, or very fast depolarization during the energy relaxation process from the photo-excited to the luminescent level of the singlet manifold.

Because of the importance of the instrumental response during the rising part of the PL signal, one can not arrive at a reliable value of  $r(t, \lambda)$  while either  $S_{\parallel}(t, \lambda)$  or  $S_{\perp}(t, \lambda)$  increase rapidly. We therefore calculate  $r(t, \lambda)$  only during the decay of the PL signals, with  $t = 0$  being defined as the time at which the PL signals reach their maximum. Figure 7.4 shows our results for the time-dependent anisotropy for the same set of wavelengths as in Fig. 7.2. In all measurements the PLA decays as a function of time, not reaching a steady-state value within our time window (1 ns). Additionally, the PLA of the solution is, at all times, substantially larger than that of the film. For  $t \geq 0.2$  ns the PLA is well described by an exponential time dependence; this applies to all wavelengths both in solution and in the film. By fitting our data for  $t \geq 0.2$  ns with an exponential we obtain the associated decay times, of order 1 – 3 ns.

Figure 7.5 shows the values of  $r(0)$ , i.e., the maximum value of the photoluminescence anisotropy. For the solution we find a, basically, wavelength independent value of  $r(0)$ , except at the shortest wavelengths. Curve (a) of Fig. 7.4 shows that the increased value of  $r(0)$  at  $\lambda = 472$  nm is due to an enhanced contribution of the fast-decaying component of  $r(t)$ . The value of  $r(0)$  for the film is seen to be strongly wavelength dependent.

## 7.5 Discussion

Reviewing all our experimental results for the *solution* we note that the photo-physics in that system is essentially *wavelength independent* except at the shortest wavelengths. This is summarized succinctly by the relevant curves of Figs. 7.3 and 7.5. The photoluminescence decay can be described by a single exponential, yielding a PL decay time of  $\approx 0.65$  ns. The photoluminescence anisotropy is substantial and has a long-lived component that is well described by an exponential time dependence, with a time constant of a few ns. This component of the PLA decay can be attributed to orientational diffusion of the polymer in its solvent [119]. The weak, fast decaying component of the anisotropy is associated with dipole-dipole-coupling-induced loss of orientation during (intrachain) energy migration along the polymer backbone [140, 150, 155]. This is supported by our data that show that this fast-decaying component is quite a bit larger at the shortest wavelength than at longer wavelengths (see Fig. 7.4). The photoluminescence at short wavelengths is entirely due to excitons that have not migrated, whereas at longer wavelengths the emission is due to excitons that have been populated directly or through an intrachain energy transfer process. Interchain energy transfer can be excluded because of the low probability of interchain overlap in solution.

The results for the *film* are in sharp contrast with those of the solution. Here we observe a *strong wavelength dependence* (see Figs. 7.2, 7.3, 7.4 and 7.5) and decay curves that can not be described by a single exponential. As discussed earlier this behavior is due to interchain processes, all-important in the film, and virtually absent in the solution.

Combining the results of Fig. 7.5 with those of Fig. 7.1, one notices that the anisotropy is very weak ( $r(0) < 0.06$ ,  $S_{\parallel}/S_{\perp} < 1.2$ ) and essentially featureless over the main body of the emission spectrum of the film. This small value of the anisotropy supports the earlier made assumption that, in this wavelength interval, the emission originates predominantly in species that have not been populated directly in the photo-excitation process. In the extreme red wing, where the photoluminescence decays slowest (see Fig. 7.3), these have interchain character and are collectively called excimers. These interchain species are generally believed to have reduced oscillator strengths, hence the slow decay of the photoluminescence (see Fig. 7.3). Less far in the red wing the emission may well be due to both excitons and excimers, the excitonic emitting states having been (partly) populated through an intrachain energy transfer process.

In the extreme blue wing of the emission spectrum the PLA is strongly wavelength dependent, as shown by Fig. 7.5 also. Here the value of  $r(0)$  is comparable to that in solution (see Fig. 7.4). This suggests that, at these wavelengths, the same

species (a singlet exciton) is responsible for the emission by both the film and the solution. Nonradiative processes such as intrachain transfer rapidly deplete this exciton population, inducing the fast initial decay of the PL. The dipole-dipole coupling that is believed to be responsible for (part of) these transfer process causes the observed rapid loss of anisotropy at these wavelengths. The slowly decaying tail of the luminescence attests to the presence of excited species that emit at these wavelengths at much later times. We believe that these are not excimers or other low-energy interchain species. Rather, we attribute this emission to the isolated excitons, introduced earlier. These communicate only weakly with their environment, as shown by their slow nonradiative decay and slow depolarization.

It is interesting to make a connection to measurements of the transient gain in thin films of this and similar PPVs. The transient gain can be quite considerable initially, but is, almost universally, seen to decay rapidly, on a time scale of tens of picoseconds. It is tempting to connect the fast decay of the gain in polymer films with the rapid decay of the initially excited species. Hence, we postulate that the gain is exclusively related to the exciton population, while a considerable part of the photoluminescence is related to the population of excimers. The mere fact that the photoluminescence quantum efficiency of a conjugated polymer is particularly high thus does not guarantee that it is especially suitable as a gain material in a laser. Rather, in order to make a good optically pumped polymer laser, one has to reduce the interchain coupling in the film. This discussion puts into context the recent extensive efforts to control and reduce interchain effects in conjugated polymers [37, 143, 152, 156–159]. Note, however, that interchain coupling is essential for any kind of charge transport, i.e., for the development of injection-type polymer lasers.

A description of the lasing process in thin films of conjugated polymers in terms of a standard four-level system is, in this scenario, not to the point. An interesting question is why the excimers in conjugated polymers do not give rise to lasing. A curious aspect of excimer lasing in conjugated polymers is that the energy transfer process that populates the excimer states enhances the Stokes shift. In standard laser physics, a large Stokes shift is considered to be advantageous. The reduced oscillator strength of the excimers should not pose a problem in view of the many laser systems that are based on very low oscillator-strengths optical transitions. Obviously, the crucial question concerns whether the excimer emission is self-absorbed by the material, i.e., whether (photo-induced) absorption by excimers or other interchain species will overwhelm the gain.

## **7.6 Conclusion**

We have studied the photophysics of a phenyl-substituted PPV, dissolved in a common organic solvent, and as a thin film by performing time-domain measurements of the spectrally resolved photoluminescence and its anisotropy across the full emission spectrum of the material. As for many conjugated polymers, the emission by the film is red-shifted as compared to that of the solution. The overall picture is that the measured properties for the dissolved polymer are wavelength independent, while the luminescent properties of the film vary considerably with wavelength. These observations thereby confirm the results obtained by others in that the photoluminescence in the film has, for the most part, a different origin as that in solution. While in solution the emission is dominated by the radiative decay of singlet excitons, in the film the main contribution comes from interchain species such as excimers.

We have paid particular attention to the blue wing of the photoluminescence spectrum where the differences between film and solution are smallest. In that spectral region the film photoluminescence (and its anisotropy) is dominated by a quickly decaying component, the decay being caused by intrachain relaxation. Once this component has decayed away, we measure an emission that slowly gets weaker. We attribute this emission to isolated excitons that only weakly interact with their surroundings.

In the final part of this chapter we speculate on the connection between photoluminescence and gain in films of conjugated polymers. We discuss whether the long-living emitter in the film can be exploited for lasing.



## References

---

- [1] A. J. Heeger, *Rev. Mod. Phys.* **73**, 681 (2001).
- [2] A. G. MacDiarmid, *Rev. Mod. Phys.* **73**, 701 (2001).
- [3] H. Shirakawa, *Rev. Mod. Phys.* **73**, 713 (2001).
- [4] H. Sirringhaus, N. Tessler, and R. H. Friend, *Science* **280**, 1741 (1998).
- [5] D. M. de Leeuw, *Phys. World* **12**, 31 (1999).
- [6] B. Crone, A. Dodabalapur, Y. Y. Lin, R. W. Filas, Z. Bao, A. LaDuca, R. Sarpeshkar, H. E. Katz, and W. Li, *Nature* **403**, 521 (2000).
- [7] G. Horowitz, in *Semiconducting polymers*, edited by G. Hadziioannou and P. F. van Hutten (Wiley-VCH, Weinheim, 2000).
- [8] T. Kawase, H. Sirringhaus, R. H. Friend, and T. Shimoda, *Adv. Mater.* **11**, 1601 (2001).
- [9] C. J. Brabec and N. S. Sariciftci, in *Semiconducting polymers*, edited by G. Hadziioannou and P. F. van Hutten (Wiley-VCH, Weinheim, 2000).
- [10] J. H. Burroughes, D. D. C. Bradley, A. R. Brown, R. N. Marks, K. Mackay, R. H. Friend, P. L. Burns, and A. B. Holmes, *Nature* **347**, 539 (1990).
- [11] J. R. Sheats, H. Antoniadis, M. Hueschen, W. Leonard, J. Miller, R. Moon, D. Roitman, and A. Stocking, *Science* **273**, 884 (1996).
- [12] A. J. Heeger and J. Long, *Optics and Photonics News* **7**, 24 (1996).
- [13] R. H. Friend, J. H. Burroughes, and T. Shimoda, *Phys. World* **12**, 35 (1999).
- [14] J. Kido, *Phys. World* **12**, 27 (1999).
- [15] W. R. Salaneck, R. H. Friend, and J. L. Brédas, *Phys. Rep.* **319**, 231 (1999).
- [16] W. P. Su, J. R. Schrieffer, and A. J. Heeger, *Phys. Rev. Lett.* **42**, 1698 (1979).
- [17] A. J. Heeger, S. Kivelson, R. J. Schrieffer, and W. P. Su, *Rev. Mod. Phys.* **60**, 781 (1988).
- [18] P.W.M. Blom and M. C. J. M. Vissenberg, *Phys. Rev. Lett.* **80**, 3819 (1998).
- [19] H. Bässler, in *Semiconducting polymers*, edited by G. Hadziioannou and P. F. van Hutten (Wiley-VCH, Weinheim, 2000).
- [20] H. C. F. Martens, *Charge transport in conjugated polymers and polymer devices* (PhD-thesis, Leiden University, The Netherlands, 2000).
- [21] A. Kraft, A. C. Grimsdale, and A. B. Holmes, *Angew. Chem. Int. Ed.* **37**, 403 (1998).
- [22] P. L. Burn, A. B. Holmes, A. Kraft, D. D. C. Bradley, A. R. Brown, R. H. Friend, and R. W. Gymer, *Nature* **356**, 47 (1992).

- 
- [23] M. Jandke, P. Strohriegl, J. Gmeiner, W. Brütting, and M. Schwoerer, *Adv. Mater.* **11**, 1518 (1999).
- [24] A. Bolognesi, C. Botta, D. Facchinetti, M. Jandke, K. Kreger, P. Strohriegl, A. Relini, R. Rolandi, and S. Blumstengel, *Adv. Mater.* **13**, 1072 (2001).
- [25] M. Berggren, O. Inganäs, G. Gustafsson, J. Rasmusson, M. R. Andersson, T. Hjertberg, and O. Wennerström, *Nature* **372**, 444 (1994).
- [26] M. D. McGehee, T. Bergstedt, C. Zhang, A. P. Saab, M. B. O'Regan, G. C. Bazan, V. I. Srdanov, and A. J. Heeger, *Adv. Mater.* **11**, 1349 (1999).
- [27] R. Kersting, U. Lemmer, M. Deussen, H. J. Bakker, R. F. Mahrt, H. Kurz, V. I. Arkhipov, H. Bässler, and E. O. Göbel, *Phys. Rev. Lett.* **73**, 1440 (1994).
- [28] S. Tasch, G. Kranzelbinder, G. Leising, and U. Scherf, *Phys. Rev. B* **55**, 5079 (1997).
- [29] I. D. W. Samuel, G. Rumbles, C. J. Collison, B. Crystall, S. C. Moratti, and A. B. Holmes, *Synth. Met.* **76**, 15 (1996).
- [30] I. D. W. Samuel, G. Rumbles, C. J. Collison, R. H. Friend, S. C. Moratti, and A. B. Holmes, *Synth. Met.* **84**, 497 (1997).
- [31] M. Yan, L. J. Rothberg, E. W. Kwock, and T. M. Miller, *Phys. Rev. Lett.* **75**, 1992 (1995).
- [32] W. Graupner, G. Leising, G. Lanzani, M. Nisoli, S. De Silvestri, and U. Scherf, *Phys. Rev. Lett.* **76**, 847 (1996).
- [33] B. J. Schwartz, F. Hide, M. R. Andersson, and A. J. Heeger, *Chem. Phys. Lett.* **265**, 327 (1997).
- [34] A. Dogariu, D. Vacar, and A. J. Heeger, *Synth. Met.* **101**, 202 (1999).
- [35] G. J. Denton, N. Tessler, N. T. Harrison, and R. H. Friend, *Phys. Rev. Lett.* **78**, 733 (1997).
- [36] D. Vacar, A. Dogariu, and A. J. Heeger, *Chem. Phys. Lett.* **290**, 58 (1998).
- [37] T.-Q. Nguyen, I. B. Martini, J. Liu, and B. J. Schwartz, *J. Phys. Chem. B* **104**, 237 (2000).
- [38] D. Moses, *Appl. Phys. Lett.* **60**, 3215 (1992).
- [39] H. J. Brouwer, V. V. Krasnikov, A. Hilberer, J. Wildeman, and G. Hadziioannou, *Appl. Phys. Lett.* **66**, 3404 (1995).
- [40] F. Hide, B. J. Schwartz, M. A. Díaz-García, and A. J. Heeger, *Chem. Phys. Lett.* **256**, 424 (1996).
- [41] W. Holzer, A. Penzkofer, S. H. Gong, A. D. Davey, and W. J. Blau, *Optical and Quantum Electronics* **29**, 713 (1997).
- [42] X. Long, A. Malinowski, D. D. C. Bradley, M. Inbasekaran, and E. P. Woo, *Chem. Phys. Lett.* **272**, 6 (1997).
- [43] N. Tessler, G. J. Denton, and R. H. Friend, *Nature* **382**, 695 (1996).

- [44] A. Schulzgen, C. Spiegelberg, M. M. Morrell, S. B. Mendes, B. Kippelen, N. Peyghambarian, M. F. Nabor, E. A. Mash, and P. M. Allemand, *Appl. Phys. Lett.* **72**, 269 (1998).
- [45] S. Stagira, M. Zavelani-Rossi, M. Nisoli, S. DeSilvestri, G. Lanzani, C. Zenz, P. Mataloni, and G. Leising, *Appl. Phys. Lett.* **73**, 2860 (1998).
- [46] S. V. Frolov, A. Fujii, D. Chinn, Z. V. Vardeny, K. Yoshino, and R. V. Gregory, *Appl. Phys. Lett.* **72**, 2811 (1998).
- [47] Y. Kawabe, Ch. Spiegelberg, A. Schültzgen, M. F. Nabor, B. Kippelen, E. A. Mash, P. M. Allemand, M. Kuwata-Gonokami, K. Takeda, and N. Peyghambarian, *Appl. Phys. Lett.* **72**, 141 (1998).
- [48] M. Berggren, A. Dodabalapur, R. E. Slusher, A. Timko, and O. Nalamasu, *Appl. Phys. Lett.* **72**, 410 (1998).
- [49] M. D. McGehee, M. A. Díaz-García, F. Hide, R. Gupta, E. K. Miller, D. Moses, and A. J. Heeger, *Appl. Phys. Lett.* **72**, 1536 (1998).
- [50] S. Riechel, U. Lemmer, J. Feldmann, T. Benstem, W. Kowalsky, U. Scherf, A. Gombert, and V. Wittwer, *Appl. Phys. B.* **71**, 897 (2000).
- [51] R. Gupta, M. Stevenson, A. Dogariu, M. D. McGehee, J. Y. Park, V. Srdanov, and A. J. Heeger, *Appl. Phys. Lett.* **73**, 3492 (1998).
- [52] M. Berggren, A. Dodabalapur, R. E. Slusher, and Z. Bao, *Nature* **389**, 466 (1997).
- [53] M. Berggren, A. Dodabalapur, Z. Bao, and R. E. Slusher, *Adv. Mater.* **9**, 968 (1997).
- [54] N. Tessler, *Adv. Mater.* **11**, 363 (1999).
- [55] U. Lemmer, A. Haugeneder, C. Kallinger, and J. Feldmann, in *Semiconducting polymers*, edited by G. Hadziioannou and P. F. van Hutten (Wiley-VCH, Weinheim, 2000).
- [56] G. Kranzelbinder and G. Leising, *Rep. Prog. Phys.* **63**, 729 (2000).
- [57] M. D. McGehee and A. J. Heeger, *Adv. Mater.* **12**, 1655 (2000).
- [58] S. V. Frolov, M. Shkunov, A. Fujii, K. Yoshino, and Z. V. Vardeny, *IEEE J. Quant. Electron.* **36**, 2 (2000).
- [59] F. Hide, M. A. Díaz-García, B. J. Schwartz, M. R. Andersson, Q. Pei, and A. J. Heeger, *Science* **273**, 1833 (1996).
- [60] A. E. Siegman, *Lasers* (University Science Books, Sausalito, California, 1986).
- [61] A. Dogariu, D. Vacar, and A. J. Heeger, *Phys. Rev. B* **58**, 10218 (1998).
- [62] S. V. Frolov, M. Liess, P. A. Lane, W. Gellermann, and Z. V. Vardeny, *Phys. Rev. Lett.* **78**, 4285 (1997).
- [63] S. V. Frolov, W. Gellermann, M. Ozaki, K. Yoshino, and Z. V. Vardeny, *Phys. Rev. Lett.* **78**, 729 (1997).

- 
- [64] G. Kranzelbinder, M. Nisoli, S. Stagira, S. De Silvestri, G. Lanzani, K. Mullen, U. Scherf, W. Graupner, and G. Leising, *Appl. Phys. Lett.* **71**, 2725 (1997).
  - [65] H. Spreitzer, H. Becker, E. Kluge, W. Kreuder, H. Schenk, R. Demandt, and H. F. M. Schoo, *Adv. Mater.* **10**, 1340 (1998).
  - [66] M. F. H. Schuurmans, Q. H. F. Vreken, and D. Polder, *Adv. Atom. Mol. Phys.* **17**, 167 (1981).
  - [67] J. Klebniczki, Zs. Bor, and G. Szabó, *Appl. Phys. B.* **46**, 151 (1988).
  - [68] J. AuYeung, *Appl. Phys. Lett.* **38**, 308 (1981).
  - [69] S. Schuster and H. Haug, *J. Opt. Soc. Am. B* **13**, 1605 (1996).
  - [70] P. F. Moulton, *J. Opt. Soc. Am. B* **3**, 125 (1986).
  - [71] J. M. Eggleston, L. G. DeShazer, and K. W. Kangas, *IEEE J. Quant. Electron.* **24**, 1009 (1988).
  - [72] A. D. Deleva, Z. Y. Peshev, Z. I. Aneva, B. K. Kaprielov, E.P. Vidolova-Angelova, and D.A. Angelov, *J. Mod. Opt.* **47**, 793 (2000).
  - [73] L. W. Casperson, *J. Appl. Phys.* **47**, 4555 (1976).
  - [74] J. C. Diels and W. Rudolph, *Ultrashort laser pulse phenomena* (Academic Press, San Diego, 1996).
  - [75] G. H. C. New, *Rep. Prog. Phys.* **46**, 877 (1983).
  - [76] S. A. van den Berg, R. H. van Schoonderwoerd den Bezemer, H. F. M. Schoo, G. W. 't Hooft, and E. R. Eliel, *Opt. Lett.* **24**, 1847 (1999).
  - [77] D. T. Schaafsma and D. H. Christensen, *Phys. Rev. B* **54**, 14618 (1996).
  - [78] R. Ulbrich and M.H. Pilkuhn, *Appl. Phys. Lett.* **16**, 516 (1970).
  - [79] L. Csillag, M. Janossy, and T. Salamon, *Phys. Lett.* **26**, 436 (1968).
  - [80] U. Ganiel, A. Hardy, G. Neumann, and D. Treves, *IEEE J. Quant. Electron.* **11**, 881 (1975).
  - [81] M. Azadeh and L. W. Casperson, *J. Appl. Phys.* **83**, 2399 (1998).
  - [82] M. E. Mack, *Appl. Phys. Lett.* **15**, 166 (1969).
  - [83] C. Lin, T. K. Gustafson, and A. Dienes, *Opt. Commun.* **8**, 210 (1973).
  - [84] J. Hebling and J. Kuhl, *Opt. Lett.* **14**, 278 (1989).
  - [85] W. A. Hamel and J. P. Woerdman, *Phys. Rev. A* **40**, 2785 (1989).
  - [86] D. J. Bradley and A.J.F. Durrant, *Phys. Lett. A* **27**, 73 (1968).
  - [87] Y. Y. Hwang, C. H. Lee, and J. Wang, *Appl. Opt.* **36**, 7802 (1997).
  - [88] M. Lai, J. Nicholson, and W. Rudolph, *Opt. Commun.* **142**, 45 (1997).
  - [89] M. F. H. Tarroja, M. Sharafi, and L. W. Casperson, *J. Opt. Soc. Am. B* **6**, 1564 (1989).
  - [90] T. J. Chuang and K. B. Eisenthal, *J. Chem. Phys.* **57**, 5094 (1972).
  - [91] K. B. Eisenthal and K.H. Drexhage, *J. Chem. Phys.* **51**, 5720 (1969).

- [92] R. D. Spencer and G. Weber, *J. Chem. Phys.* **4**, 1654 (1970).
- [93] D. W. Phillion, D. J. Kuizenga, and A. E. Siegman, *Appl. Phys. Lett.* **27**, 85 (1975).
- [94] M. L. Horng, J. A. Gardecki, and M. Maroncelli, *J. Phys. Chem. A* **101**, 1030 (1997).
- [95] M. K. Singh, *Photochemistry and Photobiology* **72**, 438 (2000).
- [96] T. J. Chuang and K. B. Eisenthal, *Chem. Phys. Lett.* **11**, 368 (1971).
- [97] K. C. Rezyer and L. W. Casperson, *J. Appl. Phys.* **51**, 6083 (1980).
- [98] I. Nagata and T. Nakaya, *J. Phys. D* **6**, 1870 (1973).
- [99] D. W. Phillion, D. J. Kuizenga, and A. E. Siegman, *J. Chem. Phys.* **61**, 3828 (1974).
- [100] A. Lempicki, *Acta Phys. Pol. A* **50**, 179 (1976).
- [101] A. N. Sevchenko, A. A. Kovalev, V. A. Pilipovich, and Y. V. Razvin, *Sov. Phys. Dokl.* **13**, 226 (1968).
- [102] S. H. Jiang and L. W. Casperson, *J. Appl. Phys.* **69**, 1866 (1991).
- [103] P. P. Feofilov, *The physical basis of polarized emission* (Consultants Bureau, New York, 1961).
- [104] S. A. van den Berg, G. W. 't Hooft, and E. R. Eliel, *Phys. Rev. A* **63**, 063809 (2001).
- [105] A. K. Jansen van Doorn, M. P. van Exter, and J. P. Woerdman, *Appl. Phys. Lett.* **69**, 1041 (1996).
- [106] L. A. Westling, M. G. Raymer, and J. J. Snyder, *J. Opt. Soc. Am. B* **1**, 150 (1984).
- [107] H. de Lang and G. Bouwhuis, *Phys. Lett.* **20**, 383 (1966).
- [108] W. van Haeringen, *Phys. Rev.* **158**, 256 (1967).
- [109] D. Lenstra, *phys-rep* **59**, 299 (1980).
- [110] M. P. van Exter, M. B. Willemsen, and J. P. Woerdman, *Phys. Rev. A* **58**, 4191 (1998).
- [111] M. B. Willemsen, M. P. van Exter, and J. P. Woerdman, *Phys. Rev. Lett.* **84**, 4337 (2000).
- [112] K. Otsuka, P. Mandel, S. Bielawski, D. Derozier, and P. Glorieux, *Phys. Rev. A* **46**, 1692 (1992).
- [113] A. J. Poustie, *Opt. Lett.* **20**, 1868 (1995).
- [114] G. Bouwmans, B. Ségard, and P. Glorieux, *Opt. Commun.* **196**, 257 (2001).
- [115] S. K. Tiwari and S. C. Mehendale, *Rev. Sci. Instr.* **69**, 4245 (1998).
- [116] T. C. Damen, L. Vina, J. E. Cunningham, J. Shah, and L. J. Sham, *Phys. Rev. Lett.* **67**, 3432 (1991).
- [117] D. D. Awschalom and J. M. Kikkawa, *Phys. Today* **52**, 33 (1999).

- 
- [118] E. L. Blansett, M. G. Raymer, G. Khitrova, H. M. Gibbs, D. K. Serkland, A. A. Allerman, and K. M. Geib, *Opt. Express* **9**, 312 (2001).
- [119] S. A. van den Berg, G. W. 't Hooft, and E. R. Eliel, *Chem. Phys. Lett.* **347**, 167 (2001).
- [120] A. Costela, I. Garcia-Moreno, J. Barroso, and R. Sastre, *J. Appl. Phys.* **83**, 650 (1998).
- [121] R. Leners and G. Stéphan, *Quantum Semiclass. Opt.* **7**, 757 (1995).
- [122] A. Aiello, F. De Martini, and P. Mataloni, *Opt. Lett.* **21**, 149 (1996).
- [123] X. Wang, R.A. Linke, G. Devlin, and H. Yokoyama, *Phys. Rev. A* **47**, 2488 (1993).
- [124] M. B. Willemsen, M. U. F. Khalid, M. P. van Exter, and J. P. Woerdman, *Phys. Rev. Lett.* **82**, 4815 (1999).
- [125] J. H. Schön, Ch. Kloc, A. Dodabalapur, and B. Batlogg, *Science* **289**, 599 (2000).
- [126] R. C. Polson, G. Levina, and Z. V. Vardeny, *Appl. Phys. Lett.* **76**, 3858 (2000).
- [127] M. D. McGehee, R. Gupta, S. Veenstra, E. K. Miller, M. A. Díaz-García, and A. J. Heeger, *Phys. Rev. B* **58**, 7035 (1998).
- [128] C. Zenz, W. Graupner, S. Tasch, and G. Leising, *J. Appl. Phys.* **84**, 5445 (1998).
- [129] A. K. Sheridan, G. A. Turnbull, A. N. Safonov, and I. D. W. Samuel, *Phys. Rev. B* **62**, R 11929 (2000).
- [130] B. Schweitzer, G. Wegmann, H. Giessen, D. Hertel, H. Bässler, and R.F. Mahrt, *Appl. Phys. Lett.* **72**, 2933 (1998).
- [131] S. C. Jeoung, Y. H. Kim, D. Kim, J. Y. Han, M. S. Jang, J. I. Lee, H. K. Shim, C. M. Kim, and C. S. Yoon, *Appl. Phys. Lett.* **74**, 212 (1999).
- [132] G. Wegmann, B. Schweitzer, D. Hertel, H. Giessen, M. Oestreich, U. Scherf, K. Müllen, and R. F. Mahrt, *Chem. Phys. Lett.* **312**, 376 (1999).
- [133] C. W. Lee, K. S. Wong, J. D. Huang, S. V. Frolov, and Z. V. Vardeny, *Chem. Phys. Lett.* **314**, 564 (1999).
- [134] G. J. Denton, N. Tessler, M. A. Stevens, and R. H. Friend, *Adv. Mater.* **9**, 547 (1997).
- [135] S. V. Frolov, M. Ozaki, W. Gellermann, M. Shkunov, Z. V. Vardeny, and K. Yoshino, *Synth. Met.* **84**, 473 (1997).
- [136] G. H. Gelinck, J. M. Warman, M. Remmers, and D. Neher, *Chem. Phys. Lett.* **265**, 320 (1997).
- [137] H. Spreitzer, H. Becker, and P. Stössel, Substituted poly(arylene vinylenes), method for the production thereof and their use in electroluminescent devices, Patent nr. WO 01/34722, 2001.

- [138] A. Yariv, *Quantum Electronics* (Wiley, New York, 1988).
- [139] A. Haugeneder, M. Neges, C. Kallinger, W. Spirkl, U. Lemmer, J. Feldmann, M. C. Amann, and U. Scherf, *J. Appl. Phys.* **85**, 1124 (1999).
- [140] T.-Q. Nguyen, V. Doan, and B. J. Schwartz, *J. Chem. Phys.* **110**, 4068 (1999).
- [141] R. Chang, J. H. Hsu, W. S. Fann, J. Yu, S. H. Lin, Y. Z. Lee, and S. A. Chen, *Chem. Phys. Lett.* **317**, 153 (2000).
- [142] R. Jakubiak, L. J. Rothberg, W. Wan, and B. R. Hsieh, *Synth. Met.* **101**, 230 (1999).
- [143] S. A. Whitelegg, A. Buckley, M. D. Rahn, A. M. Fox, D. D. C. Bradley, L. O. Pålsson, I. D. W. Samuel, G. R. Webster, and P. L. Burn, *Synth. Met.* **119**, 575 (2001).
- [144] I. D. W. Samuel, G. Rumbles, and C. J. Collins, *Phys. Rev. B* **52**, R11573 (1995).
- [145] R. F. Mahrt, T. Pauck, U. Lemmer, U. Siegner, M. Hopmeier, R. Hennig, H. Bässler, E. O. Göbel, P. Haring Bolivar, G. Wegmann, H. Kurz, U. Scherf, and K. Müllen, *Phys. Rev. B* **54**, 1759 (1996).
- [146] L. M. Herz, C. Silva, R. H. Friend, R. T. Phillips, S. Setayesh, S. Becker, D. Marisky, and K. Müllen, *Phys. Rev. B* **64**, 195203 (2001).
- [147] S. A. Jenekhe and J. A. Osaheni, *Science* **265**, 765 (1994).
- [148] M. Yan, L. J. Rothberg, R. Papadimitrakopoulos, M. E. Galvin, and T. M. Miller, *Phys. Rev. Lett.* **72**, 1104 (1994).
- [149] G. Cerullo, G. Lanzani, S. De Silvestri, H.-J. Egelhaaf, L. Lüer, and D. Oelkrug, *Phys. Rev. B* **62**, 2429 (2000).
- [150] A. Watanabe, T. Kodaira, and O. Ito, *Chem. Phys. Lett.* **273**, 227 (1997).
- [151] T.-Q. Nguyen, J. Wu, S. H. Tolbert, and B. J. Schwartz, *Adv. Mater.* **13**, 609 (2001).
- [152] B. J. Schwartz, T.-Q. Nguyen, J. Wu, and S. H. Tolbert, *Synth. Met.* **116**, 35 (2001).
- [153] R. Kersting, U. Lemmer, R. F. Mahrt, K. Leo, H. Kurz, H. Bässler, and E. O. Göbel, *Phys. Rev. Lett.* **70**, 3820 (1993).
- [154] Th. Förster, *Ann. Physik* **2**, 55 (1948).
- [155] G. R. Hayes, I. D. W. Samuel, and R. T. Phillips, *Phys. Rev. B* **56**, 3838 (1997).
- [156] L. Chiavarone, M. Di Terlizzi, G. Scamarcio, F. Babudri, G. M. Farinola, and F. Naso, *Appl. Phys. Lett.* **75**, 2053 (1999).
- [157] R. G. Sun, Y. Z. Wang, D. K. Wang, Q. B. Zheng, E. M. Kylo, T. L. Gustafson, F. Wang, and A. J. Epstein, *Synth. Met.* **111**, 595 (2000).

- 
- [158] R. G. Sun, Y. Z. Wang, D. K. Wang, Q. B. Zheng, E. M. Kyllö, T. L. Gustafson, and A. J. Epstein, *Appl. Phys. Lett.* **76**, 634 (2000).
- [159] R. Jakubiak, Z. Bao, and L. J. Rothberg, *Synth. Met.* **116**, 41 (2001).

## Samenvatting

---

### Geleidend en lichtgevend plastic

Plastic is licht van gewicht en toch sterk, het kan gemakkelijk vorm gegeven worden, is goedkoop en vaak flexibel. Een andere belangrijke eigenschap van plastic is dat het een elektrische isolator is en dus (vrijwel) geen stroom geleidt. Plastics worden dan ook algemeen toegepast als isolatiemateriaal rondom elektriciteitskabels, in allerlei elektrische apparaten enz. Toch zijn er de afgelopen tientallen jaren al heel wat pogingen gedaan om *geleidende* plastics te ontwikkelen. Geleidend plastic biedt tal van toepassingsmogelijkheden, bijvoorbeeld als antistatische coating, maar vooral ook als goedkope plastic elektronica. In 1979 zijn MacDiarmid, Heeger en Shirakawa er voor het eerst in geslaagd geleidend plastic te synthetiseren. Voor dit en daaropvolgend werk hebben ze in 2000 de Nobelprijs voor de scheikunde gekregen.

Inmiddels zijn er ook geleidende *lichtgevende* plastics ontwikkeld. Ook deze materialen zijn wat toepassingen betreft erg veelbelovend. Met name in de wereld van de beeldschermen is de belangstelling groot. Lichtgevende plastics zijn niet alleen goedkoop en licht, ze gebruiken ook nog eens weinig energie. Dat laatste is vooral een groot voordeel voor laptops en mobiele telefoons. Verder biedt de productiemethode van dergelijke beeldschermen de mogelijkheid deze in zeer grote oppervlakken te vervaardigen, wat met de halfgeleidermaterialen zoals die nu gebruikt worden niet goed lukt.

Plastic bestaat uit lange moleculen (polymeren). Zo'n polymeer is weer een aaneenschakeling van soms wel duizenden korte identieke stukjes (monomeren). Een voorbeeld van een monomeer is schematisch weergegeven op de voorkant van dit proefschrift. Een groot voordeel van polymeren is dat ze oplosbaar zijn of, door toevoeging van de juiste moleculaire zijgroepen, oplosbaar gemaakt kunnen worden. Dit biedt zeer goede mogelijkheden voor de productie van dunne lagen en grote oppervlakken. Hierbij wordt vaak gebruik gemaakt van de zogenaamde 'spin-coating'-techniek. Door een oplossing met polymeren op een snel ronddraaiend substraat (ondergrond) te gieten, wordt een mooie gelijkmatige laag gevormd. Het oplosmiddel verdampst en er blijft een zeer dunne laag van polymeer over (ongeveer 0,0001 mm dik). Deze methode wordt gebruikt voor het maken van polymere displays. Een meer geavanceerde, maar ook goed ontwikkelde tech-

---

niek is die van 'inkjet printing'. Door daarbij in plaats van inkt een oplossing van polymeren te gebruiken, kunnen er met een heel hoge resolutie gedetailleerde patronen worden geprint, bijvoorbeeld elektronische circuits. In principe kunnen de polymeren ook op een flexibele ondergrond worden aangebracht. Dit biedt de mogelijkheid van buigzame elektronica en misschien ook van buigzame (of zelfs oprolbare) beeldschermen. Vooral dat laatste spreekt erg tot de verbeelding en kan tal van toepassingen bieden. Vooralsnog zijn er echter praktische problemen: lichtgevende polymeren degraderen onder de invloed van zuurstof en water, in het bijzonder in de aanwezigheid van (blauw) licht. Om dat te voorkomen moeten de polymeren van lucht afgeschermd worden. Glas is hiervoor geschikt, maar een doorzichtig en flexibel materiaal is op dit moment nog niet beschikbaar.

## Lichtgeven en laserwerking

Om polymeren licht te laten geven moet er op één of andere manier energie in worden gestopt om de moleculen 'aan te slaan' (exciteren). Vaak gebeurt dat door middel van een elektrische stroom. Moleculen kunnen ook energie opnemen door de absorptie van licht. De aangeslagen moleculen kunnen door verschillende processen de energie die ze hebben opgenomen weer afstaan: ze komen dan weer terug in de 'grondtoestand'. Eén van de manieren waarop de energie kan worden uitgezonden, is in de vorm van een 'lichtdeeltje', 'foton' genoemd. Dit heet 'stralend verval'. De kleur van het uitgezonden licht, zoals wij dat waarnemen, hangt af van de hoeveelheid energie per foton. Zo bevat een blauw foton meer energie dan een rood foton en zit groen daar ergens tussenin. Naast het uitzenden van fotonen kan het ook gebeuren dat de energie op een andere manier weglekt en wordt omgezet in warmte. Dit is niet-stralend verval. Het zal duidelijk zijn dat dit laatste proces niet gewenst is als je een zo groot mogelijke lichtopbrengst wilt. In de experimenten zoals beschreven in dit proefschrift worden de polymeren steeds aangeslagen met blauw licht en zenden ze groen licht uit. De kleur van het uitgezonden licht hangt af van de exacte chemische structuur van de polymeren. Er zijn ook polymeren ontwikkeld die bijvoorbeeld groen licht absorberen en rood licht uitzenden.

Voorlopig concentreren we ons alleen op stralend verval van aangeslagen moleculen. Al aan het begin van de vorige eeuw liet Einstein zien dat er in het eenvoudigste systeem dat er denkbaar is twee vormen van lichtemissie voorkomen: spontane en gestimuleerde emissie. In het eerste geval vervalt het molecuul (of atoom) onder uitzending van een foton naar de grondtoestand, zonder dat hierop van buitenaf invloed wordt uitgeoefend. Dit is een kansproces dat zijn wortels in de quantummechanica heeft. Gemiddeld genomen vervallen onze aangeslagen

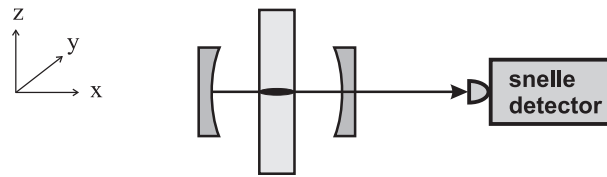
polymeermoleculen binnen een miljardste van een seconde terug naar de grondtoestand.

Een tweede mogelijkheid is dat een molecuul vervalt onder invloed van een passerend foton. In dat geval zendt het molecuul een foton uit dat een identieke kopie is van het passerende foton en dus dezelfde kleur en richting heeft. Deze twee fotonen kunnen weer andere moleculen stimuleren om ook licht uit te zenden enz. Het is eenvoudig voor te stellen dat deze gestimuleerde emissie tot een lawine-effect kan leiden. Deze manier van licht geven vindt plaats in een laser (laser betekent letterlijk: 'Light Amplification by Stimulated Emission of Radiation'). In een laser is het lichtgevende materiaal opgesloten tussen twee spiegels, zodat het licht dat wordt uitgezonden steeds door het aangeslagen materiaal heen en weer loopt en de lawine op gang kan komen. Doordat één van de spiegels een klein beetje licht doorlaat, wordt er een bundel van licht uitgezonden.

In dit proefschrift staan gestimuleerde emissie en laserwerking van lichtgevend polymeren centraal. In het bijzonder wordt de dynamica van laserwerking en lichtemissie bestudeerd.

## Korte pulsen

Voor alle experimenten die in dit proefschrift worden beschreven, is gebruik gemaakt van een lasersysteem dat zeer korte blauwe lichtpulsjes uitzendt. Deze pulsen worden gebruikt om de polymeren mee aan te slaan. De duur van zo'n 'pomppuls' is extreem kort ( $10^{-13}$  seconde), zó kort dat het licht in die tijd slechts 0,03 mm aflegt. En dan te bedenken dat licht in één seconde een afstand van ruim zeven rondjes om de aarde aflegt! Met de korte puls worden de polymeren vrijwel onmiddellijk van de grondtoestand naar de aangeslagen toestand gebracht. De pomppuls is allang weer voorbij voordat de aangeslagen moleculen terugvallen naar de grondtoestand. Het voordeel hiervan is dat het systeem na excitatie aan zichzelf is overgeleverd en dus een soort 'vrije evolutie' ondergaat. De moleculen die eenmaal naar de grondtoestand zijn teruggevallen (of dat nu via spontane of gestimuleerde emissie is) kunnen niet opnieuw aangeslagen worden omdat er geen pomplicht meer is. Dit zorgt ervoor dat de dynamica van het systeem goed gevolgd kan worden. Zo kunnen we bijvoorbeeld met een snelle detector het licht dat door een polymeer wordt uitgezonden, meten als functie van de tijd. Vlak na de pomppuls is de hoeveelheid uitgezonden licht het grootst. Dat is ook te verwachten, want dan zijn er de meeste aangeslagen moleculen. Het aantal aangeslagen moleculen neemt af en er wordt dus steeds minder licht uitgezonden. Uit deze meting kun je dus opmaken hoelang het gemiddeld duurt voordat een molecuul van de aangeslagen toestand terugvalt naar de grondtoestand. Zo'n meting



**Figuur 1:** Schematische weergave van een laser bestaande uit een cuvet met een polymeeroplossing en twee holle spiegels. De afstand tussen de spiegels is ongeveer 2,5 cm. De pomppuls komt van opzij (langs de  $y$ -as). Het donkere gebied midden in het cuvet geeft het gebied met aangeslagen polymeren aan. Het licht dat door de rechterspiegel wordt doorgelaten, wordt gemeten met de detector.

lukt natuurlijk alleen als de pomppuls veel korter is dan deze tijdsduur.

In de eerste hoofdstukken van het proefschrift wordt de korte pomppuls gebruikt, zodat de opbouw van laserwerking in een polymeerlaser kan worden gevolgd. In de resterende hoofdstukken gebruiken we de korte puls om inzicht te krijgen in de achterliggende fysica van het spontane en gestimuleerde emissieproces in dunne lagen van polymeren.

## Dit proefschrift

### Dynamica van polymeerlasers

In de hoofdstukken 2-5 gebruiken we een lichtgevend polymeer in oplossing als versterkend medium in een laser. In Fig. 1 staat een schematische voorstelling van zo'n laser. Deze bestaat uit twee spiegels, die het licht opsluiten en het meerdere malen door de polymeeroplossing sturen. De rechterspiegel laat een paar procent van het licht door, zodat het uit de laser kan ontsnappen. Het donkere gebied in het cuvet is het gebied met de aangeslagen polymeren.

Eén van de opvallende resultaten, zoals beschreven in de hoofdstukken 2 en 3, is dat het licht dat door de polymeerlaser wordt uitgezonden, bestaat uit een hele serie pulsjes, terwijl het polymeer met slechts één puls wordt aangeslagen. De basis voor het ontstaan van deze pulstrein zit hem in de verhoudingen van de diverse tijdschalen, in combinatie met het feit dat slechts een klein deel van de ruimte tussen de spiegels gevuld is met aangeslagen moleculen. Als we de rechterspiegel weghalen dan meet de detector nog maar twee lichtpulsjes. Het eerste pulsje bestaat uit het licht dat direct in de richting van de detector wordt uitgezonden. Het tweede pulsje komt via de linkerspiegel en is daarom iets later. Het valt daarbij op dat de tweede puls een stuk sterker is dan de eerste. Dat komt doordat het licht een tweede keer door het gebied met aangeslagen moleculen propageert en daar

door gestimuleerde emissie wordt versterkt. Zoals verwacht, wordt er nog slechts één lichtpuls waargenomen als ook de linkerspiegel wordt weggehaald.

Licht wordt vaak beschreven als een elektromagnetische golf. De richting waarin het elektrische veld trilt, heet de polarisatierichting. Deze staat altijd loodrecht op de voortplantingsrichting van het licht. Zo kan de polarisatie van het pomplicht, dat in Fig. 1 in de  $y$ -richting beweegt, bijvoorbeeld in de  $x$ - of de  $z$ -richting zijn. De polarisatie van de polymeerlaser, waarvan het licht in de  $x$ -richting propageert, ligt juist in het  $y-z$ -vlak. Als er gepolariseerd licht wordt gebruikt om moleculen aan te slaan, zullen deze vaak ook weer licht uitzenden met een voorkeur voor dezelfde polarisatierichting. Toch is dat lang niet altijd het geval. Als de aangeslagen moleculen reoriënteren voordat ze vervallen, blijft er van dit geheugen voor de pomppolarisatie weinig over. Dit blijkt uit hoofdstuk 4, waarin we laten zien dat een groot molecuul (een polymeer) een veel langer geheugen heeft voor de polarisatie van de pomp, dan kleine moleculen. Dit effect wordt toegeschreven aan de veel langere reoriëntatietijd van de lange polymeerketens. Een gevolg hiervan is dat een polymeerlaser veel gevoeliger is voor de pomppolarisatie dan een laser met kleine moleculen als versterkend medium. In hoofdstuk 5 wordt de koppeling tussen de polarisatierichtingen in een polymere *microlaser* in detail bestudeerd. In deze laser is de afstand tussen de spiegels slechts 0,02 mm.

### **Dynamica in polymere films**

Ook in pure films (dunne lagen) van lichtgevende polymeren blijkt gestimuleerde emissie op te kunnen treden, hoewel er in deze toestand veel concurrerende (niet-stralende en absorberende) processen zijn die nog niet volledig worden begrepen. Deze processen kunnen ervoor zorgen dat de gestimuleerde emissie niet of niet goed op gang kan komen. Het eerder genoemde lawine-effect treedt namelijk pas op als de versterking groter is dan de absorptie.

In de praktijk blijkt het zo te zijn dat er vlak na de excitatie met een korte puls vaak wel nettoversterking wordt gemeten en er dus gestimuleerde emissie optreedt, maar dat deze versterking slechts gedurende heel korte tijd in het systeem aanwezig is. Dit kan een serieuze belemmering vormen bij het maken van een laser. Als de versterking niet veel langer leeft dan de tijd die het licht nodig heeft om één keer tussen de spiegels heen en weer te lopen, komt de laser niet goed op gang: het emissieproces stopt voordat het goed en wel begonnen is. In hoofdstuk 6 wordt een eenvoudige, nieuwe methode gepresenteerd om de levensduur van de versterking te meten.

Hoofdstuk 7 gaat dieper in op het verschil tussen de processen van lichtemis-

---

sie in vloeistof, waarbij er weinig interactie is tussen de polymeerketens, en de vaste stof, waarbij interactie tussen de ketens dominant aanwezig is. In de oplossing blijft de energie van een pompfoton gelocaliseerd op de polymeerketen. In de vaste stof kan de energie overgedragen worden aan een andere, nabijgelegen keten, of kan de energie zich verspreiden over meerdere ketens. In het laatste geval ontstaat er een 'interchain state': de aangeslagen toestand is over meerdere ketens verspreid. Dit in tegenstelling tot de 'intrachain state', waarbij de aangeslagen toestand op de keten is gelocaliseerd. Na uitgebreide discussies in de literatuur, die de afgelopen jaren zijn gevoerd, wordt de lichtemissie in vaste stof nu over het algemeen toegeschreven aan 'interchain states'. Ook andere, absorberende, processen die in de oplossing niet optreden worden hieraan toegeschreven. De metingen aan zowel oplossingen als pure films, zoals gepresenteerd in hoofdstuk 7, wijzen hier ook op. We meten de lichtemissie als functie van de tijd bij verschillende golflengten van het uitgezonden licht (verschillende kleuren dus) en de polarisatie van dat licht. Toch blijkt ook uit onze metingen dat een klein deel van het licht waarschijnlijk nog steeds voortkomt uit vervallende 'intrachain states'. Meer discussies over het proces van lichtemissie en absorptie in vaste stof polymeren zullen de komende jaren zeker nog worden gevoerd.

## List of publications

---

1. *Transmission-reflection anomaly in second-harmonic generation from a monolayer*,  
S. A. van den Berg, E. W. M. van der Ham, Q. H. F. Vreken, and E. R. Eliel,  
Opt. Lett. **23**, 906 (1998).
2. *From amplified spontaneous emission to laser oscillation: dynamics in a short-cavity polymer laser*,  
S. A. van den Berg, R. H. van Schoonderwoerd den Bezemer,  
H. F. M. Schoo, G. W. 't Hooft, and E. R. Eliel,  
Opt. Lett. **24**, 1847 (1999).
3. *Pulse-train formation in a gain-switched polymer laser resulting from spatial gain inhomogeneity*,  
S. A. van den Berg, G. W. 't Hooft, and E. R. Eliel,  
Phys. Rev. A **60**, 063809 (2001).
4. *Orientational relaxation in polymer and dye solutions and its consequence for the laser threshold*,  
S. A. van den Berg, G. W. 't Hooft, and E. R. Eliel,  
Chem. Phys. Lett. **347**, 167 (2001).
5. *Study of polarization cross coupling in a polymer microlaser using double-pulse excitation*,  
S. A. van den Berg, V. A. Sautenkov, G. W. 't Hooft, and E. R. Eliel,  
Phys. Rev. A, to appear in June 2002.
6. *Measuring the gain dynamics in a conjugated polymer film*,  
S. A. van den Berg, V. A. Sautenkov, G. W. 't Hooft, and E. R. Eliel,  
Submitted for publication.
7. *Time-domain study of emissive states in a PPV*,  
V. A. Sautenkov, S. A. van den Berg, G. W. 't Hooft, and E. R. Eliel,  
Submitted for publication.
8. *Optical gain and lasing in conjugated polymers*,  
V. A. Sautenkov, S. A. van den Berg, G. W. 't Hooft, and E. R. Eliel,  
Submitted to IEEE Circuits and Devices Magazine.



## Curriculum Vitae

---

**Stephanus Anthonius van den Berg**  
geboren te Noordwijk op 6 november 1974

In 1993 behaalde ik het atheneumdiploma aan het College Leeuwenhorst te Noordwijkerhout. In september van dat jaar begon ik de studies natuurkunde en wiskunde aan de Universiteit Leiden, waarvoor ik in augustus 1994 de prope-deuses behaalde. Ik zette mijn studie voort in de natuurkunde en begon in 1996 met een experimentele stage in de werkgroep Quantumoptica, onder begeleiding van dr. E. R. Eliel en dr. E. W. M. van der Ham. Het onderzoek betrof somfrequentie en tweede harmonische generatie aan monolagen van vloeibare kristallen. Een deel hiervan werd uitgevoerd met behulp van de vrije-elektronenlaser van het FOM-instituut te Rijnhuizen. Het daaruit voortvloeiende afstudeeronderzoek beschrijft het opmerkelijke verschil tussen tweede harmonische generatie aan een monolaag in gereflecteerde en doorgelaten richting voor een  $p$ -gepolariseerde pompbundel. In oktober 1997 behaalde ik het doctoraalexamen in de experimentele natuurkunde.

Op 1 november van dat jaar trad ik als onderzoeker in opleiding in dienst van de Stichting Fundamenteel Onderzoek der Materie (FOM) om onderzoek te verrichten in de werkgroep Quantumoptica aan de Universiteit Leiden. Het onderzoek, onder begeleiding van dr. E. R. Eliel en prof. dr. G. W. 't Hooft, werd uitgevoerd in het kader van het 'Laboratorium zonder Muren'-programma, een samenwerking tussen FOM en Philips Research. Het werk omvatte het karakteriseren en ontwikkelen van kleine polymeerlasers, waarbij de nadruk lag op de (zeer snelle) dynamica van deze lasers en die van de polymeren zelf. Het opbouwen en onderhouden van een femtoseconde lasersysteem stond dan ook aan de basis van het experimentele werk.

In het kader van het promotieonderzoek heb ik deelgenomen aan de zomerschool 'QED phenomena and applications of microcavities and photonic crystals' in Cargèse, Frankrijk (1998) en de conferentie 'European Conference on Molecular Electronics' in Linköping, Zweden (1999). Ik heb voordrachten gegeven op de najaarsvergadering van de Nederlandse Natuurkundige Vereniging (Sectie Atoomfysica en Quantumelektronica) te Lunteren (1999) en op de 'Conference

---

on Lasers and Electro-Optics Europe' in Nice, Frankrijk (2000). In 2001 volgde ik een managementtraining aan het Management Development Centre van de Universiteit Nyenrode te Breukelen. Naast het onderzoek gaf ik, met plezier, eerstejaarsstudenten werkcolleges behorende bij het vak 'Optica'.

Op 1 augustus 2002 treed ik als wetenschappelijk medewerker in dienst van het Nederlands Meetinstituut te Delft.

## Nawoord

---

Graag wil ik ter afsluiting diegenen noemen die op een directe of indirecte manier van belang zijn geweest bij de totstandkoming van dit proefschrift.

Jan Post en Koos Benning van de fijnmechanische werkplaats hebben ervoor gezorgd dat mijn soms maar half uitgewerkte ideeën toch steeds tot bruikbare voorwerpen leidden, meestal met grotere nauwkeurigheid vervaardigd dan ik gevraagd had en altijd eerder klaar dan gepland. René Overgaww zorgde voor de benodigde elektronica en kreeg het voor elkaar dat mijn computer en de stappenmotor een goede wederzijdse verstandhouding kregen. Arno van Amersfoort en Leendert Prevo verstrekten de onontbeerlijke ondersteuning op het gebied van computers en hebben dan ook menig computer en printer gereanimeerd. De secretariële ondersteuning was in goede handen bij Anneke Aschoff.

Zonder lichtgevende polymeren geen polymeerlasers. Veel van deze onmisbare materialen werden ter beschikking gesteld door Philips Research en het Dutch Polymer Institute. Dr. M. M. de Kok-van Breemen en S. H. P. M. de Winter verstrekten het door Covion gesynthetiseerde polymeer HB1221.

Remco van Schoonderwoerd den Bezemer, Bas Verberg, Rogier Boogaard en Peter Lee hebben allen langere of kortere tijd als student meegewerkt aan het onderzoek. Ze hebben niet alleen een bijdrage geleverd aan het experimentele werk, ook het stellen van (lastige) vragen die de soms nogal controversiële literatuur over het onderwerp bij hen opriep was van groot belang. Vladimir Sautenkov joined the polymer project for several periods ranging from a few months to about a year. The discussions and forthcoming ideas have been of great value for part of the work described in this thesis.

Graag wil ik ook mijn collega's en oud-collega's noemen die de afgelopen jaren zowel in het lab als aan de koffietafel voor gezelligheid, ontspanning en discussie zorgden: Eric, Harald, Rob, Frans, Gerwin, Paul, Boris, Krista, Alexander, Marnix, Yngve, Jos, Sumant, Hayk, Jorrit, Javier en Erwin. De vakgroepentjes, concertbezoeken en natuurlijk de zeilmiddagen waren altijd erg gezellig.

Mijn ouders wil ik bedanken voor het bieden van de vele kansen en mogelijkheden die het fundament vormden voor mijn studie en promotie. Samen met mijn broers en zus zorgden zij voor een stabiele thuisbasis waar ik altijd terecht kon. Ten slotte, Christiane, jouw aanwezigheid en je soms verbazingwekkend oprechte belangstelling voor de inhoud van het onderzoek, hebben mij de afgelopen jaren zeer goed gedaan.

